JOURNAL OF PETROLOGY | VOLUME 48 | NUMBER 10 | PAGES 1895–1953 | 2007 | doi:10.1093/petrology/egm044

# Petrology and Mineral Chemistry of Lower Crustal Intrusions: the Chilas Complex, Kohistan (NW Pakistan)

**OLIVER JAGOUTZ[1,2]*, OTHMAR MÜNTENER[2†], PETER ULMER[1], THOMAS PETTKE[2], JEAN-PIERRE BURG[1], HAMID DAWOOD[3] AND SHAHID HUSSAIN[3]**

[1]DEPARTMENT OF EARTH SCIENCES, ETH ZURICH, SONNEGGSTRASSE 5, 8092 ZURICH, SWITZERLAND

[2]INSTITUTE OF GEOLOGICAL SCIENCES, UNIVERSITY OF BERN, BALTZERSTRASSE 1+3, 3012 BERN, SWITZERLAND

[3]PAKISTAN MUSEUM OF NATURAL HISTORY, ISLAMABAD, PAKISTAN

**RECEIVED AUGUST 7, 2006; ACCEPTED JULY 11, 2007**
**ADVANCE ACCESS PUBLICATION SEPTEMBER 3, 2007**

*Mineral major and trace element data are presented for the main rock units of the Chilas Complex, a series of lower crustal intrusions emplaced during initial rifting within the Mesozoic Kohistan (paleo)-island arc (NW Pakistan). Detailed field observations and petrological analysis, together with geochemical data, indicate that the two principal units, ultramafic rocks and gabbronorite sequences, originate from a common parental magma, but evolved along different mineral fractionation trends. Phase petrology and mineral trace element data indicate that the fractionation sequence of the ultramafic rocks is dominated by the crystallization of olivine and clinopyroxene prior to plagioclase, whereas plagioclase precedes clinopyroxene in the gabbronorites. Clinopyroxene in the ultramafic rocks (with Mg-number [$Mg/(Fe_{tot}+Mg$] up to 0·95) displays increasing $Al_2O_3$ with decreasing Mg-number. The light rare earth element depleted trace element pattern ($Ce_N/Gd_N$ ~0·5–0·3) of primitive clinopyroxenes displays no Eu anomaly. In contrast, clinopyroxenes from the gabbronorites contain plagioclase inclusions, and the trace element pattern shows pronounced negative anomalies for Sr, Pb and Eu. Trace element modeling indicates that* in situ *crystallization may account for major and trace element variations in the gabbronorite sequence, whereas the olivine-dominated ultramafic rocks show covariations between olivine Mg-number and Ni and Mn contents, pointing to the importance of crystal fractionation during their formation. A modeled parental liquid for the Chilas Complex is explained in terms of mantle- and slab-derived components, where the latter component accounts for 99% of the highly incompatible elements and between 30 and 80% of the middle rare earth elements. The geochemical characteristics of this component are similar to those of a low percentage melt or supercritical liquid derived from subducted mafic crust. However, elevated Pb/Ce ratios are best explained by additional involvement of hydrous fluids. In accordance with the crystallization sequence, the subsolidus metamorphic reactions indicate pressures of 0·5–0·7 GPa. Our data support a model of combined flux and decompression melting in the back-arc.*

KEY WORDS: *Kohistan; Island arc; gabbro; trace element modelling; lower crustal intrusion*

## INTRODUCTION

The present-day formation of continental crust is, in general, attributed to magmatic processes taking place in two distinct plate tectonic settings: active continental margins and intra-plate. Trace element similarities [e.g. enrichment of the light rare earth elements (LREE), the depletion of Nb and Ti, and enrichment of Pb with respect to the REE] between bulk crust estimates and present-day volcanism in subduction zones suggest that 80–95% of the post-Archean continental crust formed by processes similar to those taking place in present-day subduction zones (Rudnick, 1995; Barth *et al.*, 2000). Therefore, studying island arc processes provides important clues about the formation of the continental crust. Our understanding of crust formation is hampered by

†Present address: Institute of Mineralogy and Geochemistry, University of Lausanne, Anthropole, 1015 Lausanne, Switzerland.
*Corresponding author. Present address: Institute of Geological Sciences, University of Bern, Baltzerstrasse 1+3, 3012 Bern, Switzerland. E-mail: Oliver.Jagoutz@geo.unibe.ch

the scarcity of data concerning deep crustal processes. This knowledge gap mainly results from the fact that active island arcs allow direct observation of surface rocks only. Yet, the paucity of 'true' primary arc magmas in volcanic arcs indicates that intra-crustal differentiation is important. Upper and middle crustal intrusions have been studied in detail (e.g. Skaergaard, McBirney & Noyes, 1979) compared with rarely exposed lower crustal intrusions; however, the latter are more relevant to models for crustal development because potentially they link upper mantle and upper crustal processes (Annen *et al.*, 2006). Accordingly, understanding the emplacement and differentiation mechanism of deep-seated magmatic bodies is crucial to understanding continent-building processes (DeBari, 1994).

Deep-seated magmatic bodies cool more slowly than shallower intrusions. Slow crystallization may result in re-equilibration of trapped interstitial melts within early formed cumulate assemblages, and this re-equilibration may obscure the differentiation history. The process may result in enrichment of incompatible trace elements in the whole-rock samples, which may be wrongly interpreted as a differentiation effect (Cawthorn, 1996). Additionally, assimilation of crustal melts may interfere with differentiation processes (e.g. Ivrea Zone, Voshage *et al.*, 1990). Therefore, the major and trace element compositions of the magmatic mineral phases and whole-rock geochemical data are crucial to understand the magmatic differentiation mechanisms of deep-seated intrusions.

We present results from the Chilas Complex, a volumetrically important series of Mesozoic-aged calc-alkaline mafic and ultramafic intrusions emplaced in the lower to intermediate crustal segment of the Kohistan arc in NW Pakistan. The Kohistan arc is an obducted paleo-island arc exposing one of the best preserved and best exposed arc-sections worldwide. As such it offers an unrivalled opportunity to study lower island arc processes. In this paper we describe the petrography and mineral major and trace element geochemistry obtained by laser ablation inductively coupled plasma mass spectrometry (LA-ICP-MS) of the principal lithological units of the Chilas Complex.

Rare earth element (REE) modeling is used to unravel the combined effects of differentiation and trapped liquid in slowly cooled rocks. Our results show that *in situ* crystallization (Langmuir, 1989) can account for the chemical variability of the mafic rocks whereas the ultramafic rocks evolved through fractional crystallization. A parental mantle-derived hydrous magma composition for all rocks of the Chilas Complex and an evolved magma composition parental only to the gabbronorite sequence are calculated. Modeling explains the trace element composition of the parental magma in terms of mantle- and slab-derived components. The trace element composition of the modeled slab component is similar to that of a low percentage melt or supercritical liquid derived from a normal mid-ocean ridge basalt (N-MORB) source. The trace element characteristics of the slab-derived component are comparable with estimates of slab components in Mariana back-arc magmas (Stolper & Newman, 1994) and in the eruptive rocks of the Californian Cascades (Grove *et al.*, 2002).

## GEOLOGICAL SETTING AND PREVIOUS WORK

### The Kohistan arc

The Kohistan arc (Fig. 1) is a fossil Jurassic–Cretaceous island arc that was sandwiched between the Indian and Asian plates during the Himalayan collision (Tahirkheli *et al.*, 1979; Bard, 1983; Coward *et al.*, 1986; Treloar *et al.*, 1996; Searle *et al.*, 1999). To the east, the Kohistan arc is separated from the Ladakh arc by the Nanga Parbat Syntaxis, a half-window of Indian Plate gneisses undergoing rapid exhumation (Zeitler *et al.*, 1989, 1993).

The intra-oceanic Kohistan arc originated through northward subduction in the equatorial area of the Tethys Ocean (e.g. Zaman & Torii, 1999) and is essentially composed of Jurassic–Cretaceous to Tertiary igneous, volcanic and sedimentary rocks. In the southernmost part of the Kohistan arc, the Jijal Complex represents the upper mantle to lower crust transition (Jan & Howie, 1981; Jan & Windley, 1990; Ringuette *et al.*, 1999) overlain by a thick pile of metaplutonic and minor volcanic and sedimentary metamorphic rocks, considered together as the so-called Southern (Kamila) Amphibolites. The Chilas Complex (Figs 2 and 3), intruded during intra-arc rifting at the base of the arc (Khan *et al.*, 1989; Burg *et al.*, 2006) and separates these amphibolites from the Gilgit domain to the north, composed dominantly of upper crustal plutonic, volcanic and sedimentary rocks and their metamorphosed equivalents (Petterson & Windley, 1985; Pudsey *et al.*, 1985). In general, the proportional amount of volcano-sedimentary rocks in the Gilgit domain diminishes from north to south whereas plutonic units become more abundant. Accordingly, the domain has been subdivided into the so-called Kohistan Batholith in the south and volcano-sedimentary series (Chalt, Shamran and Utor volcanics and Yasin sediments) in the north.

### Chilas Complex

This study deals with the 85 Ma calc-alkaline ultramafic–mafic Chilas Complex (Figs 2 and 3) (Zeitler, 1985; Schaltegger *et al.*, 2002). Pressure and temperature estimates indicate equilibration temperatures around 600–800°C and pressures of 0·6–0·8 GPa (Jan & Howie, 1980; Bard, 1983). This magmatic complex was originally interpreted as the remnant of the gabbroic to ultramafic cumulate sequence of a fragment of oceanic crust

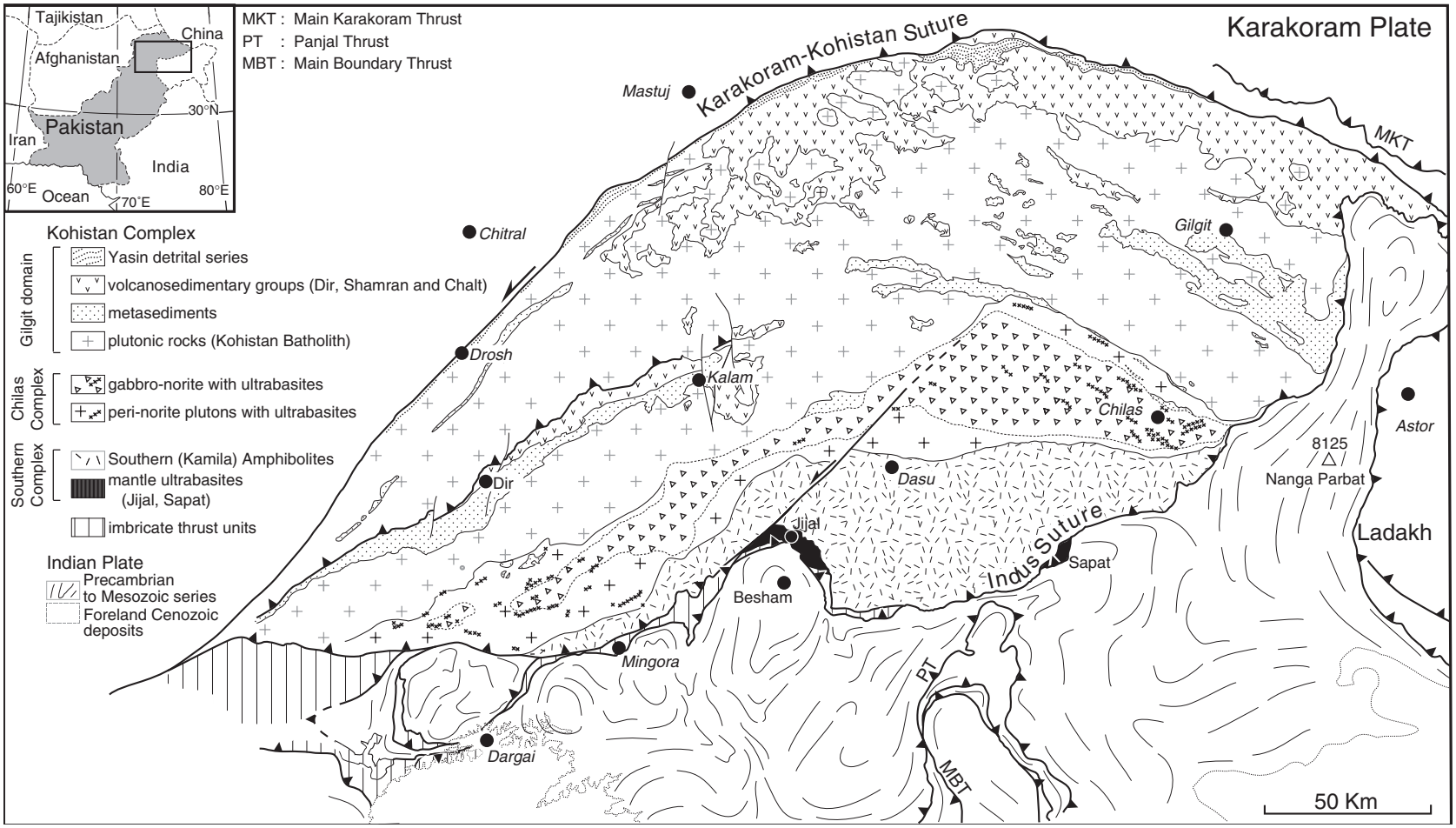


**Fig. 1.** Geology of Kohistan based on field data and extrapolations on Landsat ETM + pictures (modified after Jagoutz *et al.*, 2006).

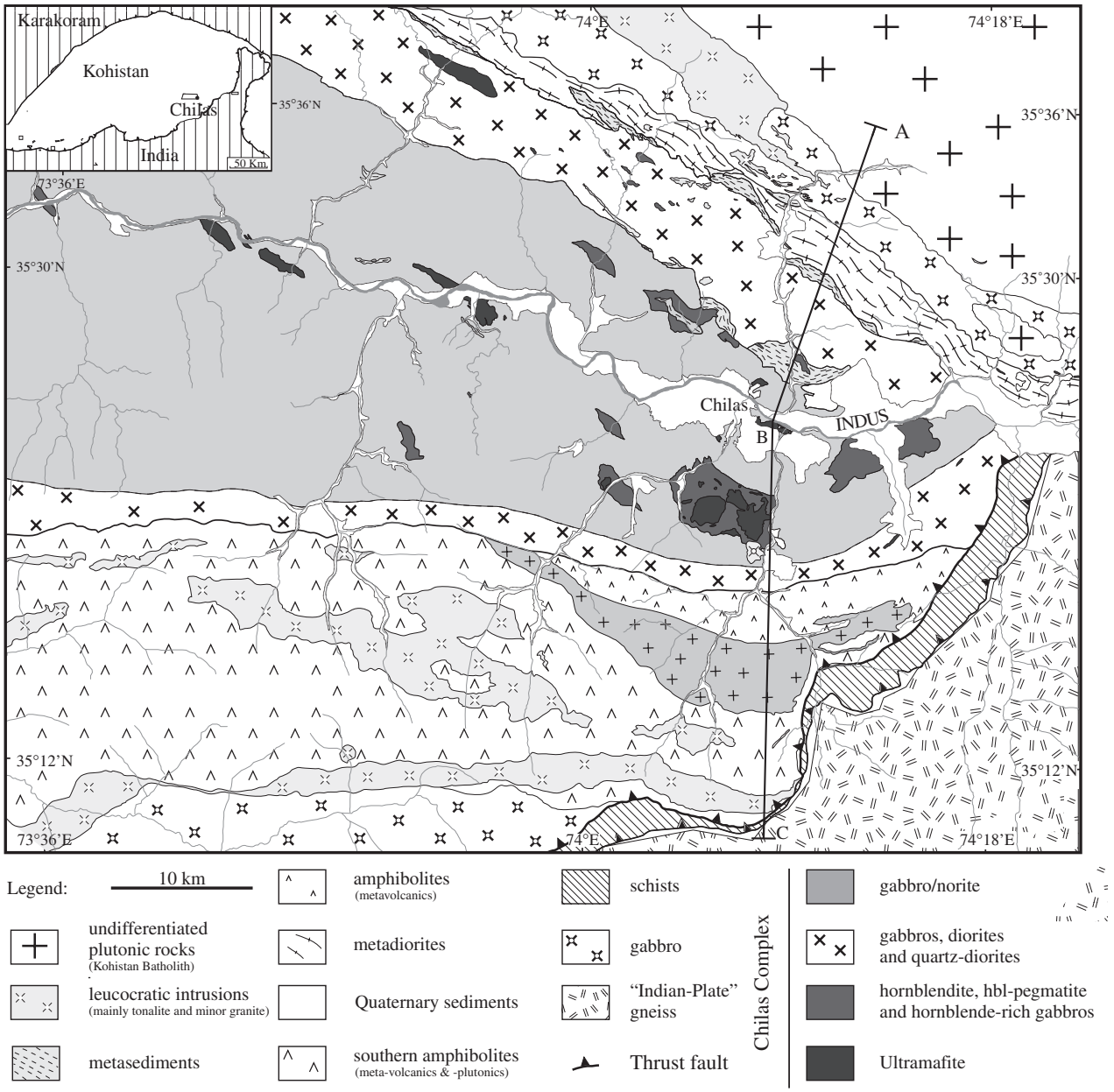


**Fig. 2.** Geological map of the Chilas Complex based on field mapping and remote sensing of Landsat ETM + data and satellite pictures from Google Earth and previously published maps (Khan & Khan, 1998; Khan *et al.*, 1999*a*, 1999*b*). Line A–C corresponds to location of the section presented in Fig. 3.

(Asrarullah & Abbas, 1979; Butt *et al.*, 1980; Chaudhry *et al.*, 1983) and later as a layered intrusion at the base of an island arc (Bard, 1983; Jan *et al.*, 1984; Khan *et al.*, 1985; Coward *et al.*, 1986; Takahashi *et al.*, 2007). The island arc affinity of the geochemical and petrological data (Khan *et al.*, 1989; Jagoutz *et al.*, 2006) rules out an oceanic origin. The large volume of mafic magma led Khan *et al.* (1989) to propose that the Chilas Complex intruded during mantle diapirism at incipient stages of back-arc spreading. This idea is supported by structural observations indicating that the Chilas Complex intruded at the base of an extending arc (Burg *et al.*, 2006). Hafnium (Hf) isotopes ($\varepsilon_{Hf} = 10{\cdot}4$), indicate a mantle source of the Chilas Complex that is different from that of the metaplutonic Southern Complex (Schaltegger *et al.*, 2002).

The Chilas Complex is composed of modally layered to homogeneous gabbronorite with subordinate (quartz) diorite and tonalite, collectively referred to as the

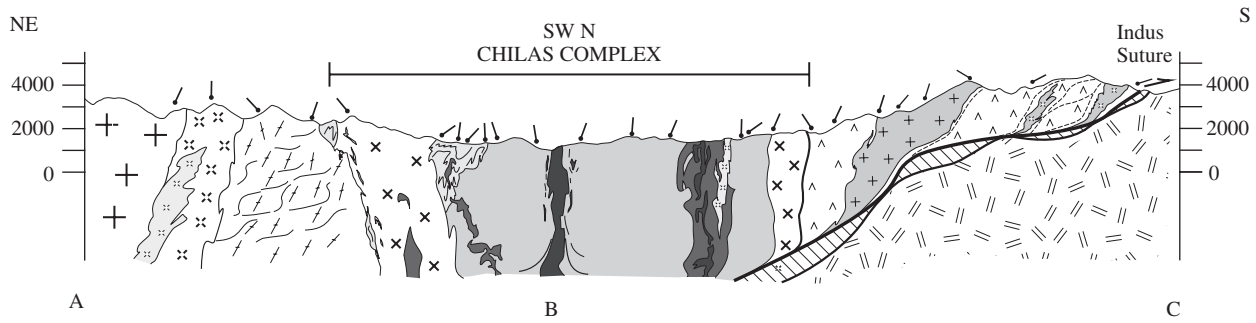


**Fig. 3.** Cross-section through Chilas Complex and adjoining units showing the overall structure and relationships between various units. Lithology as in Fig. 2.

'main gabbronorite' or the gabbronorite sequence (Khan *et al.*, 1989). Within the gabbronorite sequence, late-stage hornblende-bearing pegmatites are common. Additionally, locally hornblende-bearing (micro-)gabbroic dykes are observed. The relationships between the main gabbronorite and bodies of dunite–peridotite–pyroxenite–gabbronorite–anorthosite, which Khan *et al.* (1989) called ultramafic–mafic–anorthositic (UMA) associations, are disputed; Khan *et al.* (1985, 1989) interpreted the UMA associations as cumulates derived from picritic melts emplaced into a crystallizing magma chamber. A similar model was proposed by Niida *et al.* (1996), who interpreted the UMA associations as an ultramafic crystal-mush intrusive into a crystallizing gabbroic magma chamber. Kubo *et al.* (1996), however, argued that the UMA associations are older than the gabbronorite.

Based on facing directions of modally graded layers, the structure of the Chilas Complex has been interpreted as an antiform several tens of kilometers high with a near-vertical axial plane (Coward *et al.*, 1982, 1986). Burg *et al.* (1998), however, noted that the main gabbronorite displays a magmatic fabric with a subvertical lineation and that the axial plane of this proposed fold runs through the outcrops of UMA associations. They concluded that the facing directions do not reflect crustal-scale folding but, instead, oppositely facing margins of UMA bodies representing apices of intra-arc mantle diapirs intruding into the extending island arc. Based on detailed field and whole-rock geochemical data, Jagoutz *et al.* (2006) interpreted the ultramafic bodies as the surface expression of a vertically continuous upper mantle melt extraction system through which the mafic sequence of the Chilas Complex was fed. Our new geochemical data are not consistent with differentiation between UMA associations and the gabbronorite sequence (Khan *et al.*, 1993, 1989). We will distinguish the plagioclase-dominated mafic gabbronorite sequence (including gabbro, quartz diorites and tonalites) and the olivine- or pyroxene-dominated ultramafic sequence.

## FIELD RELATIONSHIPS AND PETROGRAPHIC OBSERVATIONS

A synopsis of field relationships between the various intrusive units has been given by Jagoutz *et al.* (2006). The kilometer-scale ultramafic bodies enclosed by the gabbronorite sequence are concentrically, but irregularly, zoned with a massive dunite core and subsequent shells of harzburgite, lherzolite, plagioclase-bearing lherzolite or olivine websterite (collectively called secondary peridotites). Relict, amphibole-bearing olivine websterite with centimeter-sized clinopyroxene (hereafter called ol-websterite) appears as xenoliths of tens-of-meter scale within the core dunite and it is therefore older. Dunite dykes (up to tens of centimeters in thickness) cross-cutting the ol-websterite have straight contacts whereas smaller, centimetre-thick veins display irregular contacts with embayment of dunite into ol-websterite. Within the dunite, xenoliths of ol-websterite, centimeters to tens of centimeters across increase in abundance towards the contact zone between massive dunite and ol-websterite.

The main part (~95%) of the ultramafic bodies is composed of homogeneous dunite with local, centimeter-sized chromite and pyroxenite veins and patches (Fig. 4a). The transition between dunite and secondary peridotite is generally gradational with increasing modal amounts of pyroxene and amphibole and decreasing amounts of olivine. However, sharp contacts between dunite and secondary peridotite exist. In the following paragraph, the transition between dunite and secondary peridotite is detailed along a section from dunite to surrounding gabbronorite.

Interstitial clinopyroxene between large olivine clasts occurs as centimeter-scale ovoid, vertically elongated patches within dunite. Where the patches are abundant, they tend to coalesce, and form lineaments. Plagioclase appears along triple junctions between large, centimeter-sized olivine grains, which display a reaction rim of pyroxene–spinel symplectite at plagioclase–olivine contacts.

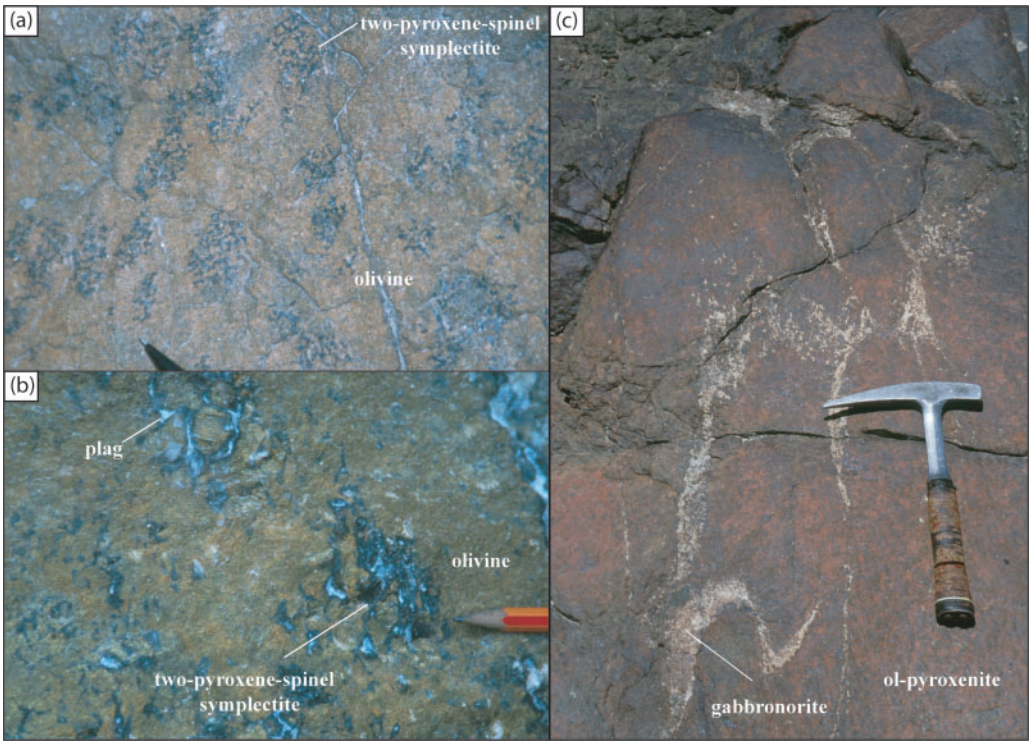


**Fig. 4.** Field relationships within the ultramafic rocks. (a) Interstitial cpx and two-pyroxene–spinel symplectite patches in dunite: the centimeter-scale patches are elongated in the third dimension and occur in increased frequency on a meter scale. (b) Symplectite forms between plagioclase and olivine. (c) Increased frequency of plagioclase in microgabbronorite patches. Over a few tens-of-centimeters diffuse patches form constrained dykes cross-cutting larger ol-pyroxenite blocks.

Patchy spheroidal to ellipsoidal clusters of this reaction texture show structures similar to the clinopyroxene patches described above (Fig. 4a). A continuous transition exists between the gabbronorite patches and patches defined by the two-pyroxene–spinel reaction texture (Fig. 4b). Gabbronorite also occurs as schlieren around ultramafic clasts (Fig. 4c) or along grain boundaries, disintegrating olivine grains in dunite (Fig. 5a). In plagioclase-dominated veins, disintegrated dunite may result in rocks with troctolitic modal composition (Fig. 5a–c). Plagioclase-bearing veins disappear along strike into planar traces defined by two-pyroxene–spinel symplectites. Around larger, meter-sized gabbronorite patches, tens-of-centimeters thick, pyroxene-rich reaction halos document the transformation of dunite into secondary peridotite and angular dunite blocks (Fig. 5d). Transformation also occurs over tens of meters, indicated by fragmented dunite blocks in secondary peridotite with various amounts of pyroxene (see Jagoutz *et al.* 2006, fig. 4d). Dunite blocks are often surrounded and possibly protected from further transformation by a sheath of pyroxenite. However, sporadic replacive dunite dykes are also observed in secondary peridotites.

Irregularly shaped xenoliths of gabbronorite within lherzolite are frequent (Fig. 5e). Taking into account the vertical attitude of both the mineral lineation and the foliation in some of the gabbronorite xenoliths, some of the 'xenoliths' in plane view may be tube-shaped in the vertical direction.

The gabbronorite–ultramafite contact is sharp but irregular (Fig. 6a), with the two rock types often interfingering (Fig. 6b). In the gabbronorite next to ultramafite, ultramafite xenoliths (Fig. 6a) are abundant. Fragmentation of larger into smaller xenoliths and 'lava-lamp'-like structures, where ultramafite blobs are detached from ultramafic fingers (Fig. 6c and d) are common. They indicate assimilation of the ultramafic rocks. Additionally, coarse-grained hornblendite, and hornblende-, pyroxene-, plagioclase-, K-feldspar-, quartz- and locally epidote-bearing pegmatites with up to meter-sized skeletal hornblende crystals, occur within the contact zone and within the mafic rocks. Patchy, irregular amoeboid meter-scale bodies of this pegmatitic material in gabbroic rocks indicate a comagmatic origin (Fig. 6e). Upward deflection of mafic layers at the contact with the ultramafite indicates syn-magmatic, differential upward movement of the ultramafic rocks with respect to the mafic sequence (Jagoutz *et al.*, 2006). A schematic representation of the field relationships is given in Fig. 7.

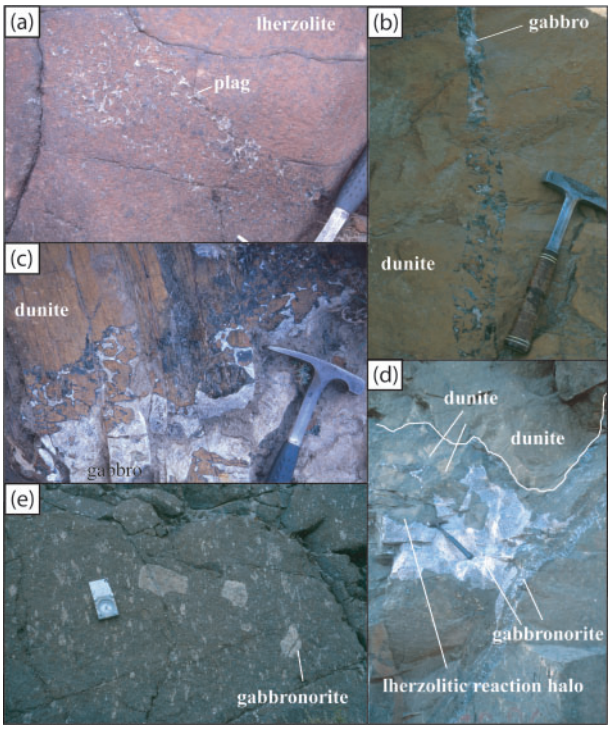


**Fig. 5.** Field relationships documenting magma transport in veins and dykes within ultramafic rocks. (a) Plagioclase occurring in an increased frequency within a dyke-like zone in secondary peridotite. (Note the occurrence of interstitial plagioclase between larger olivine grains.) (b) Along-strike transition of a mafic igneous vein into a dyke-like planar zone of pyroxene, two-pyroxene–spinel symplectite and plagioclase occurring along grain boundaries and between triple junctions of larger olivine grains. (c) Disintegration of olivine of the host rock at the contact with a mafic dyke. (Note the increased frequency of ultramafic xenoliths towards the contact with the host.) (d) Lherzolitic halo of secondary peridotite in dunite formed around a larger gabbronorite body. Dunite fragments often rimmed by a pyroxenite are preserved within the halo. (e) Numerous patches of gabbronorite 'xenoliths' within a pyroxenite matrix. Sub-vertical mineral lineation and xenoliths of ultramafite within the gabbronorite 'xenolith' indicate that many of the 'xenoliths' in plane view are tube-shaped dykes in the third dimension.

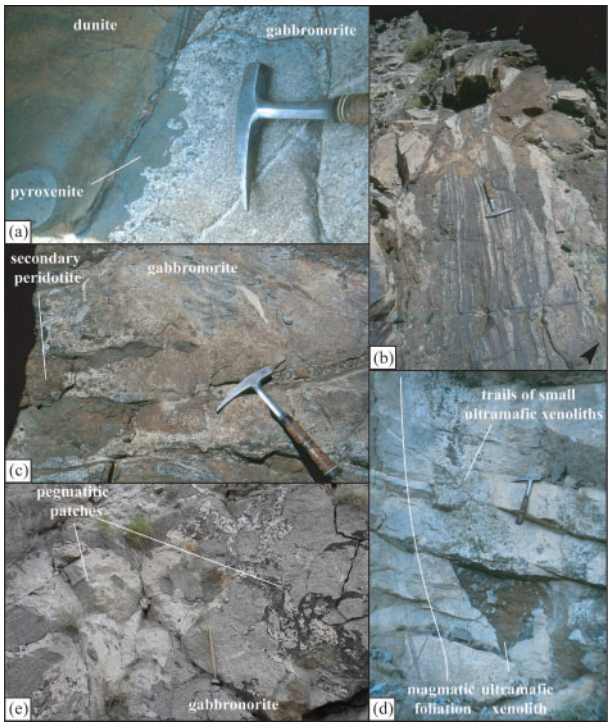


**Fig. 6.** Contact relationships between ultramafic and gabbronorite sequence. (a) Centimeter-wide zone of secondary peridotite (pyroxenite) formed at the contact between dunite and gabbronorite. The sharp but irregular contact between secondary peridotite and gabbronorite and a centimeter-wide zone of increased ultramafite xenoliths next to the contact should be noted. The 'cuspate and lobate' geometry of the contact itself indicates a similar viscosity for the gabbronorite and the secondary peridotite crystal mush during formation (from Jagoutz *et al.*, 2006). (b) Interfingering between ultramafic rocks and the gabbronorite sequence indicating mutual intrusion of both. (c) "Lava lamp" like structure: Blob of ultramafite detached from an ultramafic finger floating in a gabbronorite patch. (d) Disintegration of a large ultramafic xenolith in gabbroic host rock showing magma dynamics. (Note the absence of ultramafite clasts below the ultramafite and the trail of the clasts above, indicating a subvertical directed upwards movement of the mafic crystal mush compared to the ultramafite clasts during formation of the structure.) (e) Amoeboid and dyke-like pegmatitic patches (left, plagioclase-rich; right, amphibole-rich) in gabbronorite often occur close to or within the contact with ultramafite bodies. The structures are interpreted to represent coalescent structures of later stage interstitial melt expelled from the crystallizing gabbronorite mass. These structures are often spatially associated with increased frequency of pegmatitic dykes and can be mapped in the field (see Fig. 2).

## Petrography

Peridotite and gabbronorite samples are generally very fresh with occasional alteration being restricted along joints. The transition ol-websterite–dunite and the gradual zoning of the secondary peridotites (dunite–lherzolite–pyroxenite) from dunite towards the surrounding gabbronorite, described above, corresponds to the following petrographic changes.

### *Ultramafic rocks*

Amphibole-bearing ol-websterite has complicated textural relationships (Fig. 8a). Centimeter-scale clinopyroxene and orthopyroxene grains show exsolution lamellae of the complementary pyroxene and Cr-spinel. Pyroxenes are often rimmed by and contain inclusions of amphibole. Because the amphibole–pyroxene contacts are highly irregular (amaeboid to interlobate) amphibole 'inclusions' are likely to to be isolated as a result of 2D effects. Large (centimeter-sized) olivine grains often show kinkbands, undulose extinction and interlobate grain boundaries. Smaller, millimeter-scale olivine grains in centimeter-wide trails display straight extinction and grain boundaries with 120° triple junctions. These trails of small olivine grains cross-cut the larger olivine and pyroxene grains and also occur between pyroxene grains (Fig. 8b and c); they form an intergranular network between pyroxene

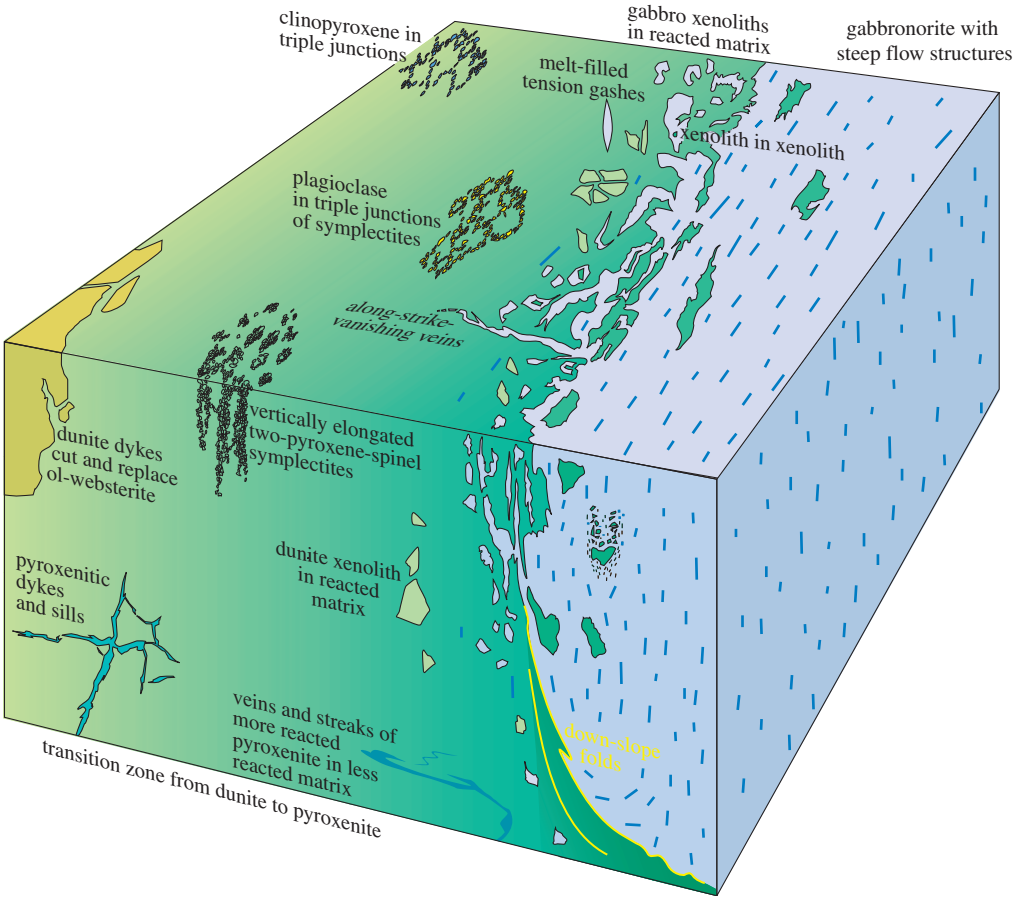


**Fig. 7.** Illustration of the contact relationships between ultramafic (greenish) and gabbronorite sequences (bluish); modified after Jagoutz *et al.* (2006). (See text for details.)

and amphibole. Grain boundaries between small olivine grains and pyroxene clasts are often irregular (Fig. 8d). The orientation of spinel exsolution trails within pyroxene can be preserved in the millimeter-scale olivine grains close to the grain boundaries (Fig. 8d).

In the field, the contact between dunite and ol-websterite is sharp. However, modal olivine decreases gradually over a few centimeters, whereas the amount of pyroxene increases. Dunite frequently has a granoblastic texture and no shape- or crystal lattice- preferred orientation is present (Jagoutz, unpublished data). Similar to what is observed in the ol-websterite, olivine has a bimodal size distribution whereby centimeter-sized grains show undulose extinction. Trails of millimeter-sized olivine grains cut across larger ones and show no feature of crystalline plasticity, which indicates multiple (re)crystallization of olivine (Fig. 9a). Accessory opaque minerals, Cr-spinel, Cr-bearing magnetite and Fe–Ni sulfide are included within olivine and along grain boundaries (Fig. 9b). Minor pyroxene occurs as centimeter-sized intergranular clusters along grain boundaries of olivine crystals and as trails (Fig. 10a and b). Pyroxene grains develop an intergranular network between larger olivine crystals (Fig. 10c). In the surrounding pyroxenites, relict olivine grains occur between partially exsolved pyroxene crystals (Fig. 10d). Closer to the contact with gabbronorite, amphibole joins the mineral assemblage. Closer to the mafic rocks, plagioclase first occurs at triple junctions between large olivine grains and pyroxene–spinel symplectites are systematically developed along olivine–plagioclase contacts. Within these symplectites, orthopyroxene nucleates close to olivine and hercynitic spinel forms symplectites with clinopyroxene and amphibole towards the plagioclase (Fig. 10e). In places, blobs and vermicular symplectites form interstitial trails between relict olivine grains (Fig. 10f). Within the contact zone between ultramafite and gabbronorite, poikilitic centimeter-sized orthopyroxene includes abundant olivine (Fig. 10g), clinopyroxene and plagioclase (Fig. 10h).

### *Mafic rocks*

The mafic rocks are dominated by gabbronorite composed of plagioclase, clinopyroxene and orthopyroxene (grain size ~0·5 cm; Fig. 11a and b). However, a broad regional

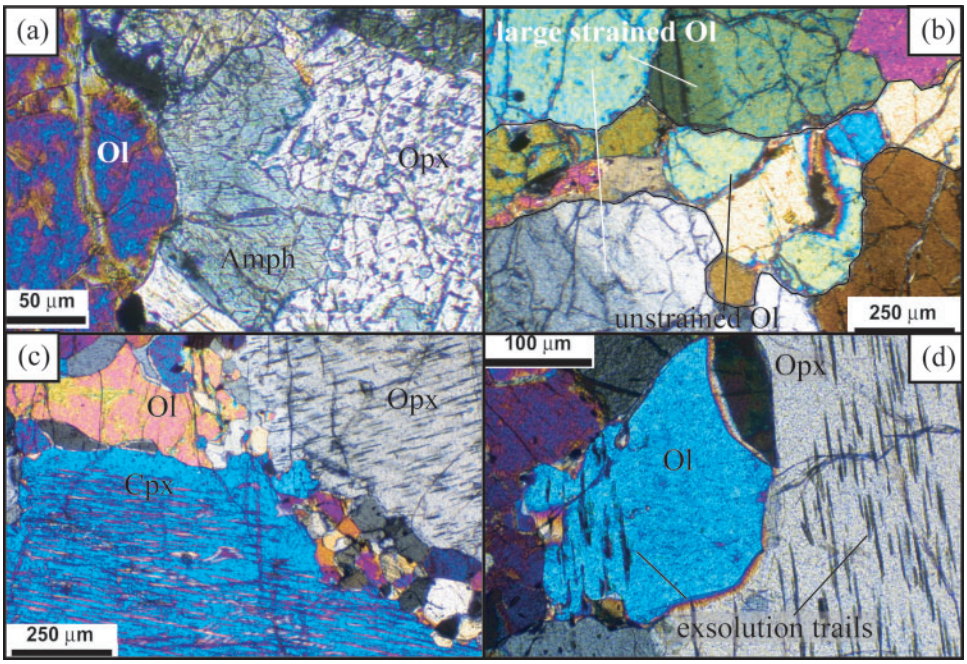


**Fig. 8.** Photomicrograph of an ol-websterite, with mineral abbreviations (Kretz, 1983). (a) Embayment of amphibole into orthopyroxene and embayment of olivine into amphibole and orthopyroxene indicate that amphibole and olivine replace orthopyroxene. (b) Trails of small unstrained olivine grains cutting through larger olivine with undulose extinction. (c) Trails of new olivine grains along grain boundaries between porphyroclastic orthopyroxene and clinopyroxene. (d) Exsolution trails of spinel in orthopyroxene are preserved in olivine grains embaying the corresponding orthopyroxene (from Jagoutz *et al.*, 2006).

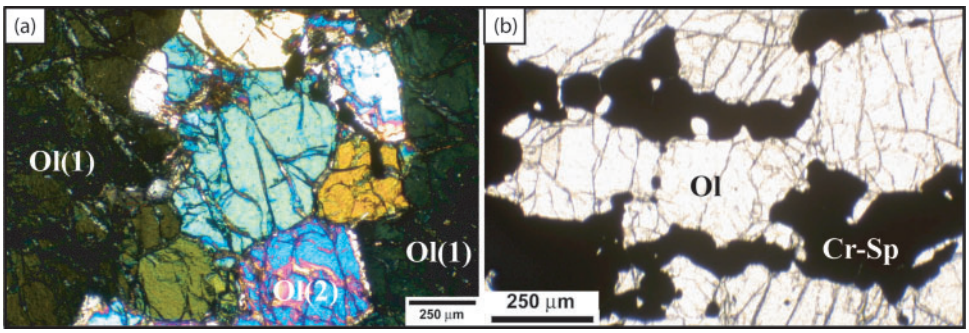


**Fig. 9.** Photomicrograph of dunite textures. (a) Trails of small olivine blasts cross-cutting a larger olivine grain. (b) Cr-rich spinels along grain boundaries of granoblastic olivine grains.

internal layering is found within the Chilas Complex, where primitive ol-bearing gabbro(norites) are more frequent towards the ultramafite bodies whereas evolved (quartz) diorite compositions are rather found towards the rim of the Complex (Figs 2 and 3). More primitive (olivine-bearing) gabbronorites generally have orthocumulate textures with clinopyroxene, orthopyroxene and amphibole as intercumulus minerals. Olivine, if present, shows reaction textures with plagioclase similar to that observed in the ultramafic rocks. Pyroxene is frequently rimmed by amphibole, and plagioclase inclusions are common (Fig. 11d). Hypidiomorphic to idiomorphic pyroxene and plagioclase are locally preserved. Twinning within plagioclase is common and typically continuous (Burg *et al.*, 2006). Undulose extinction is uncommon, but occurs rarely in quartz. Tens of centimeter thick layering, if present, is mainly defined by modal variations of plagioclase and pyroxene.

In evolved rocks amphibole is hypidiomorphic and often associated with quartz, and granophyric intergrowth between these two minerals is common (Fig. 11d). In thin section amphibole is also the nucleus of millimeter-scale cross-cutting quartz-rich veins. In the most evolved rocks K-feldspar and biotite are occasionally present.

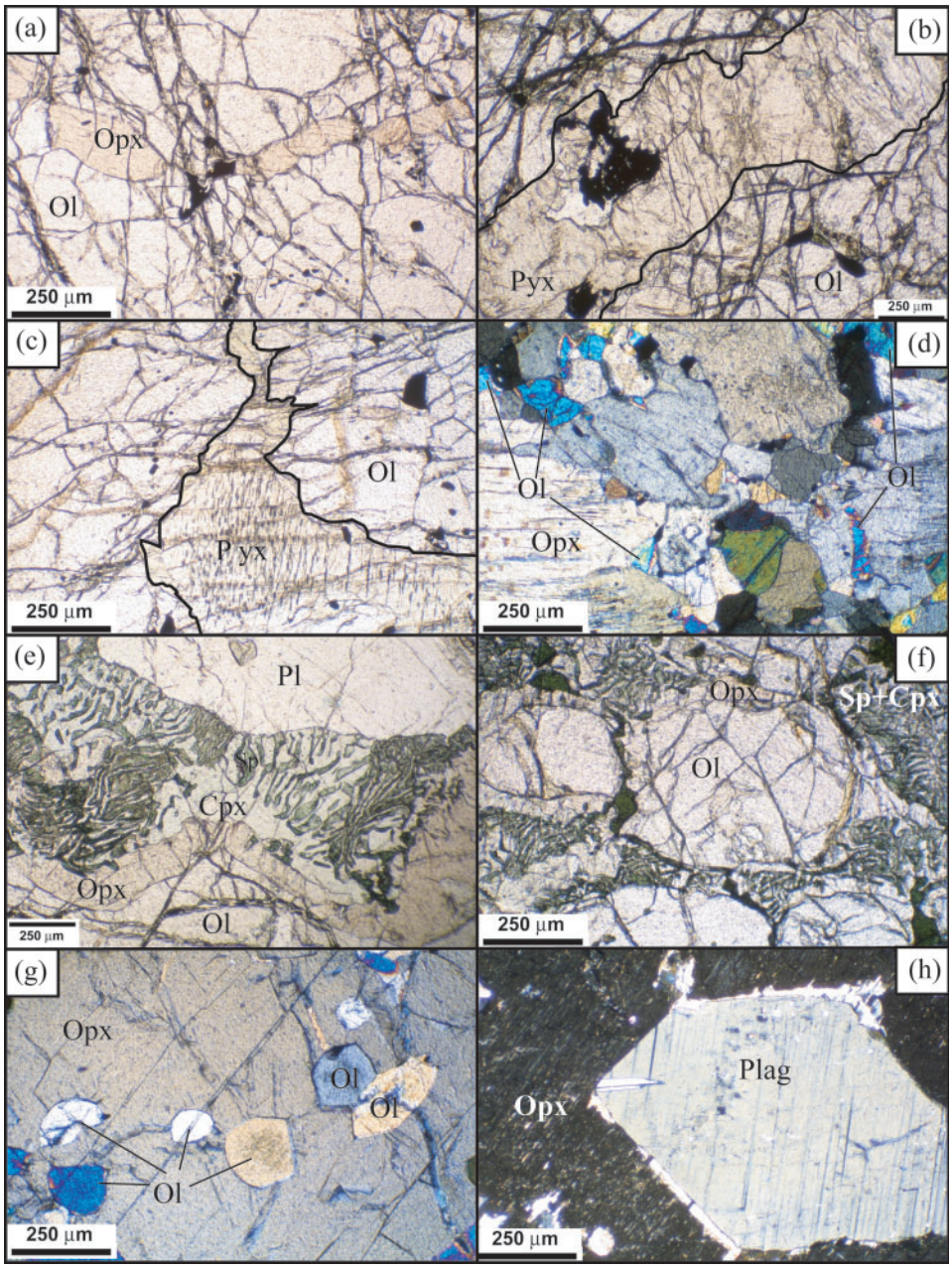


**Fig. 10.** Photomicrograph of the gradual dunite–lherzolite–pyroxenite transition. (a) Vein-like trails of orthopyroxene grains along boundaries of granoblastic olivine. (b) Veins where pyroxene content increases. (c) Large porphyroblastic pyroxene where pyroxene is abundant. (d) Relict olivine grains (high-birefringence colors) between large pyroxene crystals in pyroxenites, close to the contact with gabbronorite. (e) Two-pyroxene–spinel symplectite mineral reaction between plagioclase and olivine. (f) Same symplectitic reaction without plagioclase preserved. (g) Large poikilitic orthopyroxene with olivine inclusions and (h) with a hypidiomophic plagioclase inclusion.

*Interpretation of the field and petrographic relationships*

Field and petrographic observations can be interpreted as the result of two melt-rock reactions that took place in the ultramafic rocks, as follows.

The transition ol-websterite → dunite is due to a pyroxene-consuming, olivine-forming reaction:

$$\text{pyroxene} + \text{melt} \rightarrow \text{ol}. \quad (1)$$

This well known melt–rock reaction (e.g. Kelemen, 1990) is generally considered important in the formation of replacive dunite bodies (Boudier & Nicolas, 1972). It implies infiltration of a silica-undersaturated melt.

The textural observation of the dunite–lherzolite–pyroxenite transition indicates the opposite reaction:

$$\text{ol} + \text{melt} \rightarrow \text{pyroxene}. \quad (2)$$

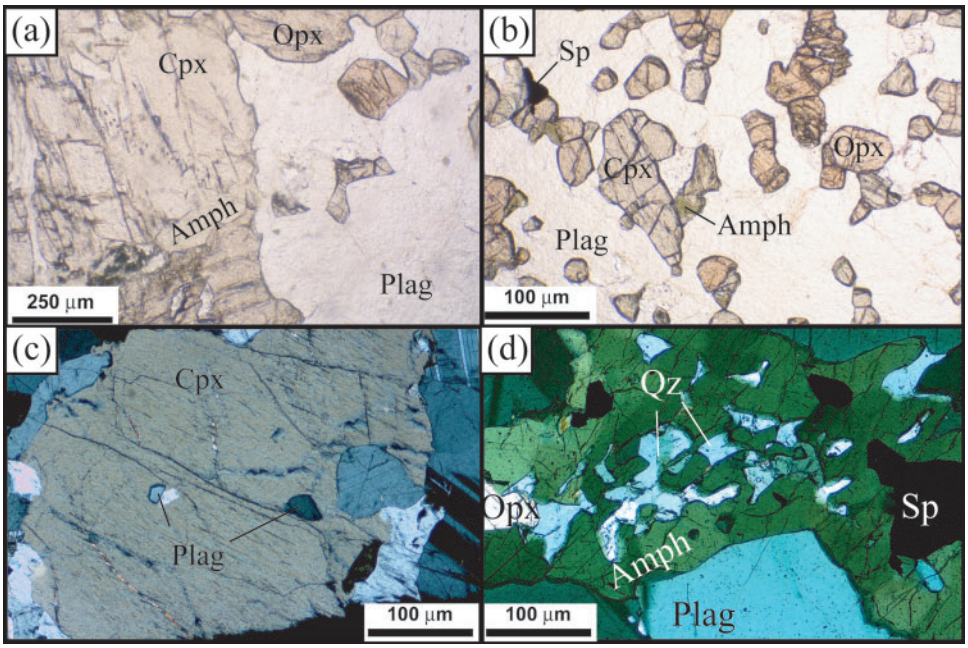


**Fig. 11.** Photomicrograph of textures in the gabbronorite. (a) Contact between ultramafic rocks on the left and gabbronorite on the right. (b) Typical texture of gabbronorite composed of plagioclase (white), orthopyroxene (reddish) and clinopyroxene (greenish). Amphibole (green) rims pyroxene. (c) Plagioclase inclusion in clinopyroxene in primitive ol-bearing gabbronorite. (d) Symplectitic intergrowth between amphibole and quartz in diorite.

Jagoutz *et al.* (2006) concluded from field observations, whole-rock geochemistry and isotope data that the ultramafic bodies are kilometer-scale upper mantle melt conduits emplaced diapirically into the lower crust and feeding the mafic part of the Chilas Complex. According to this interpretation, concentric zoning is secondary and results from re-infiltration of an interstitial liquid within a gabbronoritic crystal mush. The sporadic presence of dunite channels younger than the secondary peridotite implies that both reactions occurred contemporaneously. We present mineral major- and trace-element data to identify the inferred melt–rock reactions and to show that the ultramafic and mafic units stem from a common parental magma. However, different patches evolved at different pressures and through different fractionation mechanisms. This observation supports a diapiric emplacement of the ultramafic rocks.

## ANALYTICAL METHODS

### Electron microprobe analysis

The major element chemistry of the constituent minerals was determined by electron microprobe analysis (EMPA) (Cameca SX 50 and Jeol JXA 8200 Superprobe) at ETH Zurich and at the University of Bern. Operating parameters for the microprobe include an acceleration voltage of 15 kV, beam current of 20 nA and a beam size of 1–10 μm. Measuring times were 60 s for Ni and 20 s for the remaining elements; background counting time was half of the peak counting time. Silicates and oxides were used as standards. Detection limits are typically in the range of 0·02–0·05 wt%.

### LA-ICP–MS trace-element measurements

Whole-rock samples packed in aluminium foil were coarse crushed in a steel vessel and sieved to obtain a 200–500 μm fraction. Ten to 40 optically clear crystals per mineral per sample were hand-picked under an optical binocular and mounted in epoxy. Trace element compositions from eight samples were determined by LA-ICP-MS at ETH Zurich. The ablation system utilizes a 193 nm ArF Excimer laser (Compex 110; Lambda Physik, Göttingen, Germany) with a homogenized beam profile. A quadrupole ELAN 6100 DRC mass spectrometer was used in dual detector mode. LA-ICP-MS analytical conditions were very similar to those reported by Pettke *et al.* (2004). The background was measured for >30 s prior to each analysis and the laser signal was integrated over ~40 s. Data reduction followed the strategy detailed by Longerich *et al.* (1996), using EMPA data ($Al_2O_3$) as an internal standard. For each mineral, 5–15 analyses with a 100–120 μm laser spot size were performed within the grain cores. The uncertainty on the external analytical reproducibility reported as 2σ determined on single grains is typically better than 2% except where concentrations approach the limit of detection. Here, the counting statistics uncertainty of up to a few tens of per cent dominates the

analytical uncertainty. Data are accurate at these uncertainties (Heinrich *et al.*, 2003).

## MINERAL CHEMISTRY

The modal composition and the average mineral major and trace element chemistry is tabulated in Tables 1–10. Additional details are presented as an Electronic Appendix (available for downloading at http://www.petrology.oupjournals.org). A large dataset of individual analyses used to calculate the averaged major element compositions is available from the first author upon request. Minerals are generally homogeneous in major element chemistry but slight core-to-rim zoning is observed in some grains. Strong zoning is present in plagioclase-bearing ultramafic rocks and mafic gabbronorites (see below).

The chemical characteristics of the most important minerals are outlined below.

### Olivine

The Mg-number [Mg-number = Mg/(Fe + Mg)] of olivine varies from 0·78 to 0·90. NiO contents vary between 0·02 and 0·3 (wt %), as observed in other ultramafic complexes (e.g. Cabo Ortegal Spain; Santos *et al.*, 2002).

*Table 1: GPS location and modal composition, determined by grid counting, of analysed samples from the Chilas Complex*

| Sequence | Sample no. | GPS location | | Modal proportion* | | | | | | | | | | Rock type |
|---|---|---|---|---|---|---|---|---|---|---|---|---|---|---|
| | | Longitude (E) | Latitude (N) | ol | cpx | opx | plag | amph | symp† | sp | qz | bio | Accessory | |
| Ol-websterite | C03-43‡ | 74°08′12·4″ | 35°24′42·2″ | 26 | 56 | 6 | – | 11 | – | 1 | – | – | | Ol-websterite |
| Ol-websterite | C03-44‡ | 74°08′12·4″ | 35°24′42·2″ | 17 | 62 | 10 | – | 8 | – | 1 | – | – | | Ol-websterite |
| Ol-websterite | C03-45‡ | 74°08′12·4″ | 35°24′42·2″ | 51 | 36 | 5 | – | 6 | – | 2 | – | – | | Ol-websterite |
| Dunite | C03-50 | 74°08′12·4″ | 35°24′42·2″ | 85·7 | 2·9 | | – | – | – | 11·4 | – | – | chl | Dunite |
| Dunite | C04-16 | 74°08′15·5″ | 35°24′41·4″ | 90·2 | 0·3 | 0·5 | – | – | – | 9·0 | – | – | | Dunite |
| Dunite | C123 | 74°07′10·7″ | 35°26′17·9″ | 90·7 | 0·5 | | – | – | – | 8·8 | – | – | | Dunite |
| Dunite | C213 | 74°08′04·7″ | 35°24′52·0″ | 89·0 | 0·4 | | – | 1·8 | – | 8·8 | – | – | | Dunite |
| Dunite | C212 | 74°08′04·7″ | 35°24′52·0″ | 88·8 | 0·6 | 0·8 | – | – | – | 9·6 | – | – | serp, chl | Dunite |
| Dunite | C03-43d | 74°08′12·4″ | 35°24′42·2″ | 88·4 | 3·2 | – | – | – | – | 8·4 | – | – | chl | Dunite |
| Dunite | C37 | 74°08′49·7″ | 35°24′10·3″ | 88·4 | 4·2 | – | – | 0·3 | – | 7·0 | – | – | chl | Dunite |
| Dunite | C38 | 74°08′49·7″ | 35°24′10·3″ | 88·1 | 0·9 | 6·0 | – | 0·1 | – | 4·6 | – | – | | Dunite |
| Dunite | C174 | 74°08′27·0″ | 35°24′34·4″ | 74·0 | 4·6 | – | – | 0·8 | – | 20·0 | – | – | | Dunite |
| Dunite | C04-17 | 74°08′15·5″ | 35°24′41·4″ | 78·3 | 3·7 | 1·4 | – | 3·2 | – | 13·4 | – | – | chl | Dunite |
| Dunite | C03-46 | 74°08′12·4″ | 35°24′42·2″ | 78·6 | 3·6 | – | – | 5·2 | – | 12·5 | – | – | serp, chl | Dunite |
| Sec. peridotite | C206 | 74°08′34·0″ | 35°21′58·5″ | 79·2 | 4·6 | 4·0 | – | 2·6 | – | 9·7 | – | – | | Dunite |
| Sec. peridotite | T6 | 73°53′50·4″ | 35°29′25·9″ | 72·2 | 2·6 | 19·1 | – | 3·0 | – | 3·1 | – | – | | Harzburgite |
| Sec. peridotite | C35 | E 74°08′49·7″ | N 35°24′10·3″ | 77·0 | 4·4 | 7·6 | – | – | – | 10·8 | – | – | | Dunite |
| Sec. peridotite | C04-15 | 74°08′15·5″ | 35°24′41·4″ | 76·3 | 5·2 | 2·0 | – | 3·2 | – | 5·2 | – | – | | Dunite |
| Sec. peridotite | T4 | 73°53′50·4″ | 35°29′25·9″ | 74·6 | 11·2 | 3·4 | – | 3·1 | – | 7·1 | – | – | chl, serp | Lherzolite |
| Sec. peridotite | C03-47 | 74°08′12·4″ | 35°24′42·2″ | 78·8 | 11·6 | 1·3 | – | 2·9 | – | 5·2 | – | – | | Lherzolite |
| Sec. peridotite | C36 | 74°08′49·7″ | 35°24′10·3″ | 81·8 | 6·5 | 5·4 | – | – | – | 5·9 | – | – | | Dunite |
| Sec. peridotite | C32 | 74°08′49·7″ | 35°24′10·3″ | 87·6 | 5·6 | 0·6 | – | – | – | 6·3 | – | – | | Dunite |
| Sec. peridotite | C34 | 74°08′49·7″ | 35°24′10·3″ | 69·6 | 16·2 | 7·3 | – | – | 0·4 | 6·6 | – | – | | Lherzolite |
| Sec. peridotite | C50.1 | 74°08′49·7″ | 35°24′10·3″ | 58·5 | 15·7 | 15·9 | – | 2·0 | 1·2 | 4·6 | – | – | | Lherzolite |
| Sec. peridotite | C33 | 74°08′49·7″ | 35°24′10·3″ | 69·5 | 9·8 | 9·9 | – | | 1·4 | 7·9 | – | – | chl | Lherzolite |
| Sec. peridotite | C194 | 74°18′53·0″ | 35°24′27·0″ | 27·1 | 46·2 | 12 | 8 | 3 | 2·7 | 0·8 | – | – | | plag-Ol-websterite |
| Sec. peridotite | C218 | 74°08′06·9″ | 35°24′27·9″ | 44·0 | 29·3 | 14·0 | 4·0 | 3·7 | 4·8 | 0·2 | – | – | | plag-Ol-websterite |
| Sec. peridotite | C203 | 74°18′53·0″ | 35°24′27·0″ | 38·3 | 35·2 | 18·2 | 0·8 | | 5·7 | 1·6 | – | – | | plag-Ol-websterite |
| Sec. peridotite | C169 | 74°54′32·0″ | 35°29′19·3″ | 29·6 | 1·8 | 34·6 | 18·6 | 0·7 | 14·4 | 0·1 | – | – | | plag-Ol-websterite |
| Sec. peridotite | C171 | 74°54′32·0″ | 35°29′19·3″ | 55·6 | 1·6 | 13·6 | 1·9 | 9·4 | 16·4 | 0·1 | – | – | | plag-Ol-websterite |
| Sec. peridotite | C201 | 74°18′53·0″ | 35°24′27·0″ | 18·2 | 15·5 | 35·5 | 9·3 | 2·5 | 18·3 | 0·7 | – | – | | plag-Ol-websterite |

(continued)

*Table 1: Continued*

| Sequence | Sample no. | GPS location | | Modal proportion* | | | | | | | | | | Rock type |
|---|---|---|---|---|---|---|---|---|---|---|---|---|---|---|
| | | Longitude (E) | Latitude (N) | ol | cpx | opx | plag | amph | symp† | sp | qz | bio | Accessory | |
| Pyroxenite (sec?) | C04-9 | 73°53′33·5″ | 35°37′40·8″ | – | 20·6 | 69·0 | – | 9·3 | – | 0·9 | – | – | | Pyroxenite |
| Gabbronorite seq. | C50.4 | 74°08′49·7″ | 35°24′10·3″ | Composite contact sample between GNR and sec. peridotite | | | | | | | | | | |
| Gabbronorite seq. | C50.10 | 74°08′49·7″ | 35°24′10·3″ | Composite contact sample between GNR and sec. peridotite | | | | | | | | | | |
| Gabbronorite seq. | C66‡ | 74°07′42·0″ | 35°19′20·9″ | 22 | 3 | 6 | 60 | 4 | 5 | 1 | – | – | | ol-gabbronorite |
| Gabbronorite seq. | T3 | 73°53′50·4″ | 35°29′25·9″ | – | 12·7 | 67·9 | 14·2 | 5·0 | – | 0·2 | – | – | | gabbronorite |
| Gabbronorite seq. | C50.9 | 74°08′49·7″ | 35°24′10·3″ | – | 23·6 | 20·6 | 46·4 | 8·5 | – | 0·1 | – | – | | gabbronorite |
| Gabbronorite seq. | C48 | 74°08′49·7″ | 35°24′10·3″ | – | 6·8 | 27·0 | 60·7 | 5·2 | – | | – | – | | gabbronorite |
| Gabbronorite seq. | C41 | 74°08′49·7″ | 35°24′10·3″ | – | 21·3 | 16·1 | 56·4 | 4·0 | – | 1·4 | 0·3 | – | | gabbronorite |
| Gabbronorite seq. | C7 | 74°08′59·7″ | 35°24′32·3″ | – | 32·6 | 17·5 | 43·7 | 6·4 | – | – | – | – | | gabbronorite |
| Gabbronorite seq. | C50.6 | 74°08′49·7″ | 35°24′10·3″ | – | 8·6 | 38·0 | 49·6 | 8·6 | – | 0·1 | – | – | | gabbronorite |
| Gabbronorite seq. | C50.8 | 74°08′49·7″ | 35°24′10·3″ | – | 42·3 | 11·3 | 37·0 | 8·9 | – | 0·2 | – | – | | gabbronorite |
| Gabbronorite seq. | C50.9 | 74°08′49·7″ | 35°24′10·3″ | – | 48·9 | 16·0 | 28·2 | 6·9 | | 0·2 | – | – | | gabbronorite |
| Gabbronorite seq. | C134 | 73°49′36·1″ | 35°26′00·9″ | – | 18·4 | 5·6 | 62·1 | 6·4 | – | 2·4 | 5·0 | – | | gabbronorite |
| Gabbronorite seq. | C132 | 73°49′33·0″ | 35°23′55·4″ | | 14·7 | 9·1 | 64·0 | 7·9 | | 1·5 | 1·9 | 0·6 | | gabbronorite |
| Gabbronorite seq. | C129 | 73°48′38·1″ | 35°22′27·4″ | – | – | 3·2 | 58·3 | 10·1 | 8·6§ | 0·5 | 12·7 | 6·6 | ap, zr, ill | diorite |
| Gabbronorite seq. | C172 | 73°54′14·2″ | 35°29′21·2″ | | | | 25·7 | 61·7 | | 2·0 | 10·8 | – | | diorite |
| Gabbronorite seq. | C43 | 74°08′49·7″ | 35°24′10·3″ | – | – | – | 28·8 | 55·3 | – | 1·0 | 14·3 | – | zr, ap | diorite |
| Gabbronorite seq. | C138 | 73°49′48·5″ | 35°27′56·7″ | – | 15·3 | 9·7 | 51·8 | 7·5 | – | 4·8 | 10·7 | 0·2 | zr, ap | diorite |
| pyx–plag pegmatite | C219__peg‡ | 73°08′6·9″ | 35°24′27·9″ | – | 40 | – | 50 | 10 | – | – | – | – | | gabbro |
| hbl–plag pegmatite | C46‡ | 74°08′79·9″ | 35°23′10·3″ | – | 55 | – | 34 | – | – | – | 10 | 1 | | diorite |

*Modal compositions have been determined by grid counting (~1000 points).
†Symplectites in ol-bearing rocks are composed of two-pyroxene (± amphibole)–spinel.
‡Modal compositions of very coarse-grained and/or modally heterogeneous samples have been approximated by a combination of grid counting, field observation and, where available, CIPW norm calculation based on whole-rock analyses (Jagoutz *et al.*, 2006).
§Symplectites in evolved rocks are composed of amphibole–quartz.

*Table 2: Major element concentrations (wt %) in olivine from the Chilas Complex*

| Sample: | C03-43 ($n=8$) | | | C03-44 ($n=8$) | | | C03-45 ($n=7$) | | | T4 ($n=7$) | | |
|---|---|---|---|---|---|---|---|---|---|---|---|---|
| | Average | 2σ | 2σ mean | Average | 2σ | 2σ mean | Average | 2σ | 2σ mean | Average | 2σ | 2σ mean |
| $SiO_2$ | 39·42 | 0·52 | 0·20 | 39·54 | 1·33 | 0·50 | 39·59 | 2·14 | 0·87 | 39·70 | 0·77 | 0·32 |
| $TiO_2$ | 0·01 | 0·01 | 0·00 | 0·01 | 0·02 | 0·01 | 0·01 | 0·01 | 0·00 | 0·00 | 0·02 | 0·01 |
| $Cr_2O_3$ | 0·02 | 0·03 | 0·01 | 0·01 | 0·03 | 0·01 | 0·00 | 0·01 | 0·00 | 0·00 | 0·02 | 0·01 |
| $Al_2O_3$ | 0·00 | 0·01 | 0·00 | 0·01 | 0·02 | 0·01 | 0·01 | 0·02 | 0·01 | 0·00 | 0·00 | 0·00 |
| FeO | 17·23 | 0·28 | 0·10 | 17·26 | 0·31 | 0·12 | 14·72 | 0·31 | 0·13 | 15·56 | 1·03 | 0·42 |
| MnO | 0·30 | 0·02 | 0·01 | 0·25 | 0·03 | 0·01 | 0·24 | 0·03 | 0·01 | 0·26 | 0·03 | 0·01 |
| NiO | 0·14 | 0·02 | 0·01 | | 0·00 | | | 0·00 | | 0·20 | 0·04 | 0·02 |
| MgO | 44·97 | 0·29 | 0·11 | 43·00 | 0·86 | 0·32 | 46·10 | 0·89 | 0·36 | 44·13 | 0·70 | 0·28 |
| CaO | 0·01 | 0·02 | 0·01 | 0·02 | 0·01 | 0·01 | 0·01 | 0·02 | 0·01 | 0·01 | 0·02 | 0·01 |
| $Na_2O$ | 0·01 | 0·01 | 0·00 | 0·01 | 0·02 | 0·01 | 0·02 | 0·04 | 0·02 | 0·01 | 0·02 | 0·01 |
| $K_2O$ | 0·00 | 0·01 | 0·00 | 0·00 | 0·01 | 0·00 | 0·00 | 0·02 | 0·01 | 0·00 | 0·01 | 0·00 |

(continued)

*Table 2: Continued*

| Sample: | C03-43 ($n=8$) | | | C03-44 ($n=8$) | | | C03-45 ($n=7$) | | | T4 ($n=7$) | | |
|---|---|---|---|---|---|---|---|---|---|---|---|---|
| | Average | 2σ | 2σ mean | Average | 2σ | 2σ mean | Average | 2σ | 2σ mean | Average | 2σ | 2σ mean |
| Total | 102·11 | | | 100·11 | | | 100·70 | | | 99·88 | | |
| Si | 0·975 | 0·009 | 0·003 | 1·002 | 0·030 | 0·011 | 0·982 | 0·040 | 0·016 | 1·002 | 0·013 | 0·005 |
| Ti | 0·000 | 0·000 | 0·000 | 0·000 | 0·000 | 0·000 | 0·000 | 0·000 | 0·000 | 0·000 | 0·000 | 0·000 |
| Cr | 0·000 | 0·001 | 0·000 | 0·000 | 0·001 | 0·000 | 0·000 | 0·000 | 0·000 | 0·000 | 0·000 | 0·000 |
| Al | 0·000 | 0·000 | 0·000 | 0·000 | 0·001 | 0·000 | 0·000 | 0·000 | 0·000 | 0·000 | 0·000 | 0·000 |
| Fe | 0·356 | 0·005 | 0·002 | 0·366 | 0·006 | 0·002 | 0·306 | 0·009 | 0·004 | 0·328 | 0·020 | 0·008 |
| Mn | 0·006 | 0·000 | 0·000 | 0·005 | 0·001 | 0·000 | 0·005 | 0·001 | 0·000 | 0·006 | 0·001 | 0·000 |
| Ni | 0·003 | 0·000 | 0·000 | | | | | | | 0·004 | 0·001 | 0·000 |
| Mg | 1·658 | 0·009 | 0·004 | 1·625 | 0·032 | 0·012 | 1·705 | 0·039 | 0·016 | 1·660 | 0·029 | 0·012 |
| Ca | 0·000 | 0·000 | 0·000 | 0·000 | 0·000 | 0·000 | 0·000 | 0·000 | 0·000 | 0·000 | 0·000 | 0·000 |
| Na | 0·000 | 0·001 | 0·000 | 0·000 | 0·001 | 0·000 | 0·001 | 0·002 | 0·001 | 0·000 | 0·001 | 0·001 |
| K | 0·000 | 0·000 | 0·000 | 0·000 | 0·000 | 0·000 | 0·000 | 0·000 | 0·000 | 0·000 | 0·000 | 0·000 |
| Mg-no. | 0·823 | 0·003 | 0·001 | 0·816 | 0·005 | 0·002 | 0·848 | 0·005 | 0·002 | 0·835 | 0·011 | 0·004 |

| Sample: | T6 ($n=31$) | | | T3 ($n=9$) | | | C03-50 ($n=10$) | | | C04-16 ($n=12$) | | |
|---|---|---|---|---|---|---|---|---|---|---|---|---|
| | Average | 2σ | 2σ mean | Average | 2σ | 2σ mean | Average | 2σ | 2σ mean | Average | 2σ | 2σ mean |
| $SiO_2$ | 39·37 | 0·41 | 0·07 | 39·79 | 1·03 | 0·37 | 40·07 | 0·46 | 0·15 | 38·90 | 0·84 | 0·25 |
| $TiO_2$ | 0·01 | 0·02 | 0·00 | 0·01 | 0·02 | 0·01 | 0·01 | 0·02 | 0·01 | 0·01 | 0·01 | 0·00 |
| $Cr_2O_3$ | 0·02 | 0·10 | 0·02 | 0·01 | 0·02 | 0·01 | 0·00 | 0·00 | 0·00 | 0·01 | 0·02 | 0·01 |
| $Al_2O_3$ | 0·00 | 0·01 | 0·00 | 0·03 | 0·07 | 0·03 | 0·01 | 0·03 | 0·01 | 0·00 | 0·01 | 0·00 |
| FeO | 17·34 | 1·48 | 0·27 | 16·72 | 0·70 | 0·25 | 16·37 | 0·31 | 0·10 | 18·65 | 0·28 | 0·08 |
| MnO | 0·25 | 0·04 | 0·01 | 0·25 | 0·04 | 0·01 | 0·27 | 0·05 | 0·02 | 0·30 | 0·04 | 0·01 |
| NiO | 0·22 | 0·06 | 0·01 | | 0·00 | | 0·00 | 0·00 | 0·00 | 0·17 | 0·02 | 0·01 |
| MgO | 42·66 | 1·10 | 0·20 | 43·03 | 1·22 | 0·43 | 44·81 | 0·39 | 0·13 | 43·30 | 0·30 | 0·09 |
| CaO | 0·02 | 0·03 | 0·01 | 0·02 | 0·03 | 0·01 | 0·01 | 0·01 | 0·00 | 0·01 | 0·01 | 0·00 |
| $Na_2O$ | 0·01 | 0·03 | 0·01 | 0·03 | 0·06 | 0·02 | 0·00 | 0·01 | 0·00 | 0·01 | 0·03 | 0·01 |
| $K_2O$ | 0·00 | 0·01 | 0·00 | 0·01 | 0·01 | 0·00 | 0·00 | 0·01 | 0·00 | 0·00 | 0·01 | 0·00 |
| Total | 99·90 | | | 99·91 | | | 101·55 | | | 101·34 | | |
| Si | 1·002 | 0·009 | 0·002 | 1·009 | 0·027 | 0·010 | 0·995 | 0·009 | 0·003 | 0·9768 | 0·0129 | 0·0039 |
| Ti | 0·000 | 0·000 | 0·000 | 0·000 | 0·000 | 0·000 | 0·000 | 0·000 | 0·000 | 0·0001 | 0·0003 | 0·0001 |
| Cr | 0·000 | 0·002 | 0·000 | 0·000 | 0·001 | 0·000 | 0·000 | 0·000 | 0·000 | 0·0001 | 0·0003 | 0·0001 |
| Al | 0·000 | 0·000 | 0·000 | 0·001 | 0·001 | 0·001 | 0·000 | 0·001 | 0·000 | 0·0001 | 0·0002 | 0·0001 |
| Fe | 0·369 | 0·031 | 0·006 | 0·355 | 0·014 | 0·005 | 0·340 | 0·005 | 0·002 | 0·3916 | 0·0073 | 0·0022 |
| Mn | 0·005 | 0·001 | 0·000 | 0·005 | 0·001 | 0·000 | 0·006 | 0·001 | 0·000 | 0·0063 | 0·0008 | 0·0002 |
| Ni | 0·004 | 0·001 | 0·000 | | 0·000 | | 0·000 | 0·000 | 0·000 | 0·0033 | 0·0005 | 0·0001 |
| Mg | 1·618 | 0·035 | 0·006 | 1·627 | 0·037 | 0·013 | 1·658 | 0·010 | 0·003 | 1·6208 | 0·0096 | 0·0029 |
| Ca | 0·000 | 0·001 | 0·000 | 0·001 | 0·001 | 0·000 | 0·000 | 0·000 | 0·000 | 0·0003 | 0·0003 | 0·0001 |
| Na | 0·001 | 0·001 | 0·000 | 0·002 | 0·003 | 0·001 | 0·000 | 0·001 | 0·000 | 0·0004 | 0·0012 | 0·0004 |
| K | 0·000 | 0·000 | 0·000 | 0·000 | 0·000 | 0·000 | 0·000 | 0·000 | 0·000 | 0·0001 | 0·0003 | 0·0001 |
| Mg-no. | 0·814 | 0·016 | 0·003 | 0·821 | 0·009 | 0·003 | 0·830 | 0·003 | 0·001 | 0·805 | 0·003 | 0·001 |

(continued)

*Table 2: Continued*

| Sample: | C123 ($n=10$) | | | C213 ($n=10$) | | | C212 ($n=7$) | | | C03-43d ($n=9$) | | |
|---|---|---|---|---|---|---|---|---|---|---|---|---|
| | Average | 2σ | 2σ mean | Average | 2σ | 2σ mean | Average | 2σ | 2σ mean | Average | 2σ | 2σ mean |
| $SiO_2$ | 39·55 | 0·34 | 0·11 | 40·02 | 0·32 | 0·11 | 39·72 | 0·39 | 0·15 | 39·44 | 0·24 | 0·08 |
| $TiO_2$ | 0·01 | 0·02 | 0·01 | 0·01 | 0·02 | 0·01 | 0·01 | 0·02 | 0·01 | 0·01 | 0·02 | 0·01 |
| $Cr_2O_3$ | 0·01 | 0·02 | 0·01 | 0·02 | 0·03 | 0·01 | 0·01 | 0·03 | 0·01 | 0·00 | 0·01 | 0·00 |
| $Al_2O_3$ | 0·01 | 0·03 | 0·01 | 0·00 | 0·02 | 0·01 | 0·00 | 0·02 | 0·01 | 0·00 | 0·01 | 0·00 |
| FeO | 12·38 | 0·26 | 0·09 | 15·36 | 0·44 | 0·15 | 17·98 | 0·24 | 0·09 | 16·15 | 0·41 | 0·15 |
| MnO | 0·21 | 0·03 | 0·01 | 0·26 | 0·03 | 0·01 | 0·28 | 0·05 | 0·02 | 0·27 | 0·05 | 0·02 |
| NiO | 0·00 | 0·00 | 0·00 | 0·17 | 0·03 | 0·01 | 0·18 | 0·01 | 0·00 | 0·19 | 0·04 | 0·02 |
| MgO | 47·91 | 0·57 | 0·19 | 43·91 | 0·53 | 0·18 | 42·96 | 0·44 | 0·17 | 45·67 | 0·47 | 0·16 |
| CaO | 0·01 | 0·01 | 0·00 | 0·01 | 0·02 | 0·01 | 0·01 | 0·01 | 0·00 | 0·01 | 0·01 | 0·00 |
| $Na_2O$ | 0·00 | 0·01 | 0·00 | 0·00 | 0·01 | 0·00 | 0·01 | 0·03 | 0·01 | 0·01 | 0·04 | 0·02 |
| $K_2O$ | 0·00 | 0·01 | 0·00 | 0·00 | 0·01 | 0·00 | 0·01 | 0·02 | 0·01 | 0·00 | 0·01 | 0·00 |
| Total | 100·08 | | | 99·65 | | | 101·06 | | | 101·75 | | |
| Si | 0·9763 | 0·0054 | 0·0018 | 1·0122 | 0·0071 | 0·0024 | 1·0003 | 0·0065 | 0·0025 | 0·974 | 0·006 | 0·002 |
| Ti | 0·0001 | 0·0003 | 0·0001 | 0·0002 | 0·0004 | 0·0001 | 0·0001 | 0·0003 | 0·0001 | 0·000 | 0·000 | 0·000 |
| Cr | 0·0002 | 0·0005 | 0·0002 | 0·0003 | 0·0006 | 0·0002 | 0·0002 | 0·0006 | 0·0002 | 0·000 | 0·000 | 0·000 |
| Al | 0·0003 | 0·0009 | 0·0003 | 0·0001 | 0·0005 | 0·0002 | 0·0001 | 0·0005 | 0·0002 | 0·000 | 0·000 | 0·000 |
| Fe | 0·2555 | 0·0059 | 0·0020 | 0·3247 | 0·0090 | 0·0030 | 0·3786 | 0·0060 | 0·0023 | 0·334 | 0·010 | 0·003 |
| Mn | 0·0043 | 0·0007 | 0·0002 | 0·0032 | 0·0008 | 0·0003 | 0·0036 | 0·0009 | 0·0003 | 0·006 | 0·001 | 0·000 |
| Ni | 0·0000 | 0·0000 | 0·0000 | 0·0034 | 0·0005 | 0·0002 | 0·0037 | | 0·0001 | 0·004 | 0·001 | 0·000 |
| Mg | 1·7628 | 0·0093 | 0·0031 | 1·6553 | 0·0114 | 0·0038 | 1·6123 | 0·0051 | 0·0019 | 1·682 | 0·011 | 0·004 |
| Ca | 0·0002 | 0·0003 | 0·0001 | 0·0003 | 0·0005 | 0·0002 | 0·0002 | 0·0003 | 0·0001 | 0·000 | 0·000 | 0·000 |
| Na | 0·0002 | 0·0005 | 0·0002 | 0·0001 | 0·0005 | 0·0002 | 0·0006 | 0·0016 | 0·0006 | 0·000 | 0·002 | 0·001 |
| K | 0·0001 | 0·0002 | 0·0001 | 0·0001 | 0·0002 | 0·0001 | 0·0002 | 0·0005 | 0·0002 | 0·000 | 0·000 | 0·000 |
| Mg-no. | 0·873 | 0·003 | 0·001 | 0·836 | 0·005 | 0·002 | 0·810 | 0·003 | 0·001 | 0·834 | 0·005 | 0·002 |

| Sample: | C34 ($n=13$) | | | C35 ($n=9$) | | | C36 ($n=25$) | | | C37 ($n=20$) | | |
|---|---|---|---|---|---|---|---|---|---|---|---|---|
| | Average | 2σ | 2σ mean | Average | 2σ | 2σ mean | Average | 2σ | 2σ mean | Average | 2σ | 2σ mean |
| $SiO_2$ | 39·58 | 0·20 | 0·06 | 39·27 | 0·71 | 0·25 | 39·55 | 1·09 | 0·22 | 40·09 | 0·44 | 0·10 |
| $TiO_2$ | 0·01 | 0·03 | 0·01 | 0·00 | 0·01 | 0·00 | 0·01 | 0·04 | 0·01 | 0·01 | 0·02 | 0·00 |
| $Cr_2O_3$ | 0·00 | 0·02 | 0·00 | 0·05 | 0·14 | 0·05 | 0·01 | 0·03 | 0·01 | 0·00 | 0·01 | 0·00 |
| $Al_2O_3$ | 0·00 | 0·01 | 0·00 | 0·01 | 0·02 | 0·01 | 0·01 | 0·02 | 0·00 | 0·01 | 0·04 | 0·01 |
| FeO | 17·02 | 0·59 | 0·17 | 17·39 | 1·20 | 0·42 | 16·65 | 1·23 | 0·25 | 16·23 | 0·78 | 0·18 |
| MnO | 0·26 | 0·06 | 0·02 | 0·27 | 0·04 | 0·01 | 0·25 | 0·04 | 0·01 | 0·24 | 0·04 | 0·01 |
| NiO | 0·12 | 0·05 | 0·01 | 0·12 | 0·06 | 0·02 | 0·12 | 0·05 | 0·01 | 0·13 | 0·06 | 0·01 |
| MgO | 42·98 | 0·52 | 0·15 | 43·24 | 0·78 | 0·28 | 43·49 | 0·84 | 0·17 | 43·73 | 0·65 | 0·15 |
| CaO | 0·00 | 0·01 | 0·00 | 0·02 | 0·04 | 0·01 | 0·01 | 0·02 | 0·00 | 0·01 | 0·02 | 0·00 |
| $Na_2O$ | 0·01 | 0·03 | 0·01 | 0·03 | 0·09 | 0·03 | 0·01 | 0·04 | 0·01 | 0·03 | 0·15 | 0·03 |
| $K_2O$ | 0·00 | 0·01 | 0·00 | 0·02 | 0·03 | 0·01 | 0·01 | 0·03 | 0·01 | 0·01 | 0·03 | 0·01 |
| Total | 100·00 | | | 100·42 | | | 100·11 | | | 100·49 | | |
| Si | 1·003 | 0·004 | 0·001 | 0·992 | 0·024 | 0·009 | 0·998 | 0·030 | 0·006 | 1·007 | 0·009 | 0·002 |
| Ti | 0·000 | 0·001 | 0·000 | 0·000 | 0·000 | 0·000 | 0·000 | 0·001 | 0·000 | 0·000 | 0·000 | 0·000 |
| Cr | 0·000 | 0·000 | 0·000 | 0·000 | 0·000 | 0·000 | 0·000 | 0·000 | 0·000 | 0·000 | 0·001 | 0·000 |

(continued)

*Table 2: Continued*

| Sample: | C34 ($n=13$) | | | C35 ($n=9$) | | | C36 ($n=25$) | | | C37 ($n=20$) | | |
|---|---|---|---|---|---|---|---|---|---|---|---|---|
| | Average | 2σ | 2σ mean | Average | 2σ | 2σ mean | Average | 2σ | 2σ mean | Average | 2σ | 2σ mean |
| Al | 0·000 | 0·000 | 0·000 | 0·001 | 0·004 | 0·001 | 0·000 | 0·001 | 0·000 | 0·000 | 0·000 | 0·000 |
| Fe | 0·361 | 0·013 | 0·004 | 0·367 | 0·023 | 0·008 | 0·351 | 0·026 | 0·005 | 0·341 | 0·015 | 0·004 |
| Mn | 0·006 | 0·001 | 0·000 | 0·006 | 0·001 | 0·000 | 0·005 | 0·001 | 0·000 | 0·005 | 0·001 | 0·000 |
| Ni | 0·002 | 0·001 | 0·000 | 0·002 | 0·001 | 0·000 | 0·002 | | 0·000 | 0·003 | 0·001 | 0·000 |
| Mg | 1·624 | 0·016 | 0·005 | 1·628 | 0·017 | 0·006 | 1·637 | 0·025 | 0·005 | 1·637 | 0·017 | 0·004 |
| Ca | 0·000 | 0·000 | 0·000 | 0·001 | 0·001 | 0·000 | 0·000 | 0·000 | 0·000 | 0·000 | 0·000 | 0·000 |
| Na | 0·001 | 0·001 | 0·000 | 0·002 | 0·004 | 0·002 | 0·001 | 0·002 | 0·000 | 0·002 | 0·007 | 0·002 |
| K | 0·000 | 0·000 | 0·000 | 0·001 | 0·001 | 0·000 | 0·000 | 0·001 | 0·000 | 0·000 | 0·001 | 0·000 |
| Mg-no. | 0·818 | 0·007 | 0·002 | 0·816 | 0·010 | 0·004 | 0·823 | 0·011 | 0·002 | 0·828 | 0·007 | 0·002 |

| Sample: | C03-47 ($n=9$) | | | C03-46 ($n=7$) | | | C32 ($n=9$) | | | C33 ($n=10$) | | |
|---|---|---|---|---|---|---|---|---|---|---|---|---|
| | Average | 2σ | 2σ mean | Average | 2σ | 2σ mean | Average | 2σ | 2σ mean | Average | 2σ | 2σ mean |
| $SiO_2$ | 39·41 | 0·13 | 0·13 | 40·07 | 0·45 | 0·16 | 39·18 | 1·10 | 0·39 | 39·63 | 0·44 | 0·15 |
| $TiO_2$ | 0·01 | 0·01 | 0·01 | 0·00 | 0·02 | 0·01 | 0·01 | 0·03 | 0·01 | 0·01 | 0·02 | 0·01 |
| $Cr_2O_3$ | 0·00 | 0·00 | 0·00 | 0·01 | 0·02 | 0·01 | 0·01 | 0·02 | 0·01 | 0·01 | 0·04 | 0·01 |
| $Al_2O_3$ | 0·00 | 0·01 | 0·01 | 0·00 | 0·01 | 0·00 | 0·14 | 0·17 | 0·06 | 0·11 | 0·12 | 0·04 |
| FeO | 16·41 | 0·37 | 0·37 | 14·83 | 0·39 | 0·14 | 17·12 | 0·61 | 0·22 | 17·10 | 0·39 | 0·13 |
| MnO | 0·30 | 0·05 | 0·05 | 0·24 | 0·04 | 0·01 | 0·26 | 0·04 | 0·02 | 0·26 | 0·03 | 0·01 |
| NiO | 0·15 | 0·02 | 0·02 | 0·15 | 0·03 | 0·01 | 0·11 | 0·10 | 0·04 | 0·15 | 0·08 | 0·03 |
| MgO | 45·41 | 0·45 | 0·45 | 46·77 | 0·37 | 0·13 | 43·55 | 1·11 | 0·39 | 43·85 | 0·99 | 0·33 |
| CaO | 0·02 | 0·03 | 0·03 | 0·01 | 0·01 | 0·00 | 0·01 | 0·02 | 0·01 | 0·01 | 0·02 | 0·01 |
| $Na_2O$ | 0·00 | 0·00 | 0·00 | 0·01 | 0·03 | 0·01 | 0·04 | 0·07 | 0·03 | 0·01 | 0·02 | 0·01 |
| $K_2O$ | 0·00 | 0·01 | 0·01 | 0·01 | 0·01 | 0·00 | 0·03 | 0·04 | 0·01 | 0·00 | 0·01 | 0·00 |
| Total | 101·70 | | | 102·10 | | | 100·45 | | | 101·13 | | |
| Si | 0·9753 | 0·0045 | 0·0045 | 0·9809 | 0·0087 | 0·0031 | 0·9875 | 0·0231 | 0·0082 | 0·9923 | 0·0089 | 0·0030 |
| Ti | 0·0001 | 0·0003 | 0·0003 | 0·0001 | 0·0003 | 0·0001 | 0·0002 | 0·0005 | 0·0002 | 0·0002 | 0·0004 | 0·0001 |
| Cr | 0·0000 | 0·0001 | 0·0001 | 0·0002 | 0·0004 | 0·0001 | 0·0001 | 0·0004 | 0·0001 | 0·0001 | 0·0008 | 0·0003 |
| Al | 0·0001 | 0·0002 | 0·0002 | 0·0001 | 0·0003 | 0·0001 | 0·0040 | 0·0050 | 0·0018 | 0·0034 | 0·0034 | 0·0011 |
| Fe | 0·3396 | 0·0081 | 0·0081 | 0·3035 | 0·0083 | 0·0029 | 0·3608 | 0·0158 | 0·0056 | 0·3581 | 0·0109 | 0·0036 |
| Mn | 0·0062 | 0·0011 | 0·0011 | 0·0050 | 0·0008 | 0·0003 | 0·0055 | 0·0009 | 0·0003 | 0·0055 | 0·0007 | 0·0002 |
| Ni | 0·0030 | 0·0004 | 0·0004 | 0·0029 | 0·0005 | 0·0002 | 0·0023 | 0·0021 | 0·0007 | 0·0030 | 0·0016 | 0·0005 |
| Mg | 1·6751 | 0·0144 | 0·0144 | 1·7063 | 0·0087 | 0·0031 | 1·6362 | 0·0322 | 0·0114 | 1·6365 | 0·0166 | 0·0055 |
| Ca | 0·0005 | 0·0008 | 0·0008 | 0·0003 | 0·0002 | 0·0001 | 0·0002 | 0·0004 | 0·0001 | 0·0003 | 0·0005 | 0·0002 |
| Na | 0·0000 | 0·0000 | 0·0000 | 0·0005 | 0·0015 | 0·0005 | 0·0022 | 0·0036 | 0·0013 | 0·0003 | 0·0008 | 0·0003 |
| K | 0·0001 | 0·0002 | 0·0002 | 0·0002 | 0·0004 | 0·0001 | 0·0009 | 0·0013 | 0·0005 | 0·0002 | 0·0005 | 0·0002 |
| Mg-no. | 0·831 | 0·002 | 0·005 | 0·849 | 0·004 | 0·001 | 0·819 | 0·008 | 0·003 | 0·820 | 0·006 | 0·002 |

(continued)

Significant variations are observed within single grains, even if there is no systematic zoning. The NiO and MnO contents for a given Mg-number are systematically lower than expected for average mantle olivine composition (Takahashi *et al.*, 1987), which suggests a magmatic origin. A compositional gap exists between Mg-number 0·87 and 0·85 (Fig. 12). In Mg-rich olivine the Mg-number is negatively correlated with MnO content

*Table 2: Continued*

| Sample: | C38 ($n=24$) | | | C50.1 ($n=18$) | | | C174 ($n=32$) | | | C206 ($n=16$) | | |
|---|---|---|---|---|---|---|---|---|---|---|---|---|
| | Average | 2σ | 2σ mean | Average | 2σ | 2σ mean | Average | 2σ | 2σ mean | Average | 2σ | 2σ mean |
| $SiO_2$ | 39·05 | 0·83 | 0·17 | 39·33 | 0·76 | 0·18 | 40·76 | 1·14 | 0·20 | 39·61 | 1·20 | 0·31 |
| $TiO_2$ | 0·02 | 0·03 | 0·01 | 0·01 | 0·02 | 0·01 | 0·01 | 0·02 | 0·00 | 0·01 | 0·02 | 0·00 |
| $Cr_2O_3$ | 0·01 | 0·03 | 0·01 | 0·01 | 0·03 | 0·01 | 0·09 | 0·31 | 0·05 | 0·01 | 0·02 | 0·00 |
| $Al_2O_3$ | 0·13 | 0·16 | 0·03 | 0·01 | 0·02 | 0·01 | 0·17 | 0·39 | 0·07 | 0·02 | 0·03 | 0·01 |
| FeO | 17·02 | 1·07 | 0·22 | 18·45 | 0·86 | 0·20 | 9·76 | 2·46 | 0·44 | 14·89 | 0·54 | 0·14 |
| MnO | 0·25 | 0·04 | 0·01 | 0·25 | 0·07 | 0·02 | 0·15 | 0·06 | 0·01 | 0·23 | 0·03 | 0·01 |
| NiO | 0·14 | 0·07 | 0·01 | 0·13 | 0·08 | 0·02 | 0·20 | 0·10 | 0·02 | 0·18 | 0·06 | 0·02 |
| MgO | 43·71 | 0·85 | 0·18 | 41·21 | 2·13 | 0·50 | 49·77 | 2·14 | 0·38 | 45·99 | 0·81 | 0·21 |
| CaO | 0·02 | 0·04 | 0·01 | 0·00 | 0·02 | 0·00 | 0·01 | 0·02 | 0·00 | 0·01 | 0·03 | 0·01 |
| $Na_2O$ | 0·04 | 0·10 | 0·02 | 0·02 | 0·04 | 0·01 | 0·02 | 0·05 | 0·01 | 0·01 | 0·02 | 0·00 |
| $K_2O$ | 0·02 | 0·06 | 0·01 | 0·01 | 0·02 | 0·01 | 0·02 | 0·04 | 0·01 | 0·01 | 0·01 | 0·00 |
| Total | 100·39 | | | 99·43 | | | 100·95 | | | 100·95 | | |
| Si | 0·984 | 0·020 | 0·004 | 1·011 | 0·030 | 0·007 | 0·988 | 0·031 | 0·006 | 0·982 | 0·021 | 0·006 |
| Ti | 0·000 | 0·001 | 0·000 | 0·000 | 0·000 | 0·000 | 0·000 | 0·000 | 0·000 | 0·000 | 0·000 | 0·000 |
| Cr | 0·000 | 0·001 | 0·000 | 0·000 | 0·001 | 0·000 | 0·002 | 0·006 | 0·001 | 0·000 | 0·000 | 0·000 |
| Al | 0·004 | 0·005 | 0·001 | 0·000 | 0·001 | 0·000 | 0·005 | 0·011 | 0·002 | 0·001 | 0·001 | 0·000 |
| Fe | 0·359 | 0·023 | 0·005 | 0·397 | 0·025 | 0·006 | 0·198 | 0·050 | 0·009 | 0·309 | 0·011 | 0·003 |
| Mn | 0·005 | 0·001 | 0·000 | 0·005 | 0·002 | 0·000 | 0·003 | 0·001 | 0·000 | 0·005 | 0·001 | 0·000 |
| Ni | 0·003 | 0·001 | 0·000 | 0·003 | 0·002 | 0·000 | 0·004 | 0·002 | 0·000 | 0·004 | 0·001 | 0·000 |
| Mg | 1·642 | 0·024 | 0·005 | 1·579 | 0·053 | 0·013 | 1·798 | 0·048 | 0·008 | 1·700 | 0·025 | 0·006 |
| Ca | 0·000 | 0·001 | 0·000 | 0·000 | 0·000 | 0·000 | 0·000 | 0·001 | 0·000 | 0·000 | 0·001 | 0·000 |
| Na | 0·002 | 0·005 | 0·001 | 0·001 | 0·002 | 0·001 | 0·001 | 0·002 | 0·000 | 0·000 | 0·001 | 0·000 |
| K | 0·001 | 0·002 | 0·000 | 0·000 | 0·001 | 0·000 | 0·000 | 0·001 | 0·000 | 0·000 | 0·000 | 0·000 |
| Mg-no. | 0·821 | 0·011 | 0·002 | 0·799 | 0·015 | 0·004 | 0·901 | 0·024 | 0·004 | 0·846 | 0·006 | 0·002 |

| Sample: | C04-15 ($n=23$) | | | C04-17 ($n=9$) | | | C194 ($n=3$) | | | C201 ($n=4$) | | |
|---|---|---|---|---|---|---|---|---|---|---|---|---|
| | Average | 2σ | 2σ mean | Average | Stabw | 2σ mean | Average | 2σ | 2σ mean | Average | 2σ | 2σ mean |
| $SiO_2$ | 39·12 | 1·27 | 0·27 | 39·23 | 0·42 | 0·15 | 38·48 | 0·57 | 0·40 | 38·35 | 1·39 | 0·81 |
| $TiO_2$ | 0·01 | 0·02 | 0·00 | 0·00 | 0·01 | 0·00 | 0·00 | 0·00 | 0·00 | 0·01 | 0·03 | 0·02 |
| $Cr_2O_3$ | 0·01 | 0·02 | 0·00 | 0·01 | 0·02 | 0·01 | 0·01 | 0·03 | 0·02 | 0·02 | 0·04 | 0·02 |
| $Al_2O_3$ | 0·01 | 0·04 | 0·01 | 0·00 | 0·01 | 0·00 | 1·15 | 1·29 | 0·92 | 0·02 | 0·04 | 0·02 |
| FeO | 18·96 | 0·36 | 0·08 | 16·25 | 0·24 | 0·08 | 20·89 | 0·27 | 0·19 | 19·28 | 2·04 | 1·18 |
| MnO | 0·26 | 0·14 | 0·03 | 0·28 | 0·04 | 0·02 | 0·30 | 0·01 | 0·01 | 0·26 | 0·03 | 0·01 |
| NiO | 0·15 | 0·05 | 0·01 | 0·20 | 0·04 | 0·01 | 0·13 | 0·04 | 0·03 | 0·18 | 0·10 | 0·06 |
| MgO | 42·08 | 2·47 | 0·53 | 45·06 | 0·30 | 0·11 | 39·94 | 0·38 | 0·27 | 41·05 | 0·22 | 0·13 |
| CaO | 0·01 | 0·02 | 0·00 | 0·01 | 0·01 | 0·00 | 0·02 | 0·02 | 0·02 | 0·01 | 0·02 | 0·01 |
| $Na_2O$ | 0·01 | 0·03 | 0·01 | 0·00 | 0·01 | 0·00 | 0·01 | 0·02 | 0·01 | 0·03 | 0·04 | 0·02 |
| $K_2O$ | 0·01 | 0·01 | 0·00 | 0·00 | 0·01 | 0·00 | 0·00 | 0·01 | 0·01 | 0·01 | 0·02 | 0·01 |
| Total | 101·18 | | | 101·05 | | | 100·94 | | | 99·21 | | |
| Si | 0·9938 | 0·0497 | 0·0106 | 0·9774 | 0·0082 | 0·0029 | 0·9845 | 0·0114 | 0·0080 | 0·9906 | 0·0357 | 0·0206 |
| Ti | 0·0002 | 0·0004 | 0·0001 | 0·0001 | 0·0003 | 0·0001 | 0·0000 | 0·0000 | 0·0000 | 0·0002 | 0·0006 | 0·0003 |
| Cr | 0·0002 | 0·0005 | 0·0001 | 0·0001 | 0·0004 | 0·0001 | 0·0002 | 0·0006 | 0·0005 | 0·0003 | 0·0008 | 0·0004 |

(continued)

*Table 2: Continued*

| Sample: | C04-15 ($n=23$) | | | C04-17 ($n=9$) | | | C194 ($n=3$) | | | C201 ($n=4$) | | |
|---|---|---|---|---|---|---|---|---|---|---|---|---|
| | Average | 2σ | 2σ mean | Average | Stabw | 2σ mean | Average | 2σ | 2σ mean | Average | 2σ | 2σ mean |
| Al | 0·0003 | 0·0012 | 0·0002 | 0·0001 | 0·0003 | 0·0001 | 0·0347 | 0·0387 | 0·0274 | 0·0006 | 0·0014 | 0·0008 |
| Fe | 0·4028 | 0·0144 | 0·0031 | 0·3386 | 0·0053 | 0·0019 | 0·4469 | 0·0060 | 0·0042 | 0·4165 | 0·0439 | 0·0253 |
| Mn | 0·0056 | 0·0028 | 0·0006 | 0·0060 | 0·0009 | 0·0003 | 0·0066 | 0·0002 | 0·0001 | 0·0056 | 0·0005 | 0·0003 |
| Ni | 0·0030 | 0·0009 | 0·0002 | 0·0040 | 0·0007 | 0·0003 | 0·0027 | | 0·0006 | 0·0038 | 0·0023 | 0·0013 |
| Mg | 1·5929 | 0·0614 | 0·0131 | 1·6734 | 0·0103 | 0·0036 | 1·5233 | 0·0317 | 0·0224 | 1·5806 | 0·0095 | 0·0055 |
| Ca | 0·0004 | 0·0006 | 0·0001 | 0·0002 | 0·0003 | 0·0001 | 0·0004 | 0·0007 | 0·0005 | 0·0002 | 0·0004 | 0·0002 |
| Na | 0·0007 | 0·0016 | 0·0004 | 0·0001 | 0·0003 | 0·0001 | 0·0005 | 0·0009 | 0·0007 | 0·0014 | 0·0019 | 0·0011 |
| K | 0·0002 | 0·0003 | 0·0001 | 0·0001 | 0·0002 | 0·0001 | 0·0002 | 0·0004 | 0·0003 | 0·0003 | 0·0004 | 0·0003 |
| Mg-no. | 0·798 | 0·012 | 0·003 | 0·832 | 0·003 | 0·001 | 0·773 | 0·003 | 0·002 | 0·791 | 0·018 | 0·011 |

| Sample: | C218 ($n=32$) | | | C66 ($n=8$) | | | C171 ($n=11$) | | | C203 ($n=11$) | | |
|---|---|---|---|---|---|---|---|---|---|---|---|---|
| | Average | 2σ | 2σ mean | Average | 2σ | 2σ mean | Average | 2σ | 2σ mean | Average | 2σ | 2σ mean |
| $SiO_2$ | 38·62 | 0·51 | 0·09 | 37·85 | 1·19 | 0·42 | 38·51 | 0·78 | 0·25 | 39·37 | 0·81 | 0·26 |
| $TiO_2$ | 0·01 | 0·02 | 0·00 | 0·00 | 0·00 | 0·00 | 0·01 | 0·02 | 0·01 | 0·00 | 0·00 | 0·00 |
| $Cr_2O_3$ | 0·01 | 0·04 | 0·01 | 0·00 | 0·01 | 0·00 | 0·01 | 0·01 | 0·00 | 0·01 | 0·02 | 0·00 |
| $Al_2O_3$ | 0·77 | 1·16 | 0·21 | 0·16 | 0·13 | 0·05 | 0·35 | 0·16 | 0·05 | 0·06 | 0·12 | 0·04 |
| FeO | 19·98 | 0·83 | 0·15 | 20·28 | 0·34 | 0·12 | 16·85 | 0·61 | 0·19 | 19·38 | 0·65 | 0·21 |
| MnO | 0·28 | 0·05 | 0·01 | 0·27 | 0·04 | 0·01 | 0·24 | 0·03 | 0·01 | 0·27 | 0·05 | 0·01 |
| NiO | 0·16 | 0·09 | 0·02 | 0·15 | 0·07 | 0·02 | 0·19 | 0·06 | 0·02 | 0·18 | 0·05 | 0·02 |
| MgO | 41·31 | 1·28 | 0·23 | 42·17 | 0·41 | 0·14 | 43·63 | 0·91 | 0·29 | 41·99 | 0·99 | 0·31 |
| CaO | 0·02 | 0·06 | 0·01 | 0·01 | 0·02 | 0·01 | 0·01 | 0·01 | 0·00 | 0·01 | 0·02 | 0·01 |
| $Na_2O$ | 0·01 | 0·03 | 0·01 | 0·01 | 0·03 | 0·01 | 0·01 | 0·03 | 0·01 | 0·01 | 0·03 | 0·01 |
| $K_2O$ | 0·00 | 0·01 | 0·00 | 0·00 | 0·01 | 0·01 | 0·00 | 0·01 | 0·00 | 0·00 | 0·01 | 0·00 |
| Total | 101·18 | | | 100·90 | | | 99·81 | | | 101·28 | | |
| Si | 0·9798 | 0·0137 | 0·0025 | 0·9602 | 0·0220 | 0·0078 | 0·9753 | 0·0182 | 0·0057 | 0·9953 | 0·0222 | 0·0070 |
| Ti | 0·0001 | 0·0003 | 0·0001 | 0·0000 | 0·0001 | 0·0000 | 0·0001 | 0·0003 | 0·0001 | 0·0000 | 0·0001 | 0·0000 |
| Cr | 0·0003 | 0·0009 | 0·0002 | 0·0000 | 0·0002 | 0·0001 | 0·0001 | 0·0003 | 0·0001 | 0·0002 | 0·0003 | 0·0001 |
| Al | 0·0229 | 0·0347 | 0·0062 | 0·0048 | 0·0038 | 0·0013 | 0·0105 | 0·0047 | 0·0015 | 0·0019 | 0·0035 | 0·0011 |
| Fe | 0·4240 | 0·0180 | 0·0032 | 0·4304 | 0·0059 | 0·0021 | 0·3569 | 0·0138 | 0·0044 | 0·4098 | 0·0140 | 0·0044 |
| Mn | 0·0061 | 0·0011 | 0·0002 | 0·0057 | 0·0008 | 0·0003 | 0·0053 | 0·0006 | 0·0002 | 0·0059 | 0·0010 | 0·0003 |
| Ni | 0·0033 | 0·0018 | 0·0003 | 0·0030 | 0·0014 | 0·0005 | 0·0039 | 0·0012 | 0·0004 | 0·0036 | 0·0010 | 0·0003 |
| Mg | 1·5622 | 0·0422 | 0·0076 | 1·5949 | 0·0207 | 0·0073 | 1·6470 | 0·0262 | 0·0083 | 1·5823 | 0·0254 | 0·0080 |
| Ca | 0·0006 | 0·0014 | 0·0003 | 0·0002 | 0·0004 | 0·0002 | 0·0002 | 0·0004 | 0·0001 | 0·0002 | 0·0004 | 0·0001 |
| Na | 0·0006 | 0·0014 | 0·0003 | 0·0005 | 0·0012 | 0·0004 | 0·0005 | 0·0015 | 0·0005 | 0·0007 | 0·0016 | 0·0005 |
| K | 0·0002 | 0·0004 | 0·0001 | 0·0002 | 0·0004 | 0·0002 | 0·0002 | 0·0004 | 0·0001 | 0·0001 | 0·0004 | 0·0001 |
| Mg-no. | 0·787 | 0·011 | 0·002 | 0·787 | 0·003 | 0·001 | 0·822 | 0·008 | 0·002 | 0·794 | 0·007 | 0·002 |

because of uniform Fe/Mn ratios. For olivine with lower Mg-number values no correlation with MnO exists and MnO concentrations are about two times more variable. CaO is generally low ($\leq$0·02 wt%) and uncorrelated with Mg-number.

## Clinopyroxene

Clinopyroxene is extremely rich in Mg (Mg-number up to 0·95). Ternary end-member composition plots of orthopyroxene and clinopyroxene indicate a moderate Fe enrichment with differentiation (Khan *et al.*, 1989). The $Al_2O_3$

*Table 3: Major element concentrations (wt %) in clinopyroxene from the Chilas Complex*

| Sample: | C03-45 ($n=23$) | | | T3 ($n=21$) | | | T6 ($n=19$) | | | T4 ($n=6$) | | |
|---|---|---|---|---|---|---|---|---|---|---|---|---|
| | Average | 2σ | 2σ mean | Average | 2σ | 2σ mean | Average | 2σ | 2σ mean | Average | 2σ | 2σ mean |
| $SiO_2$ | 52·10 | 1·92 | 0·82 | 51·85 | 1·57 | 0·72 | 52·44 | 0·73 | 0·34 | 52·80 | 2·44 | 2·19 |
| $TiO_2$ | 0·29 | 0·32 | 0·14 | 0·47 | 0·16 | 0·07 | 0·33 | 0·08 | 0·04 | 0·26 | 0·29 | 0·26 |
| $Cr_2O_3$ | 0·42 | 0·33 | 0·14 | 0·33 | 0·09 | 0·04 | 0·28 | 0·15 | 0·07 | 0·25 | 0·32 | 0·29 |
| $Al_2O_3$ | 2·77 | 2·82 | 1·20 | 2·75 | 0·66 | 0·30 | 2·68 | 0·44 | 0·21 | 2·15 | 2·50 | 2·24 |
| $Fe_2O_3$ | 2·07 | 3·11 | 1·33 | 3·31 | 1·88 | 0·86 | 1·99 | 1·08 | 0·51 | 2·40 | 1·18 | 1·06 |
| FeO | 1·62 | 4·21 | 1·79 | 1·62 | 1·96 | 0·90 | 2·28 | 1·03 | 0·48 | 1·26 | 0·71 | 0·63 |
| MnO | 0·10 | 0·05 | 0·02 | 0·13 | 0·05 | 0·02 | 0·13 | 0·03 | 0·01 | 0·12 | 0·04 | 0·04 |
| NiO | 0·03 | 0·04 | 0·02 | | | | 0·03 | 0·04 | 0·02 | 0·04 | 0·03 | 0·03 |
| MgO | 15·94 | 2·49 | 1·06 | 15·49 | 0·63 | 0·29 | 16·08 | 0·40 | 0·19 | 16·42 | 1·37 | 1·23 |
| CaO | 24·90 | 2·19 | 0·93 | 24·59 | 1·06 | 0·49 | 24·09 | 0·77 | 0·36 | 25·00 | 0·84 | 0·75 |
| $Na_2O$ | 0·12 | 0·14 | 0·06 | 0·34 | 0·11 | 0·05 | 0·22 | 0·07 | 0·03 | 0·14 | 0·16 | 0·15 |
| $K_2O$ | 0·00 | 0·01 | 0·01 | 0·00 | 0·01 | 0·01 | 0·01 | 0·01 | 0·01 | 0·00 | 0·00 | 0·00 |
| Total | 100·35 | | | 100·88 | | | 100·54 | | | 100·84 | | |
| Si | 1·9015 | 0·0435 | 0·0185 | 1·8895 | 0·0326 | 0·0150 | 1·9103 | 0·0202 | 0·0095 | 1·9154 | 0·0763 | 0·0682 |
| Ti | 0·0081 | 0·0089 | 0·0038 | 0·0129 | 0·0044 | 0·0020 | 0·0090 | 0·0023 | 0·0011 | 0·0072 | 0·0080 | 0·0072 |
| Cr | 0·0121 | 0·0096 | 0·0041 | 0·0095 | 0·0027 | 0·0012 | 0·0079 | 0·0044 | 0·0021 | 0·0072 | 0·0092 | 0·0082 |
| Al | 0·1199 | 0·1237 | 0·0527 | 0·1181 | 0·0279 | 0·0128 | 0·1148 | 0·0189 | 0·0089 | 0·0922 | 0·1073 | 0·0960 |
| $Fe^{3+}$ | 0·1031 | 0·0584 | 0·0249 | 0·0910 | 0·0530 | 0·0243 | 0·0545 | 0·0295 | 0·0139 | 0·0657 | 0·0326 | 0·0291 |
| $Fe^{2+}$ | 0·0043 | 0·0159 | 0·0068 | 0·0492 | 0·0595 | 0·0273 | 0·0694 | 0·0316 | 0·0149 | 0·0381 | 0·0213 | 0·0190 |
| Mn | 0·0024 | 0·0025 | 0·0010 | 0·0039 | 0·0015 | 0·0007 | 0·0039 | 0·0009 | 0·0004 | 0·0036 | 0·0013 | 0·0011 |
| Ni | 0·7863 | 0·0430 | 0·0184 | | | 0·0000 | 0·0009 | 0·0012 | 0·0006 | 0·0012 | 0·0009 | 0·0008 |
| Mg | 0·9141 | 0·0385 | 0·0164 | 0·8413 | 0·0365 | 0·0167 | 0·8732 | 0·0190 | 0·0090 | 0·8878 | 0·0695 | 0·0621 |
| Ca | 0·6685 | 0·9393 | 0·4005 | 0·9602 | 0·0428 | 0·0197 | 0·9402 | 0·0235 | 0·0111 | 0·9719 | 0·0283 | 0·0253 |
| Na | 0·0039 | 0·0072 | 0·0031 | 0·0243 | 0·0081 | 0·0037 | 0·0155 | 0·0047 | 0·0022 | 0·0100 | 0·0118 | 0·0106 |
| K | 0·0002 | 0·0006 | 0·0002 | 0·0002 | 0·0005 | 0·0002 | 0·0003 | 0·0005 | 0·0002 | 0·0001 | 0·0002 | 0·0001 |
| Mg-no. | 0·896 | 0·044 | 0·019 | 0·857 | 0·020 | 0·009 | 0·876 | 0·014 | 0·006 | 0·895 | 0·041 | 0·037 |
| Fs | 0·002 | 0·008 | 0·003 | 0·025 | 0·030 | 0·014 | 0·035 | 0·016 | 0·007 | 0·019 | 0·011 | 0·010 |
| Wo | 0·307 | 0·442 | 0·188 | 0·433 | 0·024 | 0·011 | 0·430 | 0·012 | 0·006 | 0·449 | 0·054 | 0·048 |
| En | 0·588 | 0·388 | 0·165 | 0·421 | 0·018 | 0·008 | 0·437 | 0·009 | 0·004 | 0·445 | 0·035 | 0·031 |

| Sample: | C03-43 ($n=8$) | | | C03-44 ($n=22$) | | | C174 ($n=28$) | | | C34 ($n=5$) | | |
|---|---|---|---|---|---|---|---|---|---|---|---|---|
| | Average | 2σ | 2σ mean | Average | 2σ | 2σ mean | Average | 2σ | 2σ mean | Average | 2σ | 2σ mean |
| $SiO_2$ | 51·29 | 1·38 | 1·04 | 52·32 | 1·47 | 0·64 | 51·78 | 2·85 | 1·08 | 52·25 | 1·00 | 1·00 |
| $TiO_2$ | 0·28 | 0·05 | 0·03 | 0·24 | 0·08 | 0·03 | 0·25 | 0·14 | 0·05 | 0·26 | 0·21 | 0·21 |
| $Cr_2O_3$ | 0·43 | 0·11 | 0·08 | 0·33 | 0·16 | 0·07 | 0·50 | 0·35 | 0·13 | 0·22 | 0·25 | 0·25 |
| $Al_2O_3$ | 2·59 | 0·65 | 0·49 | 2·69 | 0·79 | 0·35 | 1·92 | 1·16 | 0·44 | 2·79 | 0·80 | 0·80 |
| $Fe_2O_3$ | 3·91 | 0·32 | 0·24 | 2·33 | 3·26 | 1·42 | 2·27 | 1·85 | 0·70 | 0·07 | 0·26 | 0·26 |
| FeO | 0·00 | 0·00 | 0·00 | 1·73 | 3·21 | 1·40 | 0·38 | 1·42 | 0·54 | 3·65 | 0·38 | 0·38 |
| MnO | 0·12 | 0·03 | 0·02 | 0·12 | 0·04 | 0·02 | 0·09 | 0·04 | 0·01 | 0·11 | 0·04 | 0·04 |
| NiO | | | | | | | 0·02 | 0·06 | 0·02 | 0·03 | 0·03 | 0·03 |
| MgO | 16·29 | 0·63 | 0·48 | 15·39 | 1·94 | 0·85 | 17·14 | 0·82 | 0·31 | 15·63 | 0·64 | 0·64 |

(continued)

*Table 3: Continued*

| Sample: | C03-43 ($n=8$) | | | C03-44 ($n=22$) | | | C174 ($n=28$) | | | C34 ($n=5$) | | |
|---|---|---|---|---|---|---|---|---|---|---|---|---|
| | Average | 2σ | 2σ mean | Average | 2σ | 2σ mean | Average | 2σ | 2σ mean | Average | 2σ | 2σ mean |
| CaO | 25·76 | 0·85 | 0·64 | 25·43 | 1·02 | 0·44 | 24·92 | 0·71 | 0·27 | 23·72 | 1·18 | 1·18 |
| $Na_2O$ | 0·16 | 0·08 | 0·06 | 0·12 | 0·10 | 0·04 | 0·09 | 0·08 | 0·03 | 0·07 | 0·02 | 0·02 |
| $K_2O$ | 0·00 | 0·01 | 0·01 | 0·00 | 0·01 | 0·01 | 0·00 | 0·01 | 0·01 | 0·01 | 0·03 | 0·03 |
| Total | 100·98 | | | 100·70 | | | 99·35 | | | 98·80 | | |
| Si | 1·8600 | 0·0326 | 0·0247 | 1·9086 | 0·0689 | 0·0301 | 1·8972 | 0·0799 | 0·0302 | 1·9341 | 0·0296 | 0·0296 |
| Ti | 0·0100 | 0·0011 | 0·0008 | 0·0067 | 0·0021 | 0·0009 | 0·0068 | 0·0039 | 0·0015 | 0·0074 | 0·0059 | 0·0059 |
| Cr | 0·0100 | 0·0032 | 0·0024 | 0·0095 | 0·0045 | 0·0020 | 0·0144 | 0·0103 | 0·0039 | 0·0064 | 0·0073 | 0·0073 |
| Al | 0·1200 | 0·0246 | 0·0186 | 0·1157 | 0·0341 | 0·0149 | 0·0832 | 0·0507 | 0·0191 | 0·1219 | 0·0357 | 0·0357 |
| $Fe^{3+}$ | 0·1100 | 0·0077 | 0·0059 | 0·0637 | 0·0892 | 0·0390 | 0·0625 | 0·0512 | 0·0194 | 0·0020 | 0·0071 | 0·0071 |
| $Fe^{2+}$ | 0·0000 | 0·0000 | 0·0000 | 0·0530 | 0·0990 | 0·0432 | 0·0116 | 0·0434 | 0·0164 | 0·1129 | 0·0126 | 0·0126 |
| Mn | 0·0000 | 0·0010 | 0·0008 | 0·0036 | 0·0013 | 0·0006 | 0·0028 | 0·0012 | 0·0005 | 0·0035 | 0·0013 | 0·0013 |
| Ni | | | | | | | 0·0007 | 0·0016 | 0·0006 | 0·0008 | 0·0010 | 0·0010 |
| Mg | 0·8800 | 0·0416 | 0·0315 | 0·8364 | 0·0931 | 0·0406 | 0·9361 | 0·0434 | 0·0164 | 0·8622 | 0·0329 | 0·0329 |
| Ca | 1·0000 | 0·0239 | 0·0181 | 0·9939 | 0·0407 | 0·0177 | 0·9783 | 0·0293 | 0·0111 | 0·9405 | 0·0403 | 0·0403 |
| Na | 0·0100 | 0·0054 | 0·0041 | 0·0088 | 0·0071 | 0·0031 | 0·0061 | 0·0055 | 0·0021 | 0·0047 | 0·0015 | 0·0015 |
| K | 0·0000 | 0·0005 | 0·0004 | 0·0003 | 0·0005 | 0·0002 | 0·0002 | 0·0006 | 0·0002 | 0·0005 | 0·0014 | 0·0014 |
| Mg-no. | 0·890 | 0·011 | 0·009 | 0·877 | 0·024 | 0·011 | 0·927 | 0·016 | 0·006 | 0·882 | 0·011 | 0·011 |
| Fs | 0·000 | 0·000 | 0·000 | 0·026 | 0·050 | 0·022 | 0·006 | 0·022 | 0·008 | 0·056 | 0·006 | 0·006 |
| Wo | 0·450 | 0·018 | 0·014 | 0·454 | 0·032 | 0·014 | 0·453 | 0·030 | 0·011 | 0·439 | 0·023 | 0·023 |
| En | 0·440 | 0·021 | 0·016 | 0·418 | 0·047 | 0·020 | 0·468 | 0·022 | 0·008 | 0·432 | 0·016 | 0·016 |

| Sample: | C169 ($n=3$) | | | C50.4 ($n=5$) | | | C50.10 ($n=19$) | | | C50.9 ($n=4$) | | |
|---|---|---|---|---|---|---|---|---|---|---|---|---|
| | Average | 2σ | 2σ mean | Average | 2σ | 2σ mean | Average | 2σ | 2σ mean | Average | 2σ | 2σ mean |
| $SiO_2$ | 50·57 | 0·96 | | 50·45 | 0·99 | 0·99 | 51·96 | 1·24 | 0·59 | 50·63 | 0·33 | 0·38 |
| $TiO_2$ | 0·37 | 0·09 | | 0·50 | 0·08 | 0·08 | 0·43 | 0·26 | 0·12 | 0·51 | 0·11 | 0·12 |
| $Cr_2O_3$ | 0·47 | 0·18 | | 0·22 | 0·11 | 0·11 | 0·24 | 0·10 | 0·05 | 0·23 | 0·06 | 0·07 |
| $Al_2O_3$ | 3·89 | 0·68 | | 3·41 | 0·30 | 0·30 | 3·22 | 1·19 | 0·56 | 3·20 | 0·24 | 0·27 |
| $Fe_2O_3$ | 3·01 | 0·87 | | 3·57 | 1·79 | 1·79 | 1·05 | 0·99 | 0·46 | 3·62 | 1·20 | 1·38 |
| FeO | 1·88 | 1·50 | | 3·00 | 1·27 | 1·27 | 4·73 | 0·70 | 0·33 | 2·67 | 1·12 | 1·29 |
| MnO | 0·14 | 0·04 | | 0·19 | 0·07 | 0·07 | 0·14 | 0·03 | 0·02 | 0·17 | 0·05 | 0·06 |
| NiO | 0·01 | 0·03 | | 0·03 | 0·05 | 0·05 | 0·02 | 0·04 | 0·02 | 0·02 | 0·04 | 0·05 |
| MgO | 15·02 | 0·34 | | 14·92 | 0·67 | 0·67 | 14·81 | 0·62 | 0·29 | 14·92 | 0·40 | 0·46 |
| CaO | 23·14 | 0·41 | | 22·87 | 0·43 | 0·43 | 23·14 | 0·98 | 0·46 | 23·17 | 0·42 | 0·49 |
| $Na_2O$ | 0·50 | 0·08 | | 0·36 | 0·11 | 0·11 | 0·34 | 0·18 | 0·08 | 0·39 | 0·08 | 0·09 |
| $K_2O$ | 0·00 | 0·00 | | 0·01 | 0·02 | 0·02 | 0·01 | 0·02 | 0·01 | 0·02 | 0·01 | 0·01 |
| Total | 99·03 | | | 99·51 | | | 100·09 | | | 99·55 | | |
| Si | 1·8739 | 0·0041 | | 1·8716 | 0·0319 | 0·0319 | 1·9121 | 0·0399 | 0·0188 | 1·8766 | 0·0223 | 0·0258 |
| Ti | 0·0105 | 0·0026 | | 0·0139 | 0·0023 | 0·0023 | 0·0120 | 0·0072 | 0·0034 | 0·0142 | 0·0030 | 0·0034 |
| Cr | 0·1700 | 0·0275 | | 0·0065 | 0·0031 | 0·0031 | 0·0070 | 0·0030 | 0·0014 | 0·0068 | 0·0016 | 0·0019 |
| Al | 0·0138 | 0·0056 | | 0·1489 | 0·0128 | 0·0128 | 0·1395 | 0·0516 | 0·0243 | 0·1398 | 0·0100 | 0·0116 |
| $Fe^{3+}$ | 0·0841 | 0·0257 | | 0·0995 | 0·0502 | 0·0502 | 0·0291 | 0·0272 | 0·0128 | 0·1009 | 0·0327 | 0·0378 |
| $Fe^{2+}$ | 0·0581 | 0·0452 | | 0·0930 | 0·0397 | 0·0397 | 0·1455 | 0·0222 | 0·0104 | 0·0827 | 0·0352 | 0·0406 |

(continued)

*Table 3: Continued*

| Sample: | C169 ($n=3$) | | | C50.4 ($n=5$) | | | C50.10 ($n=19$) | | | C50.9 ($n=4$) | | |
|---|---|---|---|---|---|---|---|---|---|---|---|---|
| | Average | 2σ | 2σ mean | Average | 2σ | 2σ mean | Average | 2σ | 2σ mean | Average | 2σ | 2σ mean |
| Mn | 0·0044 | 0·0013 | | 0·0061 | 0·0023 | 0·0023 | 0·0044 | 0·0010 | 0·0005 | 0·0054 | 0·0018 | 0·0021 |
| Ni | 0·0003 | 0·0010 | | 0·0008 | 0·0016 | 0·0016 | 0·0007 | 0·0012 | 0·0006 | 0·0005 | 0·0012 | 0·0013 |
| Mg | 0·8297 | 0·0140 | | 0·8248 | 0·0303 | 0·0303 | 0·8124 | 0·0252 | 0·0119 | 0·8243 | 0·0185 | 0·0214 |
| Ca | 0·9188 | 0·0332 | | 0·9087 | 0·0178 | 0·0178 | 0·9124 | 0·0427 | 0·0201 | 0·9200 | 0·0145 | 0·0168 |
| Na | 0·0364 | 0·0060 | | 0·0255 | 0·0081 | 0·0081 | 0·0242 | 0·0124 | 0·0058 | 0·0283 | 0·0056 | 0·0064 |
| K | 0·0001 | 0·0002 | | 0·0005 | 0·0008 | 0·0008 | 0·0005 | 0·0009 | 0·0004 | 0·0007 | 0·0003 | 0·0003 |
| Mg-no. | 0·854 | 0·023 | | 0·811 | 0·014 | 0·014 | 0·823 | 0·016 | 0·008 | 0·818 | 0·010 | 0·011 |
| Fs | 0·029 | 0·023 | | 0·047 | 0·020 | 0·020 | 0·073 | 0·011 | 0·005 | 0·041 | 0·018 | 0·020 |
| Wo | 0·456 | 0·016 | | 0·397 | 0·022 | 0·022 | 0·419 | 0·034 | 0·016 | 0·405 | 0·009 | 0·010 |
| En | 0·415 | 0·007 | | 0·413 | 0·015 | 0·015 | 0·407 | 0·012 | 0·006 | 0·412 | 0·009 | 0·010 |

| Sample: | C129 ($n=5$) | | | C132 ($n=21$) | | | C138 ($n=8$) | | | C203 ($n=10$) | | |
|---|---|---|---|---|---|---|---|---|---|---|---|---|
| | Average | 2σ | 2σ mean | Average | 2σ | 2σ mean | Average | 2σ | 2σ mean | Average | 2σ | 2σ mean |
| $SiO_2$ | 51·94 | 0·76 | 0·76 | 51·51 | 1·17 | 0·52 | 51·30 | 0·84 | 0·60 | 50·36 | 2·93 | 1·95 |
| $TiO_2$ | 0·21 | 0·04 | 0·04 | 0·26 | 0·13 | 0·06 | 0·20 | 0·05 | 0·04 | 0·34 | 0·37 | 0·25 |
| $Cr_2O_3$ | 0·03 | 0·05 | 0·05 | 0·03 | 0·05 | 0·02 | 0·01 | 0·03 | 0·02 | 0·48 | 0·72 | 0·48 |
| $Al_2O_3$ | 2·26 | 0·48 | 0·48 | 2·52 | 0·48 | 0·21 | 2·29 | 0·20 | 0·14 | 4·68 | 2·29 | 1·53 |
| $Fe_2O_3$ | 1·06 | 1·40 | 1·40 | 1·21 | 1·77 | 0·79 | 1·61 | 1·01 | 0·72 | 3·49 | 3·51 | 2·34 |
| FeO | 7·82 | 1·92 | 1·92 | 7·53 | 2·14 | 0·96 | 8·24 | 1·13 | 0·80 | 2·12 | 2·40 | 1·60 |
| MnO | 0·25 | 0·10 | 0·10 | 0·24 | 0·12 | 0·05 | 0·29 | 0·09 | 0·07 | 0·14 | 0·05 | 0·03 |
| NiO | 0·01 | 0·04 | 0·04 | 0·00 | 0·02 | 0·01 | 0·00 | 0·00 | 0·00 | 0·02 | 0·04 | 0·03 |
| MgO | 13·42 | 0·91 | 0·91 | 13·01 | 0·99 | 0·44 | 12·52 | 0·37 | 0·26 | 14·95 | 1·11 | 0·74 |
| CaO | 22·06 | 1·56 | 1·56 | 22·33 | 0·71 | 0·32 | 22·19 | 0·64 | 0·45 | 23·34 | 1·21 | 0·80 |
| $Na_2O$ | 0·42 | 0·10 | 0·10 | 0·48 | 0·03 | 0·02 | 0·48 | 0·04 | 0·03 | 0·39 | 0·14 | 0·09 |
| $K_2O$ | 0·01 | 0·03 | 0·03 | 0·02 | 0·02 | 0·01 | 0·02 | 0·02 | 0·01 | 0·00 | 0·01 | 0·01 |
| Total | 99·50 | | | 99·14 | | | 98·97 | | 0·00 | 100·30 | | |
| Si | 1·9496 | 0·0116 | 0·0116 | 1·9420 | 0·0187 | 0·0083 | 1·9455 | 0·0105 | 0·0074 | 1·8468 | 0·1020 | 0·0680 |
| Ti | 0·0058 | 0·0012 | 0·0012 | 0·0073 | 0·0037 | 0·0017 | 0·0057 | 0·0015 | 0·0011 | 0·0095 | 0·0102 | 0·0068 |
| Cr | 0·0009 | 0·0014 | 0·0014 | 0·0009 | 0·0016 | 0·0007 | 0·0002 | 0·0008 | 0·0005 | 0·0140 | 0·0209 | 0·0139 |
| Al | 0·0998 | 0·0214 | 0·0214 | 0·1121 | 0·0203 | 0·0091 | 0·1023 | 0·0092 | 0·0065 | 0·2023 | 0·0998 | 0·0665 |
| $Fe^{3+}$ | 0·0301 | 0·0395 | 0·0395 | 0·0493 | 0·1250 | 0·0559 | 0·0458 | 0·0292 | 0·0206 | 0·0963 | 0·0972 | 0·0648 |
| $Fe^{2+}$ | 0·2456 | 0·0613 | 0·0613 | 0·2228 | 0·1221 | 0·0546 | 0·2612 | 0·0349 | 0·0247 | 0·0649 | 0·0738 | 0·0492 |
| Mn | 0·0080 | 0·0033 | 0·0033 | 0·0078 | 0·0038 | 0·0017 | 0·0094 | 0·0031 | 0·0022 | 0·0044 | 0·0014 | 0·0009 |
| Ni | 0·0003 | 0·0011 | 0·0011 | 0·0001 | 0·0005 | 0·0002 | 0·0000 | 0·0000 | 0·0000 | 0·0005 | 0·0012 | 0·0008 |
| Mg | 0·7512 | 0·0505 | 0·0505 | 0·7309 | 0·0491 | 0·0219 | 0·7078 | 0·0166 | 0·0118 | 0·8169 | 0·0595 | 0·0397 |
| Ca | 0·8872 | 0·0553 | 0·0553 | 0·9020 | 0·0264 | 0·0118 | 0·9018 | 0·0258 | 0·0182 | 0·9169 | 0·0428 | 0·0285 |
| Na | 0·0307 | 0·0076 | 0·0076 | 0·0348 | 0·0025 | 0·0011 | 0·0351 | 0·0033 | 0·0023 | 0·0274 | 0·0097 | 0·0065 |
| K | 0·0004 | 0·0014 | 0·0014 | 0·0010 | 0·0010 | 0·0005 | 0·0008 | 0·0007 | 0·0005 | 0·0002 | 0·0005 | 0·0004 |
| Mg-no. | 0·732 | 0·045 | 0·045 | 0·729 | 0·059 | 0·026 | 0·698 | 0·017 | 0·012 | 0·835 | 0·031 | 0·021 |
| Fs | 0·123 | 0·031 | 0·031 | 0·111 | 0·061 | 0·027 | 0·131 | 0·017 | 0·012 | 0·032 | 0·037 | 0·025 |
| Wo | 0·419 | 0·033 | 0·033 | 0·424 | 0·012 | 0·005 | 0·424 | 0·014 | 0·010 | 0·388 | 0·061 | 0·041 |
| En | 0·376 | 0·025 | 0·025 | 0·365 | 0·025 | 0·011 | 0·354 | 0·008 | 0·006 | 0·409 | 0·030 | 0·020 |

(continued)

*Table 3: Continued*

| Sample: | C206 ($n=5$) | | | C35 ($n=10$) | | | C03-17 ($n=11$) | | | C03-15 ($n=10$) | | |
|---|---|---|---|---|---|---|---|---|---|---|---|---|
| | Average | 2σ | 2σ mean | Average | 2σ | 2σ mean | Average | 2σ | 2σ mean | Average | 2σ | 2σ mean |
| $SiO_2$ | 52·34 | 1·07 | 1·07 | 51·83 | 0·91 | 0·61 | 52·12 | 0·85 | 0·54 | 51·66 | 0·99 | 0·66 |
| $TiO_2$ | 0·17 | 0·11 | 0·11 | 0·31 | 0·14 | 0·09 | 0·27 | 0·15 | 0·09 | 0·33 | 0·14 | 0·10 |
| $Cr_2O_3$ | 0·28 | 0·34 | 0·34 | 0·39 | 0·19 | 0·13 | 0·34 | 0·28 | 0·18 | 0·31 | 0·25 | 0·17 |
| $Al_2O_3$ | 1·79 | 1·45 | 1·45 | 3·26 | 0·74 | 0·49 | 2·40 | 0·86 | 0·54 | 2·81 | 1·18 | 0·78 |
| $Fe_2O_3$ | 3·08 | 0·71 | 0·71 | 2·20 | 2·87 | 1·91 | 2·87 | 0·64 | 0·41 | 3·03 | 0·88 | 0·58 |
| FeO | 0·21 | 0·69 | 0·69 | 1·86 | 2·38 | 1·59 | 0·94 | 0·69 | 0·44 | 1·40 | 0·99 | 0·66 |
| MnO | 0·09 | 0·02 | 0·02 | 0·11 | 0·05 | 0·03 | 0·14 | 0·05 | 0·03 | 0·14 | 0·06 | 0·04 |
| NiO | 0·02 | 0·03 | 0·03 | 0·02 | 0·04 | 0·03 | 0·02 | 0·03 | 0·02 | 0·01 | 0·02 | 0·01 |
| MgO | 17·27 | 0·56 | 0·56 | 15·95 | 0·68 | 0·45 | 16·62 | 0·56 | 0·35 | 16·41 | 1·08 | 0·72 |
| CaO | 24·89 | 1·18 | 1·18 | 24·32 | 0·80 | 0·53 | 24·60 | 0·51 | 0·32 | 24·09 | 1·51 | 1·00 |
| $Na_2O$ | 0·06 | 0·09 | 0·09 | 0·15 | 0·08 | 0·05 | 0·07 | 0·05 | 0·03 | 0·09 | 0·05 | 0·03 |
| $K_2O$ | 0·00 | 0·00 | 0·00 | 0·01 | 0·02 | 0·01 | 0·00 | 0·00 | 0·00 | 0·00 | 0·01 | 0·01 |
| Total | 100·20 | | | 100·40 | | | 100·39 | | | 100·29 | | |
| Si | 1·9046 | 0·0409 | 0·0409 | 1·8912 | 0·0464 | 0·0309 | 1·8992 | 0·0261 | 0·0165 | 1·8874 | 0·0310 | 0·0207 |
| Ti | 0·0048 | 0·0029 | 0·0029 | 0·0084 | 0·0037 | 0·0025 | 0·0073 | 0·0040 | 0·0025 | 0·0091 | 0·0039 | 0·0026 |
| Cr | 0·0080 | 0·0098 | 0·0098 | 0·0114 | 0·0057 | 0·0038 | 0·0099 | 0·0081 | 0·0052 | 0·0089 | 0·0072 | 0·0048 |
| Al | 0·0769 | 0·0618 | 0·0618 | 0·1402 | 0·0316 | 0·0211 | 0·1032 | 0·0369 | 0·0233 | 0·1208 | 0·0508 | 0·0339 |
| $Fe^{3+}$ | 0·0843 | 0·0197 | 0·0197 | 0·0757 | 0·0691 | 0·0461 | 0·0788 | 0·0177 | 0·0112 | 0·0834 | 0·0244 | 0·0162 |
| $Fe^{2+}$ | 0·0064 | 0·0207 | 0·0207 | 0·0415 | 0·0640 | 0·0427 | 0·0287 | 0·0210 | 0·0133 | 0·0429 | 0·0301 | 0·0200 |
| Mn | 0·0030 | 0·0005 | 0·0005 | 0·0035 | 0·0015 | 0·0010 | 0·0044 | 0·0014 | 0·0009 | 0·0044 | 0·0018 | 0·0012 |
| Ni | 0·0006 | 0·0009 | 0·0009 | 0·0005 | 0·0011 | 0·0008 | 0·0006 | 0·0007 | 0·0005 | 0·0004 | 0·0006 | 0·0004 |
| Mg | 0·9366 | 0·0375 | 0·0375 | 0·8674 | 0·0264 | 0·0176 | 0·9025 | 0·0293 | 0·0185 | 0·8935 | 0·0571 | 0·0381 |
| Ca | 0·9704 | 0·0502 | 0·0502 | 0·9507 | 0·0214 | 0·0143 | 0·9603 | 0·0193 | 0·0122 | 0·9430 | 0·0599 | 0·0399 |
| Na | 0·0046 | 0·0061 | 0·0061 | 0·0104 | 0·0054 | 0·0036 | 0·0050 | 0·0036 | 0·0023 | 0·0061 | 0·0033 | 0·0022 |
| K | 0·0001 | 0·0002 | 0·0002 | 0·0005 | 0·0010 | 0·0006 | 0·0000 | 0·0000 | 0·0000 | 0·0001 | 0·0004 | 0·0002 |
| Mg-no. | 0·912 | 0·024 | 0·024 | 0·881 | 0·015 | 0·010 | 0·894 | 0·011 | 0·007 | 0·876 | 0·016 | 0·011 |
| Fs | 0·003 | 0·010 | 0·010 | 0·021 | 0·032 | 0·021 | 0·014 | 0·010 | 0·007 | 0·021 | 0·015 | 0·010 |
| Wo | 0·450 | 0·051 | 0·051 | 0·423 | 0·015 | 0·010 | 0·478 | 0·009 | 0·006 | 0·469 | 0·030 | 0·020 |
| En | 0·469 | 0·019 | 0·019 | 0·434 | 0·013 | 0·009 | 0·452 | 0·015 | 0·009 | 0·447 | 0·029 | 0·019 |

| Sample: | C50.1 ($n=2$) | | | C194 ($n=6$) | | | C201 ($n=14$) | | | C218 ($n=31$) | | |
|---|---|---|---|---|---|---|---|---|---|---|---|---|
| | Average | 2σ | 2σ mean | Average | 2σ | 2σ mean | Average | 2σ | 2σ mean | Average | 2σ | 2σ mean |
| $SiO_2$ | 52·18 | 0·08 | | 50·94 | 1·39 | 1·13 | 50·96 | 1·28 | 0·71 | 51·31 | 1·33 | 0·49 |
| $TiO_2$ | 0·14 | 0·14 | | 0·29 | 0·36 | 0·29 | 0·32 | 0·34 | 0·19 | 0·31 | 0·18 | 0·07 |
| $Cr_2O_3$ | 0·04 | 0·10 | | 0·34 | 0·49 | 0·40 | 0·25 | 0·38 | 0·21 | 0·32 | 0·34 | 0·12 |
| $Al_2O_3$ | 2·52 | 2·29 | | 5·29 | 0·59 | 0·48 | 3·94 | 1·24 | 0·69 | 3·39 | 1·52 | 0·56 |
| $Fe_2O_3$ | 0·82 | 2·32 | | 3·17 | 2·27 | 1·85 | 4·38 | 1·05 | 0·58 | 3·37 | 2·42 | 0·88 |
| FeO | 3·35 | 3·37 | | 2·59 | 1·95 | 1·59 | 0·61 | 0·97 | 0·54 | 1·23 | 2·20 | 0·80 |
| MnO | 0·11 | 0·01 | | 0·15 | 0·07 | 0·05 | 0·14 | 0·06 | 0·03 | 0·13 | 0·04 | 0·01 |
| NiO | 0·01 | 0·01 | | 0·04 | 0·09 | 0·07 | 0·04 | 0·07 | 0·04 | 0·02 | 0·05 | 0·02 |
| MgO | 15·62 | 1·75 | | 15·06 | 0·45 | 0·37 | 15·46 | 1·13 | 0·63 | 15·98 | 1·58 | 0·58 |

(continued)

*Table 3: Continued*

| Sample: | C50.1 ($n=2$) | | | C194 ($n=6$) | | | C201 ($n=14$) | | | C218 ($n=31$) | | |
|---|---|---|---|---|---|---|---|---|---|---|---|---|
| | Average | 2σ | 2σ mean | Average | 2σ | 2σ mean | Average | 2σ | 2σ mean | Average | 2σ | 2σ mean |
| CaO | 23·83 | 0·88 | | 22·90 | 0·76 | 0·62 | 24·29 | 1·11 | 0·62 | 24·32 | 1·38 | 0·50 |
| $Na_2O$ | 0·13 | 0·14 | | 0·46 | 0·09 | 0·07 | 0·39 | 0·24 | 0·14 | 0·13 | 0·08 | 0·03 |
| $K_2O$ | 0·01 | 0·01 | | 0·02 | 0·02 | 0·02 | 0·02 | 0·04 | 0·02 | 0·01 | 0·02 | 0·01 |
| Total | 98·74 | | | 101·26 | | | 100·80 | | | 100·52 | | |
| Si | 1·9351 | 0·0143 | | 1·8475 | 0·0359 | 0·0293 | 1·8560 | 0·0296 | 0·0164 | 1·8722 | 0·0401 | 0·0147 |
| Ti | 0·0040 | 0·0040 | | 0·0078 | 0·0098 | 0·0080 | 0·0087 | 0·0092 | 0·0051 | 0·0085 | 0·0050 | 0·0018 |
| Cr | 0·0010 | 0·0027 | | 0·0098 | 0·0140 | 0·0114 | 0·0074 | 0·0110 | 0·0061 | 0·0093 | 0·0099 | 0·0036 |
| Al | 0·1101 | 0·1001 | | 0·2262 | 0·0238 | 0·0194 | 0·1692 | 0·0543 | 0·0301 | 0·1459 | 0·0660 | 0·0241 |
| $Fe^{3+}$ | 0·0230 | 0·0649 | | 0·0867 | 0·0628 | 0·0513 | 0·1201 | 0·0277 | 0·0154 | 0·0925 | 0·0663 | 0·0242 |
| $Fe^{2+}$ | 0·1038 | 0·1041 | | 0·0784 | 0·0589 | 0·0481 | 0·0186 | 0·0298 | 0·0165 | 0·0375 | 0·0675 | 0·0246 |
| Mn | 0·0032 | 0·0006 | | 0·0047 | 0·0021 | 0·0017 | 0·0043 | 0·0019 | 0·0010 | 0·0040 | 0·0012 | 0·0004 |
| Ni | 0·0002 | 0·0006 | | 0·0013 | 0·0024 | 0·0020 | 0·0012 | 0·0020 | 0·0011 | 0·0007 | 0·0015 | 0·0006 |
| Mg | 0·8634 | 0·1015 | | 0·8141 | 0·0193 | 0·0158 | 0·8389 | 0·0528 | 0·0293 | 0·8691 | 0·0824 | 0·0301 |
| Ca | 0·9468 | 0·0400 | | 0·8902 | 0·0340 | 0·0277 | 0·9477 | 0·0376 | 0·0209 | 0·9506 | 0·0510 | 0·0186 |
| Na | 0·0093 | 0·0098 | | 0·0324 | 0·0066 | 0·0054 | 0·0273 | 0·0173 | 0·0096 | 0·0094 | 0·0058 | 0·0021 |
| K | 0·0004 | 0·0004 | | 0·0009 | 0·0010 | 0·0008 | 0·0007 | 0·0016 | 0·0009 | 0·0003 | 0·0007 | 0·0002 |
| Mg-no. | 0·872 | 0·048 | | 0·831 | 0·021 | 0·017 | 0·858 | 0·023 | 0·013 | 0·870 | 0·023 | 0·008 |
| Fs | 0·052 | 0·052 | | 0·039 | 0·029 | 0·024 | 0·009 | 0·015 | 0·008 | 0·019 | 0·034 | 0·012 |
| Wo | 0·442 | 0·027 | | 0·373 | 0·017 | 0·014 | 0·407 | 0·027 | 0·015 | 0·417 | 0·034 | 0·012 |
| En | 0·432 | 0·051 | | 0·408 | 0·010 | 0·008 | 0·420 | 0·026 | 0·015 | 0·435 | 0·041 | 0·015 |

| Sample: | C66 ($n=13$) | | | C48 ($n=15$) | | | C41 ($n=22$) | | | C7 ($n=12$) | | |
|---|---|---|---|---|---|---|---|---|---|---|---|---|
| | Average | 2σ | 2σ mean | Average | 2σ | 2σ mean | Average | 2σ | 2σ mean | Average | 2σ | 2σ mean |
| $SiO_2$ | 50·39 | 2·68 | 1·55 | 50·11 | 1·69 | 0·91 | 51·521 | 1·21 | 0·38 | 51·14 | 1·41 | 0·85 |
| $TiO_2$ | 0·24 | 0·33 | 0·19 | 0·31 | 0·15 | 0·08 | 0·280 | 0·17 | 0·05 | 0·31 | 0·10 | 0·06 |
| $Cr_2O_3$ | 0·30 | 0·47 | 0·27 | 0·07 | 0·03 | 0·02 | 0·264 | 0·15 | 0·05 | 0·13 | 0·04 | 0·03 |
| $Al_2O_3$ | 3·97 | 0·81 | 0·47 | 2·70 | 0·47 | 0·25 | 3·136 | 1·52 | 0·48 | 2·65 | 0·53 | 0·32 |
| $Fe_2O_3$ | 4·48 | 2·46 | 1·42 | 5·29 | 2·31 | 1·24 | 2·728 | 1·80 | 0·57 | 3·19 | 2·41 | 1·45 |
| FeO | 1·01 | 1·95 | 1·13 | 3·73 | 2·01 | 1·07 | 4·003 | 1·60 | 0·50 | 5·09 | 1·82 | 1·10 |
| MnO | 0·15 | 0·05 | 0·03 | 0·21 | 0·05 | 0·03 | 0·191 | 0·04 | 0·01 | 0·18 | 0·06 | 0·03 |
| NiO | 0·03 | 0·05 | 0·03 | 0·01 | 0·02 | 0·01 | 0·021 | 0·05 | 0·02 | 0·01 | 0·03 | 0·02 |
| MgO | 15·66 | 1·27 | 0·73 | 14·12 | 0·51 | 0·27 | 14·611 | 0·95 | 0·30 | 14·27 | 1·16 | 0·70 |
| CaO | 23·05 | 1·75 | 1·01 | 22·39 | 0·50 | 0·27 | 23·104 | 0·89 | 0·28 | 22·36 | 0·99 | 0·60 |
| $Na_2O$ | 0·44 | 0·07 | 0·04 | 0·51 | 0·05 | 0·02 | 0·423 | 0·17 | 0·05 | 0·44 | 0·20 | 0·12 |
| $K_2O$ | 0·00 | 0·01 | 0·01 | 0·00 | 0·01 | 0·01 | 0·014 | 0·04 | 0·01 | 0·01 | 0·02 | 0·01 |
| Total | 99·70 | | | 99·47 | | | 100·29 | | 0·00 | 99·78 | | |
| Si | 1·8534 | 0·0659 | 0·0380 | 1·8748 | 0·0372 | 0·0199 | 1·8979 | 0·0416 | 0·0131 | 1·9028 | 0·0374 | 0·0226 |
| Ti | 0·0066 | 0·0091 | 0·0053 | 0·0088 | 0·0042 | 0·0023 | 0·0078 | 0·0047 | 0·0015 | 0·0087 | 0·0029 | 0·0018 |
| Cr | 0·0088 | 0·0137 | 0·0079 | 0·0019 | 0·0009 | 0·0005 | 0·0077 | 0·0045 | 0·0014 | 0·0037 | 0·0012 | 0·0008 |
| Al | 0·1723 | 0·0376 | 0·0217 | 0·1190 | 0·0210 | 0·0112 | 0·1362 | 0·0662 | 0·0209 | 0·1162 | 0·0235 | 0·0141 |
| $Fe^{3+}$ | 0·1242 | 0·0697 | 0·0402 | 0·1492 | 0·0673 | 0·0360 | 0·0755 | 0·0494 | 0·0156 | 0·0895 | 0·0678 | 0·0409 |
| $Fe^{2+}$ | 0·0308 | 0·0594 | 0·0343 | 0·1167 | 0·0618 | 0·0330 | 0·1234 | 0·0499 | 0·0158 | 0·1583 | 0·0556 | 0·0335 |

(continued)

*Table 3: Continued*

| Sample: | C66 ($n=13$) | | | C48 ($n=15$) | | | C41 ($n=22$) | | | C7 ($n=12$) | | |
|---|---|---|---|---|---|---|---|---|---|---|---|---|
| | Average | 2σ | 2σ mean | Average | 2σ | 2σ mean | Average | 2σ | 2σ mean | Average | 2σ | 2σ mean |
| Mn | 0·0046 | 0·0017 | 0·0010 | 0·0066 | 0·0017 | 0·0009 | 0·0060 | 0·0013 | 0·0004 | 0·0057 | 0·0018 | 0·0011 |
| Ni | 0·0008 | 0·0014 | 0·0008 | 0·0004 | 0·0007 | 0·0004 | 0·0006 | 0·0014 | 0·0005 | 0·0003 | 0·0009 | 0·0005 |
| Mg | 0·8582 | 0·0614 | 0·0355 | 0·7874 | 0·0302 | 0·0161 | 0·8022 | 0·0479 | 0·0151 | 0·7913 | 0·0627 | 0·0378 |
| Ca | 0·9084 | 0·0714 | 0·0412 | 0·8976 | 0·0190 | 0·0101 | 0·9118 | 0·0322 | 0·0102 | 0·8914 | 0·0402 | 0·0242 |
| Na | 0·0318 | 0·0055 | 0·0032 | 0·0372 | 0·0029 | 0·0016 | 0·0302 | 0·0121 | 0·0038 | 0·0318 | 0·0146 | 0·0088 |
| K | 0·0001 | 0·0005 | 0·0003 | 0·0003 | 0·0006 | 0·0003 | 0·0007 | 0·0017 | 0·0005 | 0·0005 | 0·0009 | 0·0005 |
| Mg-no. | 0·847 | 0·023 | 0·013 | 0·748 | 0·016 | 0·009 | 0·8012 | 0·0178 | 0·0056 | 0·761 | 0·047 | 0·028 |
| Fs | 0·015 | 0·030 | 0·017 | 0·058 | 0·031 | 0·017 | 0·0617 | 0·0250 | 0·0079 | 0·079 | 0·028 | 0·017 |
| Wo | 0·387 | 0·045 | 0·026 | 0·395 | 0·014 | 0·007 | 0·4092 | 0·0292 | 0·0092 | 0·401 | 0·023 | 0·014 |
| En | 0·430 | 0·031 | 0·018 | 0·394 | 0·015 | 0·008 | 0·4014 | 0·0242 | 0·0076 | 0·396 | 0·031 | 0·019 |

| Sample: | C171 | | | C04-9 | | | C135 ($n=9$) | | | C135 ($n=16$) | | |
|---|---|---|---|---|---|---|---|---|---|---|---|---|
| | Average | 2σ | 2σ mean | Average | 2σ | 2σ mean | Average | 2σ | 2σ mean | Average | 2σ | 2σ mean |
| $SiO_2$ | 49·98 | 0·58 | 0·52 | 51·52 | 1·37 | 0·91 | 53·49 | 0·69 | 0·49 | 53·26 | 0·47 | 0·24 |
| $TiO_2$ | 0·43 | 0·11 | 0·10 | 0·48 | 0·17 | 0·11 | 0·25 | 0·05 | 0·04 | 0·25 | 0·04 | 0·02 |
| $Cr_2O_3$ | 0·52 | 0·21 | 0·19 | 0·36 | 0·11 | 0·07 | 0·04 | 0·08 | 0·06 | 0·02 | 0·04 | 0·02 |
| $Al_2O_3$ | 3·43 | 1·03 | 0·92 | 4·31 | 0·96 | 0·64 | 2·50 | 0·16 | 0·11 | 2·38 | 0·24 | 0·13 |
| $Fe_2O_3$ | 3·76 | 1·26 | 1·13 | 1·74 | 1·23 | 0·82 | 0·00 | 0·00 | 0·00 | 0·00 | 0·00 | 0·00 |
| FeO | 0·55 | 0·93 | 0·83 | 3·21 | 1·48 | 0·99 | 9·66 | 0·62 | 0·44 | 10·08 | 1·38 | 0·71 |
| MnO | 0·12 | 0·03 | 0·03 | 0·12 | 0·05 | 0·03 | 0·25 | 0·05 | 0·03 | 0·31 | 0·03 | 0·02 |
| NiO | 0·01 | 0·03 | 0·03 | 0·00 | 0·00 | 0·00 | 0·02 | 0·05 | 0·03 | 0·01 | 0·03 | 0·01 |
| MgO | 15·95 | 1·00 | 0·89 | 15·08 | 0·72 | 0·48 | 13·10 | 0·33 | 0·23 | 12·89 | 0·47 | 0·24 |
| CaO | 23·30 | 0·91 | 0·82 | 24·10 | 1·23 | 0·82 | 21·82 | 0·84 | 0·60 | 21·75 | 1·71 | 0·88 |
| $Na_2O$ | 0·27 | 0·07 | 0·06 | 0·20 | 0·06 | 0·04 | 0·30 | 0·05 | 0·03 | 0·29 | 0·05 | 0·02 |
| $K_2O$ | 0·00 | 0·00 | 0·00 | 0·00 | 0·01 | 0·00 | 0·01 | 0·02 | 0·01 | 0·01 | 0·02 | 0·01 |
| Total | 98·32 | | | 101·14 | | | 101·44 | | | 101·25 | 0·50 | 0·26 |
| Si | 1·8614 | 0·0207 | 0·0185 | 1·8728 | 0·0391 | 0·0261 | 1·9700 | 0·0130 | 0·0092 | 1·9700 | 0·0135 | 0·0070 |
| Ti | 0·0119 | 0·0031 | 0·0028 | 0·0130 | 0·0047 | 0·0031 | 0·0100 | 0·0015 | 0·0011 | 0·0100 | 0·0011 | 0·0005 |
| Cr | 0·0152 | 0·0063 | 0·0056 | 0·1847 | 0·0413 | 0·0275 | 0·0000 | 0·0023 | 0·0016 | 0·0000 | 0·0013 | 0·0007 |
| Al | 0·1505 | 0·0453 | 0·0406 | 0·0105 | 0·0032 | 0·0021 | 0·1100 | 0·0067 | 0·0048 | 0·1000 | 0·0103 | 0·0053 |
| $Fe^{3+}$ | 0·1055 | 0·0352 | 0·0315 | 0·0477 | 0·0340 | 0·0226 | 0·0000 | 0·0000 | 0·0000 | 0·0000 | 0·0000 | 0·0000 |
| $Fe^{2+}$ | 0·0172 | 0·0289 | 0·0258 | 0·0976 | 0·0444 | 0·0296 | 0·3000 | 0·0192 | 0·0135 | 0·3100 | 0·0438 | 0·0226 |
| Mn | 0·0038 | 0·0010 | 0·0009 | 0·0037 | 0·0015 | 0·0010 | 0·0100 | 0·0014 | 0·0010 | 0·0100 | 0·0010 | 0·0005 |
| Ni | 0·0004 | 0·0009 | 0·0008 | 0·0000 | 0·0000 | 0·0000 | 0·0000 | 0·0015 | 0·0010 | 0·0000 | 0·0008 | 0·0004 |
| Mg | 0·8853 | 0·0550 | 0·0492 | 0·8171 | 0·0350 | 0·0233 | 0·7200 | 0·0173 | 0·0122 | 0·7100 | 0·0279 | 0·0144 |
| Ca | 0·9298 | 0·0357 | 0·0319 | 0·9386 | 0·0503 | 0·0335 | 0·8600 | 0·0316 | 0·0224 | 0·8600 | 0·0649 | 0·0335 |
| Na | 0·0192 | 0·0047 | 0·0042 | 0·0143 | 0·0043 | 0·0028 | 0·0200 | 0·0035 | 0·0025 | 0·0200 | 0·0034 | 0·0018 |
| K | 0·0000 | 0·0000 | 0·0000 | 0·0001 | 0·0003 | 0·0002 | 0·0000 | 0·0007 | 0·0005 | 0·0000 | 0·0012 | 0·0006 |
| Mg-no. | 0·878 | 0·020 | 0·018 | 0·849 | 0·022 | 0·015 | 0·710 | 0·012 | 0·009 | 0·700 | 0·023 | 0·012 |
| Fs | 0·009 | 0·014 | 0·013 | 0·049 | 0·022 | 0·015 | 0·150 | 0·010 | 0·007 | 0·160 | 0·022 | 0·011 |
| Wo | 0·403 | 0·021 | 0·019 | 0·467 | 0·025 | 0·017 | 0·410 | 0·016 | 0·012 | 0·410 | 0·031 | 0·016 |
| En | 0·443 | 0·028 | 0·025 | 0·409 | 0·017 | 0·012 | 0·360 | 0·009 | 0·006 | 0·360 | 0·014 | 0·007 |

(continued)

*Table 3: Continued*

| Sample: | C141 ($n=4$) | | | C219 ($n=6$) | | |
|---|---|---|---|---|---|---|
| | Average | 2σ | 2σ mean | Average | 2σ | 2σ mean |
| $SiO_2$ | 53·21 | 0·32 | 0·37 | 52·04 | 0·64 | 0·29 |
| $TiO_2$ | 0·22 | 0·06 | 0·07 | 0·39 | 0·09 | 0·04 |
| $Cr_2O_3$ | 0·02 | 0·05 | 0·05 | 0·58 | 0·10 | 0·05 |
| $Al_2O_3$ | 2·16 | 0·11 | 0·13 | 4·46 | 0·58 | 0·26 |
| $Fe_2O_3$ | 0·00 | 0·00 | 0·00 | 0·58 | 0·90 | 0·40 |
| FeO | 9·90 | 0·64 | 0·74 | 4·33 | 0·91 | 0·41 |
| MnO | 0·29 | 0·07 | 0·08 | 0·13 | 0·05 | 0·02 |
| NiO | 0·00 | 0·01 | 0·01 | 0·01 | 0·05 | 0·02 |
| MgO | 12·89 | 0·34 | 0·40 | 15·18 | 0·29 | 0·13 |
| CaO | 22·09 | 0·50 | 0·58 | 23·38 | 0·65 | 0·29 |
| $Na_2O$ | 0·26 | 0·01 | 0·02 | 0·24 | 0·09 | 0·04 |
| $K_2O$ | 0·00 | 0·01 | 0·02 | 0·00 | 0·00 | 0·00 |
| Total | 101·05 | 0·25 | 0·29 | 101·31 | 0·58 | 0·26 |
| Si | 1·9734 | 0·0062 | 0·0072 | 1·8862 | 0·0211 | 0·0094 |
| Ti | 0·0061 | 0·0016 | 0·0019 | 0·0107 | 0·0026 | 0·0012 |
| Cr | 0·0006 | 0·0013 | 0·0015 | 0·0166 | 0·0029 | 0·0013 |
| Al | 0·0943 | 0·0049 | 0·0057 | 0·1906 | 0·0250 | 0·0112 |
| $Fe^{3+}$ | 0·0000 | 0·0000 | 0·0000 | 0·0158 | 0·0246 | 0·0110 |
| $Fe^{2+}$ | 0·3071 | 0·0207 | 0·0239 | 0·1312 | 0·0276 | 0·0123 |
| Mn | 0·0091 | 0·0023 | 0·0026 | 0·0038 | 0·0016 | 0·0007 |
| Ni | 0·0001 | 0·0004 | 0·0004 | 0·0003 | 0·0014 | 0·0006 |
| Mg | 0·7127 | 0·0179 | 0·0207 | 0·8203 | 0·0169 | 0·0075 |
| Ca | 0·8776 | 0·0175 | 0·0203 | 0·9077 | 0·0226 | 0·0101 |
| Na | 0·0187 | 0·0010 | 0·0012 | 0·0168 | 0·0066 | 0·0029 |
| K | 0·0002 | 0·0007 | 0·0008 | 0·0000 | 0·0001 | 0·0000 |
| Mg-no. | 0·699 | 0·017 | 0·020 | 0·848 | 0·013 | 0·006 |
| Fs | 0·154 | 0·010 | 0·012 | 0·066 | 0·014 | 0·006 |
| Wo | 0·420 | 0·009 | 0·010 | 0·402 | 0·015 | 0·007 |
| En | 0·356 | 0·009 | 0·010 | 0·410 | 0·008 | 0·004 |

content varies systematically within clinopyroxene and can be separated into an igneous trend defined by core compositions and unzoned clinopyroxene and a metamorphic trend defined by core to rim zoning (Fig. 13). Within the igneous trend the $Al_2O_3$ content of clinopyroxenes from samples devoid of plagioclase increases with decreasing Mg-number. The $Al_2O_3$ and $Na_2O$ contents of clinopyroxene coexisting with plagioclase decrease with decreasing Mg-number. This trend has been previously noticed in pyroxenes from the Aleutian arc volcanic rocks (Kay & Kay, 1985), from lower crustal cumulates (DeBari *et al.*, 1987), in the Tonsina ultramafic–mafic assemblage (DeBari & Coleman, 1989) and in experimental studies on pyroxenites (Müntener *et al.*, 2001). However, it is not observed for low-pressure cumulates such as those of Skaergaard (DeBari & Coleman, 1989). The generally accepted explanation is that plagioclase crystallization is suppressed by high total pressure and high water pressure (Yoder & Tilley, 1962; Sisson & Grove, 1993; Panjasawatwong *et al.*, 1995). Crystallization of Al-poor olivine and pyroxene leads to Al enrichment of the residual liquids. Because the solubility of Al in pyroxene increases with increasing pressure (Kushiro & Yoder, 1966; Howells & O'Hara, 1978; Gasparik, 1984), higher crystallization pressures in Tonsina (0·95–1·1 GPa; DeBari & Coleman, 1989) than in Chilas (0·5–0·7 GPa) explain the slightly higher absolute $Al_2O_3$ content observed in Tonsina (8·85 wt%) compared with Chilas (below 6 wt% excluding one analyses of 7·28 wt%). The metamorphic trend displayed in Fig. 13 is due to a Tschermak exchange of $(Fe,Mg)SiAl_{-2}$ during cooling. In terms of major element chemistry, clinopyroxenes from ol-websterites are characterized by low Na, Al, Ti and Cr and high Mg-number, and are similar to primitive clinopyroxene from dunites and secondary peridotites.

The trace element characteristics of clinopyroxene have been determined from three ol-websterite samples (C03-43, C03-44 and C03-45), one high Mg-number dunite (C174), one plagioclase-bearing lherzolite (C218), one primitive, olivine-bearing gabbronorite (C66) and two gabbronorite samples (C7 and C48). Clinopyroxene is characterized by incompatible trace element depletion with respect to middle and heavy rare earth elements (MREE and HREE) (Fig. 14). The absolute trace element concentrations are 7–10 times higher in gabbronorite clinopyroxene than in the other samples. Gabbronorite samples display pronounced negative Pb, Sr and Eu anomalies that increase with increasing trace element concentration, indicating plagioclase fractionation prior to gabbronorite crystallization. Primitive clinopyroxene from the plagioclase-bearing lherzolite C218, however, has positive Pb and Sr spikes indicating that clinopyroxene crystallized from a melt that did not fractionate plagioclase. However, there is evidence for metamorphic re-equilibration of clinopyroxene with coexisting plagioclase (see below). Clinopyroxene REE concentrations vary by a factor of two within a single sample, whereas the Mg-number remains constant.

The clinopyroxene REE concentration in ol-websterite is low and normalized REE patterns show a slight light REE (LREE) depletion and convex-upwards pattern ($Ce_N/Yb_N = 0·43–0·76$) with enrichment of the MREE compared with the heavy REE ($Gd_N/Yb_N = 1·2–1·8$). We focused on clinopyroxene grains with high Mg-number (0·92–0·93) in dunite C174. The primitive mantle normalized concentrations display a convex-upward pattern, with $Gd_N/Yb_N \sim 1$ and $Ce_N/Gd_N \sim 0·4–0·5$. For the plagioclase-bearing lherzolite the HREE and LREE are slightly depleted with respect to the MREE ($Gd_N/Yb_N \sim 1·3–1·6$; $Ce_N/Gd_N \sim 0·3$).

*Table 4: Trace element concentrations (ppm) in clinopyroxene from the Chilas Complex*

| Sample: | C03-43 | | | C03-44 | | | C03-45 | | | C174 | | |
|---|---|---|---|---|---|---|---|---|---|---|---|---|
| *n*: | 6 | | | 15 | | | 11 | | | 6 | | |
| | Average | 2σ | 2σ mean | Average | 2σ | 2σ mean | Average | 2σ | 2σ mean | Average | 2σ | 2σ mean |
| Li | 1·83 | 0·21 | 0·18 | 1·51 | 1·04 | 0·28 | 1·54 | 0·65 | 0·25 | 1·27 | 1·08 | 0·48 |
| Sc | 106 | 4 | 4 | 104 | 70 | 19 | 97 | 19 | 7 | 89·3 | 41·7 | 18·7 |
| V | 211 | 26 | 23 | 197 | 132 | 35 | 145 | 60 | 23 | 116 | 72·2 | 32·3 |
| Cr | 4209 | 433 | 387 | 2430 | 1740 | 465 | 3253 | 2845 | 1075 | 3113 | 2705 | 1210 |
| Co | 29·8 | 2·5 | 2·3 | 31·3 | 21·5 | 5·8 | 26·8 | 6·64 | 2·51 | 19·2 | 9·76 | 4·36 |
| Ni | 139 | 14 | 12 | 129 | 89·6 | 23·9 | 114 | 24 | 9 | 122 | 65·3 | 29·2 |
| Cu | 0·112 | 0·033 | 0·038 | 0·092 | 0·082 | 0·025 | 0·142 | 0·129 | 0·065 | 0·869 | 0·414 | 0·185 |
| Zn | | | | | | | | | | 8·91 | 8·42 | 3·77 |
| Ga | 4·17 | 0·56 | 0·50 | 4·05 | 2·75 | 0·74 | 2·69 | 1·47 | 0·55 | 1·86 | 1·13 | 0·51 |
| Rb | | | | | | | | | | | | |
| Sr | 20·6 | 1·8 | 1·6 | 21·6 | 15·0 | 4·0 | 19·0 | 2·6 | 1·0 | 19·7 | 10·6 | 4·74 |
| Y | 6·05 | 0·92 | 0·83 | 5·08 | 3·42 | 0·91 | 3·28 | 1·4 | 0·52 | 3·49 | 2·29 | 1·03 |
| Zr | 6·48 | 1·00 | 0·90 | 4·78 | 3·37 | 0·90 | 3·51 | 1·42 | 0·54 | 3·72 | 2·28 | 1·02 |
| Nb | | | | | | | | | | 0·012 | 0·009 | 0·004 |
| La | 0·304 | 0·035 | 0·031 | 0·267 | 0·181 | 0·048 | 0·171 | 0·050 | 0·02 | 0·210 | 0·124 | 0·056 |
| Ce | 1·37 | 0·12 | 0·11 | 1·17 | 0·80 | 0·21 | 0·69 | 0·16 | 0·06 | 0·761 | 0·407 | 0·182 |
| Pr | 0·275 | 0·022 | 0·020 | 0·235 | 0·162 | 0·043 | 0·144 | 0·040 | 0·01 | 0·158 | 0·092 | 0·041 |
| Nd | 1·90 | 0·24 | 0·21 | 1·63 | 1·13 | 0·30 | 1·02 | 0·28 | 0·11 | 1·03 | 0·63 | 0·28 |
| Sm | 0·811 | 0·075 | 0·067 | 0·685 | 0·477 | 0·127 | 0·443 | 0·17 | 0·06 | 0·445 | 0·313 | 0·140 |
| Eu | 0·317 | 0·031 | 0·028 | 0·266 | 0·180 | 0·048 | 0·177 | 0·063 | 0·024 | 0·188 | 0·117 | 0·052 |
| Gd | 1·020 | 0·124 | 0·111 | 0·846 | 0·564 | 0·151 | 0·588 | 0·20 | 0·07 | 0·552 | 0·357 | 0·160 |
| Tb | 0·186 | 0·026 | 0·023 | 0·156 | 0·105 | 0·028 | 0·104 | 0·047 | 0·018 | 0·111 | 0·071 | 0·032 |
| Dy | 1·17 | 0·16 | 0·14 | 1·01 | 0·69 | 0·18 | 0·70 | 0·27 | 0·10 | 0·732 | 0·475 | 0·213 |
| Ho | 0·256 | 0·044 | 0·039 | 0·220 | 0·149 | 0·040 | 0·136 | 0·060 | 0·023 | 0·156 | 0·097 | 0·043 |
| Er | 0·705 | 0·112 | 0·100 | 0·551 | 0·375 | 0·100 | 0·354 | 0·20 | 0·07 | 0·413 | 0·287 | 0·128 |
| Tm | 0·088 | 0·015 | 0·014 | 0·080 | 0·055 | 0·015 | 0·051 | 0·020 | 0·008 | 0·062 | 0·040 | 0·018 |
| Yb | 0·581 | 0·107 | 0·096 | 0·499 | 0·339 | 0·091 | 0·317 | 0·1 | 0·1 | 0·429 | 0·277 | 0·124 |
| Lu | 0·083 | 0·016 | 0·015 | 0·069 | 0·046 | 0·012 | 0·047 | 0·019 | 0·007 | 0·067 | 0·036 | 0·016 |
| Hf | 0·293 | 0·049 | 0·044 | 0·223 | 0·162 | 0·043 | 0·192 | 0·056 | 0·021 | 0·177 | 0·093 | 0·042 |
| Pb | 0·074 | 0·019 | 0·017 | 0·061 | 0·042 | 0·011 | 0·077 | 0·04 | 0·01 | 0·100 | 0·033 | 0·015 |
| Th | 0·014 | 0·007 | 0·007 | 0·017 | 0·018 | 0·005 | 0·014 | 0·03 | 0·01 | 0·004 | 0·003 | 0·001 |
| U | | | | 0·005 | 0·004 | 0·001 | 0·007 | 0·01 | 0·00 | 0·002 | 0·002 | 0·001 |

| Sample: | C218 | | | C66 | | | C48 | | | C7 | | |
|---|---|---|---|---|---|---|---|---|---|---|---|---|
| *n*: | 6 | | | 7 | | | 7 | | | 9 | | |
| | Average | 2σ | 2σ mean | Average | 2σ | 2σ mean | Average | 2σ | 2σ mean | Average | 2σ | 2σ mean |
| Li | 3·93 | 1·19 | 0·45 | 1·23 | 0·14 | 0·10 | 17·3 | 1·0 | 0·4 | 10·0 | 1·2 | 0·4 |
| Sc | 96·6 | 14·0 | 5·31 | 82·7 | 10·0 | 7·57 | 145 | 10 | 4 | 138 | 6 | 2 |
| V | 275 | 53·6 | 20·3 | 216 | 38·1 | 28·84 | 419 | 54·6 | 20·6 | 385 | 37·2 | 13·1 |
| Cr | 3663 | 1018 | 385 | 2880 | 384 | 290·18 | 360 | 68 | 26 | 690 | 157 | 56 |
| Co | 38·5 | 10·44 | 3·95 | 30·3 | 2·97 | 2·25 | 46·4 | 4·47 | 1·69 | 45·3 | 2·87 | 1·02 |

(continued)

*Table 4: Continued*

| Sample: | C218 | | | C66 | | | C48 | | | C7 | | |
|---|---|---|---|---|---|---|---|---|---|---|---|---|
| *n*: | 6 | | | 7 | | | 7 | | | 9 | | |
| | Average | 2σ | 2σ mean | Average | 2σ | 2σ mean | Average | 2σ | 2σ mean | Average | 2σ | 2σ mean |
| Ni | 171 | 37·4 | 14·13 | 135 | 13·2 | 9·98 | 149 | 15·8 | 5·96 | 153 | 15·0 | 5·30 |
| Cu | 0·671 | 0·433 | 0·164 | 0·549 | 0·069 | 0·052 | 1·50 | 1·31 | 0·49 | 0·631 | 0·269 | 0·095 |
| Zn | | | | 0·000 | 0·00 | 0·00 | 55·4 | 8·89 | 3·36 | 56·0 | 5·08 | 1·80 |
| Ga | 5·04 | 1·57 | 0·59 | 5·21 | 0·74 | 0·56 | 8·02 | 1·04 | 0·39 | 7·97 | 0·98 | 0·35 |
| Rb | 0·000 | 0·000 | 0·000 | 0·020 | 0·016 | 0·02 | 0·014 | 0·012 | 0·005 | 0·015 | 0·006 | 0·003 |
| Sr | 68·5 | 51·1 | 19·30 | 20·7 | 1·9 | 1·45 | 14·7 | 2·7 | 1·04 | 13·5 | 1·3 | 0·44 |
| Y | 5·68 | 3·21 | 1·21 | 5·44 | 1·79 | 1·35 | 27·7 | 10·86 | 4·11 | 45·6 | 8·77 | 3·10 |
| Zr | 5·09 | 2·09 | 0·79 | 4·87 | 0·84 | 0·64 | 22·2 | 7·37 | 2·79 | 31·9 | 3·93 | 1·39 |
| Nb | 0·011 | 0·006 | 0·002 | 0·009 | 0·001 | 0·001 | 0·005 | 0·002 | 0·001 | 0·009 | 0·005 | 0·002 |
| La | 0·297 | 0·085 | 0·032 | 0·213 | 0·027 | 0·021 | 0·969 | 0·249 | 0·094 | 1·33 | 0·23 | 0·08 |
| Ce | 1·00 | 0·43 | 0·16 | 0·989 | 0·158 | 0·119 | 4·82 | 1·50 | 0·57 | 7·04 | 1·34 | 0·47 |
| Pr | 0·209 | 0·113 | 0·043 | 0·215 | 0·042 | 0·032 | 1·07 | 0·42 | 0·16 | 1·62 | 0·34 | 0·12 |
| Nd | 1·47 | 0·83 | 0·32 | 1·50 | 0·34 | 0·25 | 7·25 | 3·06 | 1·16 | 11·7 | 2·5 | 0·9 |
| Sm | 0·692 | 0·372 | 0·141 | 0·683 | 0·200 | 0·152 | 3·14 | 1·26 | 0·48 | 5·33 | 1·18 | 0·42 |
| Eu | 0·325 | 0·136 | 0·051 | 0·330 | 0·062 | 0·047 | 0·877 | 0·227 | 0·086 | 1·01 | 0·16 | 0·06 |
| Gd | 0·989 | 0·496 | 0·188 | 0·915 | 0·278 | 0·210 | 4·25 | 1·75 | 0·66 | 7·04 | 1·34 | 0·48 |
| Tb | 0·188 | 0·100 | 0·038 | 0·176 | 0·056 | 0·042 | 0·817 | 0·320 | 0·121 | 1·34 | 0·28 | 0·10 |
| Dy | 1·20 | 0·63 | 0·24 | 1·12 | 0·37 | 0·28 | 5·39 | 2·01 | 0·76 | 8·66 | 1·67 | 0·59 |
| Ho | 0·254 | 0·143 | 0·054 | 0·239 | 0·078 | 0·059 | 1·16 | 0·44 | 0·16 | 1·88 | 0·31 | 0·11 |
| Er | 0·639 | 0·366 | 0·138 | 0·615 | 0·197 | 0·149 | 3·07 | 1·12 | 0·42 | 4·97 | 0·86 | 0·30 |
| Tm | 0·088 | 0·048 | 0·018 | 0·083 | 0·028 | 0·021 | 0·423 | 0·163 | 0·061 | 0·684 | 0·095 | 0·034 |
| Yb | 0·579 | 0·293 | 0·111 | 0·564 | 0·167 | 0·126 | 2·87 | 0·96 | 0·36 | 4·68 | 0·83 | 0·29 |
| Lu | 0·075 | 0·043 | 0·016 | 0·078 | 0·023 | 0·018 | 0·400 | 0·141 | 0·053 | 0·637 | 0·093 | 0·033 |
| Hf | 0·313 | 0·101 | 0·038 | 0·257 | 0·045 | 0·034 | 1·19 | 0·22 | 0·08 | 1·69 | 0·26 | 0·09 |
| Pb | 0·089 | 0·045 | 0·017 | 0·051 | 0·019 | 0·014 | 0·139 | 0·043 | 0·016 | 0·123 | 0·034 | 0·012 |
| Th | 0·029 | 0·038 | 0·014 | 0·043 | 0·017 | 0·013 | 0·037 | 0·019 | 0·007 | 0·019 | 0·009 | 0·003 |
| U | 0·024 | 0·044 | 0·016 | 0·025 | 0·037 | 0·028 | 0·015 | 0·006 | 0·002 | 0·010 | 0·007 | 0·002 |

The concentration of trace element for which no value is shown is below detection limit.

*Table 5: Major element concentrations (wt %) in orthopyroxene from the Chilas Complex*

| Sample: | T6 (*n* = 5) | | | C03-44 (*n* = 4) | | | C03-50 (*n* = 3) | | | C03-17 (*n* = 3) | | |
|---|---|---|---|---|---|---|---|---|---|---|---|---|
| | Average | 2σ | 2σ mean | Average | 2σ | 2σ mean | Average | 2σ | 2σ mean | Average | 2σ | 2σ mean |
| $SiO_2$ | 54·90 | 0·54 | 0·27 | 56·44 | 2·57 | 1·48 | 57·55 | 2·33 | 2·33 | 55·30 | 0·51 | 0·36 |
| $TiO_2$ | 0·09 | 0·05 | 0·02 | 0·07 | 0·04 | 0·02 | 0·01 | 0·01 | 0·01 | 0·07 | 0·01 | 0·00 |
| $Cr_2O_3$ | 0·19 | 0·09 | 0·04 | 0·13 | 0·03 | 0·02 | 0·02 | 0·02 | 0·02 | 0·12 | 0·10 | 0·07 |
| $Al_2O_3$ | 2·28 | 0·22 | 0·11 | 1·77 | 0·42 | 0·24 | 0·02 | 0·00 | 0·00 | 1·70 | 0·51 | 0·36 |
| $Fe_2O_3$ | 0·47 | 0·71 | 0·36 | 0·80 | 2·36 | 1·36 | 0·66 | 1·86 | 1·86 | 2·97 | 0·34 | 0·24 |
| FeO | 11·03 | 0·53 | 0·27 | 10·49 | 2·33 | 1·34 | 10·41 | 1·55 | 1·55 | 8·17 | 0·10 | 0·07 |
| MnO | 0·29 | 0·04 | 0·02 | 0·27 | 0·04 | 0·02 | 0·42 | 0·20 | 0·20 | 0·34 | 0·02 | 0·01 |

(continued)

*Table 5: Continued*

| Sample: | T6 ($n=5$) | | | C03-44 ($n=4$) | | | C03-50 ($n=3$) | | | C03-17 ($n=3$) | | |
|---|---|---|---|---|---|---|---|---|---|---|---|---|
| | Average | 2σ | 2σ mean | Average | 2σ | 2σ mean | Average | 2σ | 2σ mean | Average | 2σ | 2σ mean |
| NiO | 0·06 | 0·02 | 0·01 | | 0·00 | | 0·00 | 0·00 | 0·00 | 0·03 | 0·01 | 0·00 |
| MgO | 30·15 | 0·65 | 0·32 | 30·78 | 1·46 | 0·84 | 30·01 | 6·45 | 6·45 | 32·13 | 0·30 | 0·21 |
| CaO | 0·40 | 0·17 | 0·09 | 0·44 | 0·12 | 0·07 | 0·13 | 0·22 | 0·22 | 0·30 | 0·05 | 0·04 |
| $Na_2O$ | 0·01 | 0·03 | 0·02 | 0·01 | 0·03 | 0·01 | 0·00 | 0·00 | 0·00 | 0·00 | 0·01 | 0·00 |
| $K_2O$ | 0·01 | 0·01 | 0·00 | 0·00 | 0·01 | 0·01 | 0·00 | 0·00 | 0·00 | 0·00 | 0·00 | 0·00 |
| Total | 99·88 | | | 101·21 | | | 99·22 | | | 101·13 | | |
| Si | 1·9419 | 0·0142 | 0·0071 | 1·9688 | 0·0614 | 0·0354 | 2·0565 | 0·2115 | 0·2115 | 1·9230 | 0·0089 | 0·0063 |
| Ti | 0·0024 | 0·0012 | 0·0006 | 0·0018 | 0·0011 | 0·0006 | 0·0002 | 0·0003 | 0·0003 | 0·0018 | 0·0002 | 0·0001 |
| Cr | 0·0051 | 0·0023 | 0·0011 | 0·0036 | 0·0009 | 0·0005 | 0·0006 | 0·0005 | 0·0005 | 0·0034 | 0·0027 | 0·0019 |
| Al | 0·0950 | 0·0080 | 0·0040 | 0·0728 | 0·0196 | 0·0113 | 0·0008 | 0·0001 | 0·0001 | 0·0696 | 0·0210 | 0·0148 |
| $Fe^{3+}$ | 0·0125 | 0·0186 | 0·0093 | 0·0210 | 0·0620 | 0·0358 | 0·0173 | 0·0490 | 0·0490 | 0·0776 | 0·0084 | 0·0059 |
| $Fe^{2+}$ | 0·3265 | 0·0188 | 0·0094 | 0·3060 | 0·0698 | 0·0403 | 0·3114 | 0·0657 | 0·0657 | 0·2376 | 0·0010 | 0·0007 |
| Mn | 0·0086 | 0·0011 | 0·0005 | 0·0078 | 0·0011 | 0·0006 | 0·0127 | 0·0067 | 0·0067 | 0·0100 | 0·0006 | 0·0004 |
| Ni | 0·0016 | 0·0007 | 0·0003 | | 0·0000 | | 0·0000 | 0·0000 | 0·0000 | 0·0009 | 0·0002 | 0·0001 |
| Mg | 1·5898 | 0·0126 | 0·0063 | 1·6007 | 0·0631 | 0·0364 | 1·5953 | 0·2438 | 0·2438 | 1·6650 | 0·0085 | 0·0060 |
| Ca | 0·0153 | 0·0068 | 0·0034 | 0·0166 | 0·0047 | 0·0027 | 0·0051 | 0·0087 | 0·0087 | 0·0110 | 0·0020 | 0·0014 |
| Na | 0·0010 | 0·0021 | 0·0011 | 0·0008 | 0·0018 | 0·0010 | 0·0000 | 0·0000 | 0·0000 | 0·0001 | 0·0004 | 0·0003 |
| K | 0·0003 | 0·0004 | 0·0002 | 0·0001 | 0·0004 | 0·0002 | 0·0000 | 0·0001 | 0·0001 | 0·0001 | 0·0002 | 0·0001 |
| Mg-no. | 0·824 | 0·004 | 0·002 | 0·830 | 0·009 | 0·005 | 0·829 | 0·029 | 0·029 | 0·841 | 0·003 | 0·002 |
| Fs | 0·163 | 0·009 | 0·005 | 0·153 | 0·035 | 0·020 | 0·156 | 0·033 | 0·033 | 0·119 | 0·001 | 0·000 |
| Wo | 0·036 | 0·005 | 0·003 | 0·007 | 0·031 | 0·018 | 0·000 | 0·000 | 0·000 | 0·000 | 0·000 | 0·000 |
| En | 0·796 | 0·006 | 0·003 | 0·804 | 0·033 | 0·019 | 0·798 | 0·122 | 0·122 | 0·833 | 0·004 | 0·003 |

| Sample: | C169 ($n=20$) | | | C218 ($n=16$) | | | C201 ($n=7$) | | | C194 ($n=6$) | | |
|---|---|---|---|---|---|---|---|---|---|---|---|---|
| | Average | 2σ | 2σ mean | Average | 2σ | 2σ mean | Average | 2σ | 2σ mean | Average | 2σ | 2σ mean |
| $SiO_2$ | 53·56 | 1·21 | 0·28 | 54·27 | 0·89 | 0·23 | 53·34 | 1·11 | 0·45 | 53·22 | 1·54 | 0·69 |
| $TiO_2$ | 0·08 | 0·10 | 0·02 | 0·05 | 0·05 | 0·01 | 0·05 | 0·10 | 0·04 | 0·05 | 0·09 | 0·04 |
| $Cr_2O_3$ | 0·19 | 0·18 | 0·04 | 0·14 | 0·15 | 0·04 | 0·08 | 0·12 | 0·05 | 0·07 | 0·15 | 0·07 |
| $Al_2O_3$ | 3·50 | 1·12 | 0·26 | 3·31 | 0·74 | 0·19 | 3·43 | 0·70 | 0·29 | 4·45 | 1·04 | 0·47 |
| $Fe_2O_3$ | 1·93 | 1·04 | 0·24 | 1·40 | 1·86 | 0·48 | 2·09 | 2·32 | 0·95 | 1·96 | 1·65 | 0·74 |
| FeO | 11·99 | 2·65 | 0·61 | 11·36 | 1·32 | 0·34 | 10·74 | 1·04 | 0·42 | 12·27 | 2·25 | 1·01 |
| MnO | 0·31 | 0·06 | 0·01 | 0·29 | 0·04 | 0·01 | 0·25 | 0·22 | 0·09 | 0·30 | 0·05 | 0·02 |
| NiO | 0·04 | 0·06 | 0·01 | 0·04 | 0·05 | 0·01 | 0·02 | 0·09 | 0·04 | 0·02 | 0·06 | 0·03 |
| MgO | 28·08 | 2·50 | 0·57 | 29·53 | 0·55 | 0·14 | 29·24 | 0·41 | 0·17 | 28·15 | 1·70 | 0·76 |
| CaO | 1·19 | 2·70 | 0·62 | 0·42 | 0·18 | 0·05 | 0·43 | 0·26 | 0·11 | 0·43 | 0·30 | 0·14 |
| $Na_2O$ | 0·04 | 0·17 | 0·04 | 0·01 | 0·04 | 0·01 | 0·03 | 0·03 | 0·01 | 0·07 | 0·07 | 0·03 |
| $K_2O$ | 0·01 | 0·01 | 0·00 | 0·00 | 0·01 | 0·00 | 0·01 | 0·02 | 0·01 | 0·02 | 0·03 | 0·01 |
| Total | 100·90 | | | 100·84 | | | 99·71 | | | 100·99 | | |
| Si | 1·8980 | 0·0214 | 0·0049 | 1·9100 | 0·0358 | 0·0093 | 1·8987 | 0·0292 | 0·0119 | 1·8817 | 0·0301 | 0·0135 |
| Ti | 0·0021 | 0·0026 | 0·0006 | 0·0014 | 0·0014 | 0·0003 | 0·0013 | 0·0025 | 0·0010 | 0·0013 | 0·0023 | 0·0010 |
| Cr | 0·0052 | 0·0049 | 0·0011 | 0·0040 | 0·0041 | 0·0011 | 0·0023 | 0·0032 | 0·0013 | 0·0018 | 0·0044 | 0·0020 |
| Al | 0·1459 | 0·0449 | 0·0103 | 0·1371 | 0·0303 | 0·0078 | 0·1440 | 0·0287 | 0·0117 | 0·1853 | 0·0438 | 0·0196 |
| $Fe^{3+}$ | 0·0515 | 0·0273 | 0·0063 | 0·0371 | 0·0490 | 0·0127 | 0·0561 | 0·0624 | 0·0255 | 0·0522 | 0·0440 | 0·0197 |

(continued)

*Table 5: Continued*

| Sample: | C169 ($n=20$) | | | C218 ($n=16$) | | | C201 ($n=7$) | | | C194 ($n=6$) | | |
|---|---|---|---|---|---|---|---|---|---|---|---|---|
| | Average | 2σ | 2σ mean | Average | 2σ | 2σ mean | Average | 2σ | 2σ mean | Average | 2σ | 2σ mean |
| $Fe^{2+}$ | 0·3555 | 0·0822 | 0·0189 | 0·3346 | 0·0404 | 0·0104 | 0·3196 | 0·0308 | 0·0126 | 0·3631 | 0·0698 | 0·0312 |
| Mn | 0·0093 | 0·0020 | 0·0005 | 0·0087 | 0·0012 | 0·0003 | 0·0075 | 0·0067 | 0·0027 | 0·0089 | 0·0015 | 0·0007 |
| Ni | 0·0013 | 0·0016 | 0·0004 | 0·0011 | 0·0014 | 0·0004 | 0·0007 | 0·0025 | 0·0010 | 0·0005 | 0·0016 | 0·0007 |
| Mg | 1·4833 | 0·1199 | 0·0275 | 1·5489 | 0·0205 | 0·0053 | 1·5511 | 0·0080 | 0·0033 | 1·4836 | 0·0691 | 0·0309 |
| Ca | 0·0450 | 0·1019 | 0·0234 | 0·0160 | 0·0069 | 0·0018 | 0·0162 | 0·0100 | 0·0041 | 0·0163 | 0·0119 | 0·0053 |
| Na | 0·0026 | 0·0115 | 0·0026 | 0·0009 | 0·0026 | 0·0007 | 0·0020 | 0·0022 | 0·0009 | 0·0045 | 0·0053 | 0·0024 |
| K | 0·0003 | 0·0005 | 0·0001 | 0·0002 | 0·0006 | 0·0002 | 0·0005 | 0·0007 | 0·0003 | 0·0008 | 0·0013 | 0·0006 |
| Mg-no. | 0·785 | 0·036 | 0·008 | 0·807 | 0·012 | 0·003 | 0·805 | 0·020 | 0·008 | 0·781 | 0·027 | 0·012 |
| Fs | 0·178 | 0·041 | 0·009 | 0·167 | 0·020 | 0·005 | 0·160 | 0·015 | 0·006 | 0·182 | 0·035 | 0·016 |
| Wo | 0·041 | 0·024 | 0·005 | 0·046 | 0·019 | 0·005 | 0·040 | 0·038 | 0·015 | 0·062 | 0·036 | 0·016 |
| En | 0·742 | 0·060 | 0·014 | 0·775 | 0·010 | 0·003 | 0·776 | 0·004 | 0·002 | 0·742 | 0·035 | 0·015 |

| Sample: | C34 ($n=8$) | | | C36 ($n=6$) | | | C33 ($n=3$) | | | C03-17 ($n=3$) | | |
|---|---|---|---|---|---|---|---|---|---|---|---|---|
| | Average | 2σ | 2σ mean | Average | 2σ | 2σ mean | Average | 2σ | 2σ mean | Average | 2σ | 2σ mean |
| $SiO_2$ | 55·08 | 1·95 | 0·74 | 55·53 | 1·33 | 0·60 | 54·74 | 0·79 | 0·56 | 55·30 | 0·26 | 0·36 |
| $TiO_2$ | 0·01 | 0·02 | 0·01 | 0·05 | 0·07 | 0·03 | 0·05 | 0·03 | 0·02 | 0·07 | 0·00 | 0·00 |
| $Cr_2O_3$ | 0·12 | 0·21 | 0·08 | 0·14 | 0·20 | 0·09 | 0·15 | 0·09 | 0·06 | 0·12 | 0·05 | 0·07 |
| $Al_2O_3$ | 2·17 | 1·93 | 0·73 | 2·01 | 1·90 | 0·85 | 2·78 | 0·33 | 0·23 | 1·70 | 0·26 | 0·36 |
| $Fe_2O_3$ | 0·37 | 1·45 | 0·55 | 0·00 | 0·02 | 0·01 | 2·07 | 0·39 | 0·28 | 2·97 | 0·17 | 0·24 |
| FeO | 10·90 | 1·37 | 0·52 | 10·85 | 0·36 | 0·16 | 9·49 | 1·10 | 0·78 | 8·17 | 0·05 | 0·07 |
| MnO | 0·28 | 0·06 | 0·02 | 0·25 | 0·05 | 0·02 | 0·29 | 0·03 | 0·02 | 0·34 | 0·01 | 0·01 |
| NiO | 0·03 | 0·06 | 0·02 | 0·03 | 0·04 | 0·02 | 0·04 | 0·01 | 0·01 | 0·03 | 0·00 | 0·00 |
| MgO | 30·07 | 1·29 | 0·49 | 30·30 | 1·59 | 0·71 | 30·89 | 0·13 | 0·09 | 32·13 | 0·15 | 0·21 |
| CaO | 0·24 | 0·13 | 0·05 | 0·24 | 0·26 | 0·12 | 0·41 | 0·17 | 0·12 | 0·30 | 0·03 | 0·04 |
| $Na_2O$ | 0·01 | 0·02 | 0·01 | 0·02 | 0·01 | 0·01 | 0·02 | 0·03 | 0·02 | 0·00 | 0·00 | 0·00 |
| $K_2O$ | 0·01 | 0·02 | 0·01 | 0·01 | 0·02 | 0·01 | 0·01 | 0·02 | 0·02 | 0·00 | 0·00 | 0·00 |
| Total | 99·28 | | | 99·45 | | | 100·92 | | | 101·13 | 0·53 | 0·74 |
| Si | 1·9584 | 0·0667 | 0·0252 | 1·9684 | 0·0407 | 0·0182 | 1·9129 | 0·0128 | 0·0091 | 1·9230 | 0·0045 | 0·0063 |
| Ti | 0·0003 | 0·0006 | 0·0002 | 0·0014 | 0·0019 | 0·0008 | 0·0014 | 0·0007 | 0·0005 | 0·0018 | 0·0001 | 0·0001 |
| Cr | 0·0033 | 0·0060 | 0·0023 | 0·0040 | 0·0055 | 0·0025 | 0·0042 | 0·0025 | 0·0018 | 0·0034 | 0·0014 | 0·0019 |
| Al | 0·0910 | 0·0809 | 0·0306 | 0·0842 | 0·0798 | 0·0357 | 0·1143 | 0·0147 | 0·0104 | 0·0696 | 0·0105 | 0·0148 |
| $Fe^{3+}$ | 0·0098 | 0·0389 | 0·0147 | 0·0001 | 0·0006 | 0·0003 | 0·0544 | 0·0107 | 0·0076 | 0·0776 | 0·0042 | 0·0059 |
| $Fe^{2+}$ | 0·3242 | 0·0403 | 0·0152 | 0·3216 | 0·0118 | 0·0053 | 0·2771 | 0·0301 | 0·0213 | 0·2376 | 0·0005 | 0·0007 |
| Mn | 0·0084 | 0·0018 | 0·0007 | 0·0075 | 0·0015 | 0·0007 | 0·0085 | 0·0009 | 0·0006 | 0·0100 | 0·0003 | 0·0004 |
| Ni | 0·0008 | 0·0018 | 0·0007 | 0·0008 | 0·0010 | 0·0005 | 0·0011 | 0·0003 | 0·0002 | 0·0009 | 0·0001 | 0·0001 |
| Mg | 1·5936 | 0·0551 | 0·0208 | 1·6007 | 0·0706 | 0·0316 | 1·6093 | 0·0195 | 0·0138 | 1·6650 | 0·0042 | 0·0060 |
| Ca | 0·0093 | 0·0050 | 0·0019 | 0·0092 | 0·0101 | 0·0045 | 0·0154 | 0·0060 | 0·0043 | 0·0110 | 0·0010 | 0·0014 |
| Na | 0·0007 | 0·0016 | 0·0006 | 0·0015 | 0·0010 | 0·0005 | 0·0011 | 0·0015 | 0·0011 | 0·0001 | 0·0002 | 0·0003 |
| K | 0·0003 | 0·0009 | 0·0003 | 0·0006 | 0·0011 | 0·0005 | 0·0004 | 0·0006 | 0·0004 | 0·0001 | 0·0001 | 0·0001 |
| Mg-no. | 0·827 | 0·009 | 0·003 | 0·833 | 0·011 | 0·005 | 0·829 | 0·010 | 0·007 | 0·841 | 0·002 | 0·002 |
| Fs | 0·162 | 0·020 | 0·008 | 0·161 | 0·006 | 0·003 | 0·139 | 0·015 | 0·011 | 0·119 | 0·000 | 0·000 |
| Wo | 0·031 | 0·041 | 0·016 | 0·025 | 0·033 | 0·015 | 0·026 | 0·003 | 0·002 | 0·000 | 0·000 | 0·000 |
| En | 0·797 | 0·028 | 0·011 | 0·801 | 0·036 | 0·016 | 0·805 | 0·010 | 0·007 | 0·833 | 0·002 | 0·003 |

(continued)

*Table 5: Continued*

| Sample: | C35 ($n=3$) | | | C03-15 ($n=4$) | | | C50.1 ($n=4$) | | | C50.4 ($n=12$) | | |
|---|---|---|---|---|---|---|---|---|---|---|---|---|
| | Average | 2σ | 2σ mean | Average | 2σ | 2σ mean | Average | 2σ | 2σ mean | Average | 2σ | 2σ mean |
| $SiO_2$ | 54·94 | 1·28 | 0·90 | 53·80 | 0·82 | 0·95 | 54·32 | 1·14 | 0·66 | 52·65 | 1·18 | 0·35 |
| $TiO_2$ | 0·07 | 0·06 | 0·04 | 0·06 | 0·02 | 0·02 | 0·06 | 0·08 | 0·04 | 0·15 | 0·09 | 0·03 |
| $Cr_2O_3$ | 0·12 | 0·05 | 0·04 | 0·21 | 0·08 | 0·09 | 0·15 | 0·20 | 0·11 | 0·11 | 0·06 | 0·02 |
| $Al_2O_3$ | 2·39 | 0·73 | 0·52 | 2·63 | 0·61 | 0·70 | 2·74 | 0·46 | 0·27 | 2·44 | 0·41 | 0·12 |
| $Fe_2O_3$ | 1·65 | 0·92 | 0·65 | 2·99 | 0·31 | 0·36 | 0·24 | 0·95 | 0·55 | 3·00 | 1·66 | 0·50 |
| FeO | 10·63 | 0·70 | 0·50 | 10·00 | 0·77 | 0·89 | 12·31 | 1·84 | 1·07 | 13·42 | 2·32 | 0·70 |
| MnO | 0·30 | 0·01 | 0·01 | 0·32 | 0·02 | 0·02 | 0·27 | 0·03 | 0·02 | 0·34 | 0·04 | 0·01 |
| NiO | 0·01 | 0·02 | 0·01 | 0·02 | 0·01 | 0·01 | 0·02 | 0·04 | 0·03 | 0·03 | 0·07 | 0·02 |
| MgO | 30·31 | 0·89 | 0·63 | 30·04 | 0·95 | 1·10 | 28·15 | 1·84 | 1·06 | 27·06 | 1·41 | 0·42 |
| CaO | 0·38 | 0·05 | 0·04 | 0·35 | 0·09 | 0·11 | 0·32 | 0·14 | 0·08 | 0·68 | 1·15 | 0·35 |
| $Na_2O$ | 0·05 | 0·07 | 0·05 | 0·01 | 0·01 | 0·01 | 0·07 | 0·11 | 0·06 | 0·04 | 0·05 | 0·02 |
| $K_2O$ | 0·02 | 0·02 | 0·02 | 0·00 | 0·00 | 0·00 | 0·02 | 0·01 | 0·01 | 0·01 | 0·03 | 0·01 |
| Total | 100·86 | | | 100·43 | 0·47 | 0·55 | 98·65 | | | 99·92 | | |
| Si | 1·9276 | 0·0052 | 0·0037 | 1·9012 | 0·0144 | 0·0166 | 1·9600 | 0·0422 | 0·0243 | 1·9033 | 0·0272 | 0·0082 |
| Ti | 0·0017 | 0·0013 | 0·0009 | 0·0016 | 0·0005 | 0·0006 | 0·0016 | 0·0021 | 0·0012 | 0·0040 | 0·0023 | 0·0007 |
| Cr | 0·0033 | 0·0014 | 0·0010 | 0·0058 | 0·0023 | 0·0026 | 0·0043 | 0·0055 | 0·0032 | 0·0032 | 0·0018 | 0·0005 |
| Al | 0·0990 | 0·0319 | 0·0226 | 0·1097 | 0·0261 | 0·0302 | 0·1166 | 0·0205 | 0·0119 | 0·1038 | 0·0172 | 0·0052 |
| $Fe^{3+}$ | 0·0435 | 0·0236 | 0·0167 | 0·0796 | 0·0081 | 0·0094 | 0·0065 | 0·0258 | 0·0149 | 0·0816 | 0·0456 | 0·0138 |
| $Fe^{2+}$ | 0·3118 | 0·0213 | 0·0151 | 0·2956 | 0·0245 | 0·0283 | 0·3714 | 0·0569 | 0·0328 | 0·4058 | 0·0704 | 0·0212 |
| Mn | 0·0090 | 0·0001 | 0·0001 | 0·0097 | 0·0005 | 0·0006 | 0·0082 | 0·0010 | 0·0006 | 0·0105 | 0·0011 | 0·0003 |
| Ni | 0·0003 | 0·0006 | 0·0004 | 0·0005 | 0·0004 | 0·0004 | 0·0007 | 0·0014 | 0·0008 | 0·0008 | 0·0019 | 0·0006 |
| Mg | 1·5850 | 0·0308 | 0·0218 | 1·5823 | 0·0383 | 0·0442 | 1·5136 | 0·0909 | 0·0525 | 1·4578 | 0·0737 | 0·0222 |
| Ca | 0·0144 | 0·0017 | 0·0012 | 0·0133 | 0·0037 | 0·0042 | 0·0122 | 0·0055 | 0·0032 | 0·0264 | 0·0439 | 0·0132 |
| Na | 0·0035 | 0·0044 | 0·0031 | 0·0006 | 0·0005 | 0·0005 | 0·0044 | 0·0077 | 0·0044 | 0·0024 | 0·0036 | 0·0011 |
| K | 0·0009 | 0·0009 | 0·0007 | 0·0001 | 0·0001 | 0·0001 | 0·0007 | 0·0003 | 0·0002 | 0·0006 | 0·0013 | 0·0004 |
| Mg-no. | 0·817 | 0·009 | 0·006 | 0·808 | 0·012 | 0·014 | 0·800 | 0·023 | 0·014 | 0·749 | 0·024 | 0·007 |
| Fs | 0·156 | 0·011 | 0·008 | 0·148 | 0·012 | 0·014 | 0·186 | 0·028 | 0·016 | 0·203 | 0·035 | 0·011 |
| Wo | 0·022 | 0·029 | 0·020 | 0·011 | 0·012 | 0·014 | 0·026 | 0·023 | 0·014 | 0·007 | 0·017 | 0·005 |
| En | 0·793 | 0·016 | 0·011 | 0·791 | 0·019 | 0·022 | 0·757 | 0·045 | 0·026 | 0·729 | 0·037 | 0·011 |

| Sample: | C50.10 ($n=20$) | | | C50.6 ($n=9$) | | | C50.8 ($n=2$) | | | C50.9 ($n=10$) | | |
|---|---|---|---|---|---|---|---|---|---|---|---|---|
| | Average | 2σ | 2σ mean | Average | 2σ | 2σ mean | Average | 2σ | 2σ mean | Average | 2σ | 2σ mean |
| $SiO_2$ | 54·12 | 1·19 | 0·22 | 52·41 | 1·79 | 0·63 | 53·34 | 0·68 | | 53·45 | 0·96 | 0·34 |
| $TiO_2$ | 0·10 | 0·06 | 0·01 | 0·12 | 0·06 | 0·02 | 0·12 | 0·03 | | 0·11 | 0·06 | 0·02 |
| $Cr_2O_3$ | 0·11 | 0·06 | 0·01 | 0·10 | 0·06 | 0·02 | 0·08 | 0·07 | | 0·13 | 0·03 | 0·01 |
| $Al_2O_3$ | 2·34 | 0·73 | 0·16 | 1·86 | 0·21 | 0·08 | 1·70 | 0·10 | | 1·80 | 0·39 | 0·14 |
| $Fe_2O_3$ | 0·35 | 1·19 | 0·29 | 3·54 | 2·52 | 0·89 | 1·20 | 1·47 | | 1·73 | 1·47 | 0·52 |
| FeO | 14·84 | 2·78 | 0·44 | 12·49 | 2·46 | 0·87 | 15·99 | 0·47 | | 14·58 | 1·90 | 0·67 |
| MnO | 0·30 | 0·06 | 0·01 | 0·33 | 0·03 | 0·01 | 0·31 | 0·00 | | 0·34 | 0·03 | 0·01 |
| NiO | 0·06 | 0·36 | 0·11 | 0·04 | 0·09 | 0·03 | 0·01 | 0·03 | | 0·05 | 0·09 | 0·03 |
| MgO | 27·06 | 1·91 | 0·28 | 27·63 | 0·48 | 0·17 | 26·27 | 0·72 | | 26·93 | 1·01 | 0·36 |
| CaO | 0·46 | 0·31 | 0·07 | 0·48 | 0·10 | 0·04 | 0·56 | 0·03 | | 0·68 | 1·34 | 0·47 |

(continued)

*Table 5: Continued*

| Sample: | C50.10 ($n=20$) | | | C50.6 ($n=9$) | | | C50.8 ($n=2$) | | | C50.9 ($n=10$) | | |
|---|---|---|---|---|---|---|---|---|---|---|---|---|
| | Average | 2σ | 2σ mean | Average | 2σ | 2σ mean | Average | 2σ | 2σ mean | Average | 2σ | 2σ mean |
| $Na_2O$ | 0·05 | 0·17 | 0·05 | 0·01 | 0·02 | 0·01 | 0·01 | 0·00 | | 0·03 | 0·04 | 0·02 |
| $K_2O$ | 0·02 | 0·04 | 0·01 | 0·01 | 0·02 | 0·01 | 0·01 | 0·01 | | 0·01 | 0·02 | 0·01 |
| Total | 99·81 | | | 99·01 | | | 99·58 | | | 99·84 | | |
| Si | 1·9507 | 0·0377 | 0·0058 | 1·9074 | 0·0366 | 0·0129 | 1·9433 | 0·0156 | | 1·9347 | 0·0186 | 0·0066 |
| Ti | 0·0028 | 0·0017 | 0·0004 | 0·0032 | 0·0016 | 0·0006 | 0·0033 | 0·0007 | | 0·0029 | 0·0015 | 0·0005 |
| Cr | 0·0030 | 0·0018 | 0·0004 | 0·0029 | 0·0018 | 0·0006 | 0·0022 | 0·0024 | | 0·0037 | 0·0010 | 0·0004 |
| Al | 0·0994 | 0·0302 | 0·0068 | 0·0796 | 0·0088 | 0·0031 | 0·0727 | 0·0062 | | 0·0767 | 0·0168 | 0·0059 |
| $Fe^{3+}$ | 0·0093 | 0·0321 | 0·0079 | 0·0972 | 0·0701 | 0·0248 | 0·0328 | 0·0396 | | 0·0470 | 0·0403 | 0·0142 |
| $Fe^{2+}$ | 0·4475 | 0·0894 | 0·0137 | 0·3800 | 0·0698 | 0·0247 | 0·4870 | 0·0245 | | 0·4413 | 0·0548 | 0·0194 |
| Mn | 0·0093 | 0·0018 | 0·0004 | 0·0103 | 0·0009 | 0·0003 | 0·0097 | 0·0003 | | 0·0104 | 0·0009 | 0·0003 |
| Ni | 0·0017 | 0·0102 | 0·0031 | 0·0011 | 0·0025 | 0·0009 | 0·0003 | 0·0008 | | 0·0013 | 0·0024 | 0·0009 |
| Mg | 1·4536 | 0·0790 | 0·0110 | 1·4987 | 0·0335 | 0·0118 | 1·4262 | 0·0092 | | 1·4529 | 0·0527 | 0·0186 |
| Ca | 0·0177 | 0·0120 | 0·0026 | 0·0186 | 0·0040 | 0·0014 | 0·0220 | 0·0006 | | 0·0265 | 0·0521 | 0·0184 |
| Na | 0·0038 | 0·0118 | 0·0033 | 0·0006 | 0·0014 | 0·0005 | 0·0004 | 0·0000 | | 0·0021 | 0·0030 | 0·0011 |
| K | 0·0009 | 0·0017 | 0·0004 | 0·0004 | 0·0007 | 0·0002 | 0·0004 | 0·0010 | | 0·0005 | 0·0006 | 0·0002 |
| Mg-no. | 0·761 | 0·042 | 0·006 | 0·759 | 0·007 | 0·002 | 0·733 | 0·004 | | 0·748 | 0·014 | 0·005 |
| Fs | 0·224 | 0·045 | 0·007 | 0·190 | 0·035 | 0·012 | 0·243 | 0·012 | | 0·221 | 0·027 | 0·010 |
| Wo | 0·032 | 0·023 | 0·005 | 0·002 | 0·010 | 0·004 | 0·015 | 0·021 | | 0·011 | 0·018 | 0·006 |
| En | 0·728 | 0·040 | 0·006 | 0·750 | 0·017 | 0·006 | 0·713 | 0·005 | | 0·727 | 0·026 | 0·009 |

| Sample: | C7 ($n=5$) | | | C66 ($n=10$) | | | C41 ($n=7$) | | | C48 ($n=25$) | | |
|---|---|---|---|---|---|---|---|---|---|---|---|---|
| | Average | 2σ | 2σ mean | Average | 2σ | 2σ mean | Average | 2σ | 2σ mean | Average | 2σ | 2σ mean |
| $SiO_2$ | 52·52 | 0·96 | 0·55 | 52·18 | 2·64 | 0·84 | 52·77 | 0·38 | 0·16 | 53·63 | 0·91 | 0·19 |
| $TiO_2$ | 0·10 | 0·02 | 0·01 | 0·01 | 0·02 | 0·01 | 0·06 | 0·03 | 0·01 | 0·08 | 0·05 | 0·01 |
| $Cr_2O_3$ | 0·06 | 0·04 | 0·02 | 0·03 | 0·08 | 0·03 | 0·14 | 0·09 | 0·04 | 0·07 | 0·07 | 0·01 |
| $Al_2O_3$ | 1·64 | 0·18 | 0·10 | 3·47 | 0·47 | 0·15 | 2·08 | 0·37 | 0·15 | 1·65 | 1·18 | 0·24 |
| $Fe_2O_3$ | 3·10 | 1·08 | 0·62 | 5·50 | 3·19 | 1·01 | 0·68 | 1·37 | 0·56 | 0·34 | 0·98 | 0·20 |
| FeO | 16·64 | 1·29 | 0·74 | 7·81 | 3·03 | 0·96 | 19·12 | 1·92 | 0·78 | 19·29 | 1·25 | 0·25 |
| MnO | 0·39 | 0·07 | 0·04 | 0·28 | 0·05 | 0·02 | 0·47 | 0·08 | 0·03 | 0·40 | 0·07 | 0·01 |
| NiO | 0·04 | 0·08 | 0·04 | 0·05 | 0·06 | 0·02 | 0·02 | 0·05 | 0·02 | 0·03 | 0·06 | 0·01 |
| MgO | 25·27 | 0·66 | 0·38 | 30·09 | 0·47 | 0·15 | 23·96 | 1·48 | 0·61 | 24·34 | 1·00 | 0·20 |
| CaO | 0·50 | 0·13 | 0·08 | 0·44 | 0·24 | 0·08 | 0·49 | 0·06 | 0·03 | 0·51 | 0·28 | 0·06 |
| $Na_2O$ | 0·03 | 0·04 | 0·02 | 0·01 | 0·03 | 0·01 | 0·02 | 0·03 | 0·01 | 0·04 | 0·08 | 0·02 |
| $K_2O$ | 0·01 | 0·01 | 0·01 | 0·00 | 0·01 | 0·00 | 0·00 | 0·01 | 0·00 | 0·02 | 0·07 | 0·01 |
| Total | 100·29 | | 0·64 | 99·88 | | | 99·83 | | | 100·39 | | |
| Si | 1·9197 | 0·0139 | 0·0080 | 1·8534 | 0·0530 | 0·0168 | 1·9440 | 0·0297 | 0·0121 | 1·9618 | 0·0279 | 0·0057 |
| Ti | 0·0028 | 0·0007 | 0·0004 | 0·0002 | 0·0006 | 0·0002 | 0·0017 | 0·0006 | 0·0003 | 0·0021 | 0·0013 | 0·0003 |
| Cr | 0·0017 | 0·0012 | 0·0007 | 0·0010 | 0·0023 | 0·0007 | 0·0040 | 0·0026 | 0·0010 | 0·0019 | 0·0021 | 0·0004 |
| Al | 0·0704 | 0·0077 | 0·0045 | 0·1454 | 0·0217 | 0·0069 | 0·0905 | 0·0154 | 0·0063 | 0·0712 | 0·0502 | 0·0103 |
| $Fe^{3+}$ | 0·0852 | 0·0302 | 0·0174 | 0·1475 | 0·0892 | 0·0282 | 0·0188 | 0·0377 | 0·0154 | 0·0094 | 0·0268 | 0·0055 |
| $Fe^{2+}$ | 0·5087 | 0·0399 | 0·0230 | 0·2317 | 0·0856 | 0·0271 | 0·5889 | 0·0615 | 0·0251 | 0·5900 | 0·0432 | 0·0088 |
| Mn | 0·0122 | 0·0021 | 0·0012 | 0·0084 | 0·0016 | 0·0005 | 0·0147 | 0·0026 | 0·0010 | 0·0124 | 0·0021 | 0·0004 |

(continued)

*Table 5: Continued*

| Sample: | C7 ($n=5$) | | | C66 ($n=10$) | | | C41 ($n=7$) | | | C48 ($n=25$) | | |
|---|---|---|---|---|---|---|---|---|---|---|---|---|
| | Average | 2σ | 2σ mean | Average | 2σ | 2σ mean | Average | 2σ | 2σ mean | Average | 2σ | 2σ mean |
| Ni | 0·0011 | 0·0024 | 0·0014 | 0·0015 | 0·0018 | 0·0006 | 0·0007 | 0·0015 | 0·0006 | 0·0009 | 0·0019 | 0·0004 |
| Mg | 1·3764 | 0·0222 | 0·0128 | 1·5932 | 0·0383 | 0·0121 | 1·3156 | 0·0773 | 0·0316 | 1·3268 | 0·0436 | 0·0089 |
| Ca | 0·0197 | 0·0052 | 0·0030 | 0·0166 | 0·0089 | 0·0028 | 0·0195 | 0·0024 | 0·0010 | 0·0200 | 0·0108 | 0·0022 |
| Na | 0·0020 | 0·0027 | 0·0016 | 0·0010 | 0·0017 | 0·0005 | 0·0013 | 0·0021 | 0·0008 | 0·0027 | 0·0055 | 0·0011 |
| K | 0·0002 | 0·0003 | 0·0002 | 0·0002 | 0·0004 | 0·0001 | 0·0002 | 0·0005 | 0·0002 | 0·0007 | 0·0031 | 0·0006 |
| Mg-no. | 0·699 | 0·011 | 0·006 | 0·808 | 0·009 | 0·003 | 0·684 | 0·041 | 0·017 | 0·689 | 0·018 | 0·004 |
| Fs | 0·254 | 0·020 | 0·012 | 0·116 | 0·043 | 0·014 | 0·294 | 0·031 | 0·013 | 0·295 | 0·022 | 0·004 |
| Wo | 0·000 | 0·000 | 0·000 | 0·000 | 0·000 | 0·000 | 0·030 | 0·015 | 0·006 | 0·023 | 0·023 | 0·005 |
| En | 0·689 | 0·012 | 0·007 | 0·797 | 0·019 | 0·006 | 0·658 | 0·038 | 0·016 | 0·664 | 0·022 | 0·004 |

| Sample: | C129 ($n=15$) | | | C134 ($n=12$) | | | C04-9 ($n=10$) | | | C171 ($n=2$) | | |
|---|---|---|---|---|---|---|---|---|---|---|---|---|
| | Average | 2σ | 2σ mean | Average | 2σ | 2σ mean | Average | 2σ | 2σ mean | Average | 2σ | 2σ mean |
| $SiO_2$ | 52·38 | 1·32 | 0·35 | 52·35 | 1·50 | 0·43 | 54·53 | 1·13 | 0·38 | 53·55 | 0·45 | |
| $TiO_2$ | 0·09 | 0·07 | 0·02 | 0·07 | 0·05 | 0·01 | 0·11 | 0·07 | 0·02 | 0·09 | 0·00 | |
| $Cr_2O_3$ | 0·03 | 0·04 | 0·01 | 0·03 | 0·07 | 0·02 | 0·18 | 0·11 | 0·04 | 0·17 | 0·02 | |
| $Al_2O_3$ | 1·59 | 0·23 | 0·06 | 1·82 | 1·29 | 0·37 | 3·30 | 0·58 | 0·19 | 2·57 | 0·27 | |
| $Fe_2O_3$ | 0·60 | 1·73 | 0·46 | 0·50 | 0·94 | 0·27 | 0·71 | 1·17 | 0·39 | 2·66 | 1·63 | |
| FeO | 22·43 | 2·24 | 0·60 | 22·77 | 6·37 | 1·84 | 11·94 | 1·33 | 0·44 | 9·12 | 1·84 | |
| MnO | 0·53 | 0·07 | 0·02 | 0·59 | 0·28 | 0·08 | 0·30 | 0·05 | 0·02 | 0·29 | 0·04 | |
| NiO | 0·01 | 0·04 | 0·01 | 0·02 | 0·04 | 0·01 | 0·00 | 0·00 | 0·00 | 0·05 | 0·02 | |
| MgO | 21·64 | 1·18 | 0·32 | 21·55 | 4·82 | 1·39 | 29·39 | 0·62 | 0·21 | 30·38 | 0·77 | |
| CaO | 0·66 | 0·64 | 0·17 | 0·50 | 0·18 | 0·05 | 0·49 | 0·81 | 0·27 | 0·37 | 0·05 | |
| $Na_2O$ | 0·02 | 0·03 | 0·01 | 0·01 | 0·02 | 0·01 | 0·00 | 0·01 | 0·00 | 0·01 | 0·01 | |
| $K_2O$ | 0·01 | 0·02 | 0·01 | 0·01 | 0·02 | 0·01 | 0·00 | 0·01 | 0·00 | 0·00 | 0·00 | |
| Total | 99·99 | | | 100·21 | | | 100·96 | | | 99·25 | 0·41 | |
| Si | 1·9578 | 0·0323 | 0·0086 | 1·9541 | 0·0402 | 0·0116 | 1·9173 | 0·0203 | 0·0068 | 1·9061 | 0·0276 | |
| Ti | 0·0025 | 0·0020 | 0·0005 | 0·0020 | 0·0014 | 0·0004 | 0·0029 | 0·0020 | 0·0007 | 0·0024 | 0·0001 | |
| Cr | 0·0008 | 0·0010 | 0·0003 | 0·0007 | 0·0019 | 0·0005 | 0·0051 | 0·0031 | 0·0010 | 0·0047 | 0·0006 | |
| Al | 0·0700 | 0·0102 | 0·0027 | 0·0796 | 0·0509 | 0·0147 | 0·1369 | 0·0241 | 0·0080 | 0·1076 | 0·0107 | |
| $Fe^{3+}$ | 0·0170 | 0·0489 | 0·0131 | 0·0138 | 0·0259 | 0·0075 | 0·0188 | 0·0312 | 0·0104 | 0·0712 | 0·0434 | |
| $Fe^{2+}$ | 0·7012 | 0·0721 | 0·0193 | 0·7128 | 0·2223 | 0·0642 | 0·3511 | 0·0366 | 0·0122 | 0·2716 | 0·0566 | |
| Mn | 0·0167 | 0·0022 | 0·0006 | 0·0187 | 0·0093 | 0·0027 | 0·0090 | 0·0015 | 0·0005 | 0·0088 | 0·0013 | |
| Ni | 0·0004 | 0·0011 | 0·0003 | 0·0006 | 0·0011 | 0·0003 | 0·0000 | 0·0000 | 0·0000 | 0·0015 | 0·0006 | |
| Mg | 1·2054 | 0·0584 | 0·0156 | 1·1965 | 0·2054 | 0·0593 | 1·5402 | 0·0342 | 0·0114 | 1·6116 | 0·0305 | |
| Ca | 0·0263 | 0·0253 | 0·0068 | 0·0202 | 0·0078 | 0·0022 | 0·0184 | 0·0306 | 0·0102 | 0·0141 | 0·0021 | |
| Na | 0·0016 | 0·0023 | 0·0006 | 0·0008 | 0·0017 | 0·0005 | 0·0002 | 0·0006 | 0·0002 | 0·0004 | 0·0006 | |
| K | 0·0002 | 0·0009 | 0·0002 | 0·0003 | 0·0010 | 0·0003 | 0·0001 | 0·0003 | 0·0001 | 0·0001 | 0·0001 | |
| Mg-no. | 0·627 | 0·027 | 0·007 | 0·622 | 0·108 | 0·031 | 0·806 | 0·008 | 0·003 | 0·825 | 0·008 | |
| Fs | 0·351 | 0·036 | 0·010 | 0·356 | 0·111 | 0·032 | 0·176 | 0·018 | 0·006 | 0·136 | 0·028 | |
| Wo | 0·019 | 0·023 | 0·006 | 0·027 | 0·025 | 0·007 | 0·053 | 0·018 | 0·006 | 0·013 | 0·016 | |
| En | 0·603 | 0·029 | 0·008 | 0·599 | 0·103 | 0·030 | 0·770 | 0·017 | 0·006 | 0·807 | 0·016 | |

(continued)

*Table 5: Continued*

| Sample: | C203 ($n=5$) | | | C135 ($n=10$) | | | C141 ($n=22$) | | | C135 ($n=8$) | | |
|---|---|---|---|---|---|---|---|---|---|---|---|---|
| | Average | 2σ | 2σ mean | Average | 2σ | 2σ mean | Average | 2σ | 2σ mean | Average | 2σ | 2σ mean |
| $SiO_2$ | 54·18 | 2·82 | 1·41 | 53·86 | 0·20 | 0·07 | 53·26 | 1·01 | 0·44 | 53·51 | 0·39 | 0·15 |
| $TiO_2$ | 0·03 | 0·03 | 0·02 | 0·07 | 0·01 | 0·00 | 0·08 | 0·01 | 0·00 | 0·08 | 0·03 | 0·01 |
| $Cr_2O_3$ | 0·09 | 0·04 | 0·02 | 0·02 | 0·04 | 0·01 | 0·01 | 0·03 | 0·01 | 0·01 | 0·03 | 0·01 |
| $Al_2O_3$ | 2·93 | 0·56 | 0·28 | 1·59 | 0·10 | 0·03 | 1·47 | 0·18 | 0·08 | 1·51 | 0·13 | 0·05 |
| $Fe_2O_3$ | 2·01 | 3·77 | 1·88 | 0·00 | 0·00 | 0·00 | | | | 0·00 | 0·00 | 0·00 |
| FeO | 10·95 | 3·68 | 1·84 | 23·86 | 1·02 | 0·34 | 24·67 | 0·39 | 0·17 | 24·19 | 1·18 | 0·45 |
| MnO | 0·30 | 0·05 | 0·02 | 0·60 | 0·08 | 0·03 | 0·70 | 0·03 | 0·01 | 0·67 | 0·04 | 0·01 |
| NiO | 0·02 | 0·05 | 0·02 | 0·02 | 0·06 | 0·02 | 0·01 | 0·02 | 0·01 | 0·02 | 0·06 | 0·02 |
| MgO | 29·64 | 0·52 | 0·26 | 21·29 | 0·48 | 0·16 | 20·09 | 0·66 | 0·29 | 20·45 | 0·31 | 0·12 |
| CaO | 0·32 | 0·21 | 0·11 | 0·59 | 0·09 | 0·03 | 0·69 | 0·08 | 0·04 | 0·64 | 0·08 | 0·03 |
| $Na_2O$ | 0·02 | 0·02 | 0·01 | 0·01 | 0·02 | 0·01 | 0·01 | 0·01 | 0·00 | 0·01 | 0·01 | 0·00 |
| $K_2O$ | 0·00 | 0·01 | 0·01 | 0·00 | 0·01 | 0·00 | 0·02 | 0·03 | 0·01 | 0·00 | 0·01 | 0·01 |
| Total | 100·50 | | | 101·93 | | | 101·01 | | | 101·09 | | |
| Si | 1·9135 | 0·0603 | 0·0301 | 1·9825 | 0·0152 | 0·0051 | 1·9905 | 0·0090 | 0·0039 | 1·9938 | 0·0269 | 0·0102 |
| Ti | 0·0009 | 0·0007 | 0·0004 | 0·0019 | 0·0003 | 0·0001 | 0·0024 | 0·0003 | 0·0001 | 0·0021 | 0·0007 | 0·0003 |
| Cr | 0·0025 | 0·0010 | 0·0005 | 0·0005 | 0·0012 | 0·0004 | 0·0004 | 0·0008 | 0·0004 | 0·0004 | 0·0009 | 0·0004 |
| Al | 0·1218 | 0·0210 | 0·0105 | 0·0691 | 0·0040 | 0·0013 | 0·0649 | 0·0090 | 0·0039 | 0·0663 | 0·0057 | 0·0022 |
| $Fe^{3+}$ | 0·0540 | 0·1025 | 0·0513 | 0·0000 | 0·0000 | 0·0000 | | | | | | |
| $Fe^{2+}$ | 0·3231 | 0·1026 | 0·0513 | 0·7344 | 0·0281 | 0·0094 | 0·7712 | 0·0195 | 0·0085 | 0·7538 | 0·0316 | 0·0119 |
| Mn | 0·0088 | 0·0015 | 0·0007 | 0·0188 | 0·0024 | 0·0008 | 0·0221 | 0·0009 | 0·0004 | 0·0211 | 0·0011 | 0·0004 |
| Ni | 0·0005 | 0·0013 | 0·0006 | 0·0007 | 0·0019 | 0·0006 | 0·0003 | 0·0006 | 0·0002 | 0·0006 | 0·0017 | 0·0006 |
| Mg | 1·5610 | 0·0525 | 0·0262 | 1·1680 | 0·0245 | 0·0082 | 1·1190 | 0·0207 | 0·0090 | 1·1356 | 0·0165 | 0·0062 |
| Ca | 0·0123 | 0·0081 | 0·0041 | 0·0234 | 0·0036 | 0·0012 | 0·0276 | 0·0032 | 0·0014 | 0·0256 | 0·0030 | 0·0011 |
| Na | 0·0014 | 0·0015 | 0·0007 | 0·0005 | 0·0013 | 0·0004 | 0·0006 | 0·0008 | 0·0003 | 0·0004 | 0·0009 | 0·0003 |
| K | 0·0002 | 0·0005 | 0·0002 | 0·0002 | 0·0006 | 0·0002 | 0·0009 | 0·0013 | 0·0006 | 0·0002 | 0·0007 | 0·0003 |
| Mg-no. | 0·805 | 0·006 | 0·003 | 0·614 | 0·014 | 0·005 | 0·592 | 0·010 | 0·005 | 0·601 | 0·013 | 0·005 |
| Fs | 0·162 | 0·051 | 0·026 | 0·009 | 0·001 | 0·000 | 0·386 | 0·010 | 0·004 | 0·011 | 0·001 | 0·000 |
| Wo | 0·030 | 0·040 | 0·020 | 0·014 | 0·015 | 0·005 | 0·006 | 0·006 | 0·003 | 0·006 | 0·019 | 0·007 |
| En | 0·781 | 0·027 | 0·013 | 0·364 | 0·013 | 0·004 | 0·560 | 0·010 | 0·005 | 0·375 | 0·013 | 0·005 |

*Table 6: Trace element concentrations (ppm) in orthopyroxene from the Chilas Complex*

| Sample: | C03-44 | | | C218 | | | C66 | | | C48 | | | C7 | | |
|---|---|---|---|---|---|---|---|---|---|---|---|---|---|---|---|
| *n*: | 5 | | | 8 | | | 7 | | | 7 | | | 10 | | |
| | Average | 2σ | 2σ mean | Average | 2σ | 2σ mean | Average | 2σ | 2σ mean | Average | 2σ | 2σ mean | Average | 2σ | 2σ mean |
| Li | 0·210 | 0·121 | 0·086 | 0·98 | 0·68 | 0·26 | 0·244 | 0·129 | 0·053 | 4·82 | 0·75 | 0·31 | 2·69 | 0·55 | 0·18 |
| Sc | 30·3 | 3·4 | 1·5 | 15·8 | 6·3 | 2·4 | 12·7 | 5·9 | 2·4 | 35·0 | 7·2 | 2·9 | 35·4 | 5·7 | 1·9 |
| V | 73·5 | 3·3 | 1·5 | 57·0 | 38·6 | 14·6 | 31·9 | 13·9 | 5·7 | 172 | 46 | 19 | 152 | 37 | 12 |
| Cr | 941 | 100 | 45 | 964 | 1076 | 407 | 303 | 416 | 170 | 209 | 44 | 18 | 277 | 61 | 20 |
| Co | 71·6 | 1·6 | 0·7 | 69·0 | 7·8 | 3·0 | 66·1 | 5·8 | 2·4 | 114 | 11 | 4 | 109 | 15 | 5 |

(continued)

*Table 6: Continued*

| Sample: | C03-44 | | | C218 | | | C66 | | | C48 | | | C7 | | |
|---|---|---|---|---|---|---|---|---|---|---|---|---|---|---|---|
| *n*: | 5 | | | 8 | | | 7 | | | 7 | | | 10 | | |
| | Average | 2σ | 2σ mean | Average | 2σ | 2σ mean | Average | 2σ | 2σ mean | Average | 2σ | 2σ mean | Average | 2σ | 2σ mean |
| Ni | 191 | 18 | 8 | 217 | 34 | 13 | 211 | 15 | 6 | 226 | 28 | 11 | 234 | 45 | 15 |
| Cu | 0·094 | 0·025 | 0·025 | 1·01 | 0·31 | 0·12 | 0·910 | 0·335 | 0·137 | 2·68 | 5·09 | 2·08 | 1·02 | 0·69 | 0·23 |
| Zn | | | | | | | | | | 270 | 49 | 20 | 262 | 54 | 18 |
| Ga | 3·89 | 0·54 | 0·24 | 2·30 | 0·91 | 0·34 | 3·46 | 1·15 | 0·47 | 8·19 | 1·68 | 0·68 | 7·74 | 1·30 | 0·43 |
| Sr | 0·027 | 0·008 | 0·006 | 0·258 | 0·711 | 0·269 | 0·054 | 0·074 | 0·030 | 0·200 | 0·234 | 0·095 | 0·426 | 0·948 | 0·316 |
| Y | 0·233 | 0·056 | 0·025 | 0·111 | 0·053 | 0·020 | 0·113 | 0·071 | 0·029 | 1·01 | 0·47 | 0·19 | 2·06 | 1·32 | 0·44 |
| Zr | 0·219 | 0·014 | 0·006 | 0·127 | 0·063 | 0·024 | 0·166 | 0·105 | 0·043 | 1·02 | 0·45 | 0·18 | 1·48 | 0·33 | 0·11 |
| Cs | | | | | | | | | | | | | 0·012 | 0·025 | 0·010 |
| Ba | | | | | | | | | | 0·250 | 0·437 | 0·178 | 0·187 | 0·408 | 0·154 |
| La | | | | | | | 0·004 | 0·004 | 0·003 | | | | 0·013 | 0·009 | 0·003 |
| Ce | | | | 0·006 | 0·006 | 0·003 | 0·006 | 0·010 | 0·006 | 0·010 | 0·005 | 0·002 | 0·026 | 0·023 | 0·008 |
| Pr | | | | | | | | | | 0·003 | 0·001 | 0·001 | 0·010 | 0·014 | 0·005 |
| Nd | 0·036* | | | | | | | | | 0·020 | 0·012 | 0·005 | 0·042 | 0·032 | 0·011 |
| Sm | | | | | | | | | | 0·013 | 0·007 | 0·004 | 0·039 | 0·028 | 0·009 |
| Eu | | | | 0·007 | 0·005 | 0·003 | 0·004 | 0·002 | 0·001 | 0·009 | 0·005 | 0·002 | 0·014 | 0·012 | 0·004 |
| Gd | | | | | | | | | | 0·038 | 0·027 | 0·011 | 0·078 | 0·066 | 0·022 |
| Tb | | | | | | | 0·002 | 0·001 | 0·001 | 0·009 | 0·006 | 0·002 | 0·028 | 0·025 | 0·008 |
| Dy | | | | 0·016 | 0·010 | 0·004 | 0·017 | 0·011 | 0·005 | 0·122 | 0·082 | 0·034 | 0·252 | 0·160 | 0·053 |
| Ho | 0·013 | 0·011 | 0·007 | 0·005 | 0·003 | 0·001 | 0·005 | 0·002 | 0·001 | 0·038 | 0·019 | 0·008 | 0·079 | 0·045 | 0·015 |
| Er | 0·041 | 0·035 | 0·020 | 0·024 | 0·018 | 0·007 | 0·018 | 0·012 | 0·005 | 0·168 | 0·061 | 0·025 | 0·331 | 0·203 | 0·068 |
| Tm | 0·007 | 0·002 | 0·001 | 0·005 | 0·002 | 0·001 | 0·004 | 0·002 | 0·001 | 0·038 | 0·016 | 0·006 | 0·077 | 0·037 | 0·012 |
| Yb | 0·092 | 0·077 | 0·045 | 0·053 | 0·041 | 0·016 | 0·041 | 0·031 | 0·013 | 0·428 | 0·197 | 0·080 | 0·761 | 0·389 | 0·130 |
| Lu | 0·016 | 0·003 | 0·002 | 0·010 | 0·005 | 0·002 | 0·010 | 0·008 | 0·003 | 0·084 | 0·028 | 0·011 | 0·148 | 0·061 | 0·020 |
| Hf | 0·022 | 0·032 | 0·023 | 0·010 | 0·004 | 0·002 | 0·009 | 0·007 | 0·003 | 0·052 | 0·024 | 0·010 | 0·085 | 0·038 | 0·013 |
| Ta | | | | | | | | | | | | | 0·004 | 0·006 | 0·002 |
| Pb | 0·042 | 0·021 | 0·011 | 0·032 | 0·013 | 0·005 | 0·048 | 0·039 | 0·016 | 0·063 | 0·033 | 0·014 | 0·068 | 0·048 | 0·016 |
| Th | | | | | | | | | | 0·011 | 0·035 | 0·020 | 0·004 | 0·003 | 0·001 |
| U | | | | 0·007 | 0·013 | 0·005 | 0·002 | 0·003 | 0·002 | 0·004 | 0·001 | 0·001 | 0·012 | 0·018 | 0·006 |

The concentration of trace element for which no value is shown is below detection limit.
*Author's own unpublished TIMS ID data.

*Table 7: Major element concentrations (wt %) in amphibole from the Chilas Complex*

| Sample: | C03-43 ($n=3$) | | | C03-45 ($n=12$) | | | C03-50 ($n=3$) | | |
|---|---|---|---|---|---|---|---|---|---|
| | Average | 2σ | 2σ mean | Average | 2σ | 2σ mean | Average | 2σ | 2σ mean |
| $SiO_2$ | 44·40 | 1·30 | 0·92 | 51·15 | 7·60 | 2·29 | 53·11 | 5·74 | 4·06 |
| $TiO_2$ | 1·08 | 0·12 | 0·09 | 0·36 | 0·47 | 0·14 | 0·29 | 0·31 | 0·22 |
| $Cr_2O_3$ | 0·83 | 0·07 | 0·05 | 6·55 | 7·17 | 2·16 | 0·40 | 0·35 | 0·25 |
| $Al_2O_3$ | 11·38 | 0·93 | 0·66 | 0·66 | 0·70 | 0·21 | 5·07 | 6·05 | 4·28 |
| $Fe_2O_3$ | 5·37 | 3·29 | 2·33 | 2·17 | 2·28 | 0·69 | 2·10 | 2·81 | 1·99 |
| FeO | 1·31 | 2·28 | 1·61 | 2·48 | 2·63 | 0·79 | 2·40 | 1·01 | 0·71 |
| MnO | 0·08 | 0·02 | 0·02 | 0·06 | 0·04 | 0·01 | 0·06 | 0·03 | 0·02 |

(continued)

*Table 7: Continued*

| Sample: | C03-43 ($n=3$) | | | C03-45 ($n=12$) | | | C03-50 ($n=3$) | | |
|---|---|---|---|---|---|---|---|---|---|
| | Average | 2σ | 2σ mean | Average | 2σ | 2σ mean | Average | 2σ | 2σ mean |
| NiO | 0·03 | 0·01 | 0·01 | | 0·00 | | 0·00 | 0·00 | 0·00 |
| MgO | 17·58 | 0·11 | 0·08 | 20·15 | 3·67 | 1·11 | 20·47 | 2·64 | 1·87 |
| CaO | 12·73 | 0·30 | 0·21 | 13·60 | 0·29 | 0·09 | 13·22 | 0·47 | 0·33 |
| $Na_2O$ | 1·93 | 0·00 | 0·00 | 0·98 | 1·18 | 0·36 | 0·71 | 0·90 | 0·64 |
| $K_2O$ | 0·02 | 0·00 | 0·00 | 0·02 | 0·06 | 0·02 | 0·01 | 0·03 | 0·02 |
| $H_2O$ | 2·09 | 0·01 | 0·01 | 2·16 | 0·06 | 0·02 | 2·16 | 0·01 | 0·01 |
| Total | 99·83 | | | 100·32 | | | 100·01 | | |
| Si | 6·3627 | 0·2126 | 0·1503 | 7·1116 | 0·8942 | 0·2696 | 7·3629 | 0·7575 | 0·5357 |
| Ti | 0·1166 | 0·0125 | 0·0088 | 0·0372 | 0·0493 | 0·0149 | 0·0306 | 0·0322 | 0·0228 |
| Cr | 0·0944 | 0·0079 | 0·0056 | 0·0725 | 0·0771 | 0·0232 | 0·0435 | 0·0383 | 0·0271 |
| Al | 1·9222 | 0·1498 | 0·1059 | 1·0790 | 1·1902 | 0·3589 | 0·8288 | 0·9912 | 0·7009 |
| $Fe^{3+}$ | 0·5787 | 0·3525 | 0·2492 | 0·2281 | 0·2434 | 0·0734 | 0·2197 | 0·2941 | 0·2080 |
| $Fe^{2+}$ | 0·1570 | 0·2741 | 0·1938 | 0·2892 | 0·3069 | 0·0925 | 0·2786 | 0·1160 | 0·0820 |
| Mn | 0·0099 | 0·0025 | 0·0018 | 0·0064 | 0·0043 | 0·0013 | 0·0072 | 0·0030 | 0·0021 |
| Ni | 0·0037 | 0·0011 | 0·0008 | | 0·0000 | | 0·0000 | 0·0000 | 0·0000 |
| Mg | 3·7548 | 0·0396 | 0·0280 | 4·1761 | 0·6938 | 0·2092 | 4·2287 | 0·5236 | 0·3702 |
| Ca | 1·9536 | 0·0536 | 0·0379 | 2·0269 | 0·0615 | 0·0186 | 1·9635 | 0·0617 | 0·0436 |
| Na | 0·5362 | 0·0022 | 0·0016 | 0·2647 | 0·3213 | 0·0969 | 0·1917 | 0·2436 | 0·1722 |
| K | 0·0027 | 0·0005 | 0·0004 | 0·0041 | 0·0114 | 0·0034 | 0·0022 | 0·0053 | 0·0037 |
| H | 2 | | | 2 | | | 2 | | |
| Mg-no.($Fe_{tot}$) | 0·836 | 0·016 | 0·011 | 0·888 | 0·064 | 0·019 | 0·894 | 0·053 | 0·037 |

| Sample: | C38 ($n=4$) | | | C34 ($n=6$) | | | C37 ($n=4$) | | |
|---|---|---|---|---|---|---|---|---|---|
| | Average | 2σ | 2σ mean | Average | 2σ | 2σ mean | Average | 2σ | 2σ mean |
| $SiO_2$ | 49·11 | 2·76 | 1·59 | 48·89 | 3·30 | 1·48 | 52·30 | 7·36 | 4·25 |
| $TiO_2$ | 0·35 | 0·22 | 0·13 | 0·33 | 0·13 | 0·06 | 0·19 | 0·28 | 0·16 |
| $Cr_2O_3$ | 8·93 | 3·11 | 1·79 | 0·28 | 0·28 | 0·12 | 0·37 | 0·41 | 0·23 |
| $Al_2O_3$ | 0·50 | 0·19 | 0·11 | 9·79 | 3·24 | 1·45 | 6·44 | 6·74 | 3·89 |
| $Fe_2O_3$ | 4·82 | 0·90 | 0·52 | 3·85 | 1·80 | 0·80 | 2·81 | 0·89 | 0·51 |
| FeO | 1·58 | 0·63 | 0·36 | 2·35 | 1·15 | 0·51 | 2·30 | 1·98 | 1·14 |
| MnO | 0·08 | 0·04 | 0·02 | 0·07 | 0·05 | 0·02 | 0·08 | 0·04 | 0·02 |
| NiO | 0·07 | 0·09 | 0·05 | 0·03 | 0·05 | 0·02 | 0·05 | 0·03 | 0·02 |
| MgO | 18·59 | 1·63 | 0·94 | 17·74 | 1·39 | 0·62 | 19·45 | 3·93 | 2·27 |
| CaO | 12·72 | 0·27 | 0·15 | 12·42 | 0·63 | 0·28 | 12·81 | 0·55 | 0·32 |
| $Na_2O$ | 1·35 | 0·34 | 0·20 | 1·23 | 0·99 | 0·44 | 0·75 | 0·82 | 0·48 |
| $K_2O$ | 0·03 | 0·03 | 0·01 | 0·04 | 0·06 | 0·03 | 0·01 | 0·03 | 0·02 |
| $H_2O$ | 2·15 | 0·01 | 0·01 | 2·13 | 0·02 | 0·01 | 2·16 | 0·08 | 0·05 |
| Total | 100·275 | | | 99·16 | | | 99·70 | | |
| Si | 6·8593 | 0·3730 | 0·2154 | 6·8858 | 0·4142 | 0·1853 | 7·2698 | 0·7708 | 0·4450 |
| Ti | 0·0370 | 0·0231 | 0·0134 | 0·0347 | 0·0132 | 0·0059 | 0·0204 | 0·0303 | 0·0175 |
| Cr | 0·0552 | 0·0209 | 0·0121 | 0·0315 | 0·0307 | 0·0137 | 0·0407 | 0·0461 | 0·0266 |
| Al | 1·4706 | 0·5133 | 0·2963 | 1·6267 | 0·5487 | 0·2454 | 1·0631 | 1·1416 | 0·6591 |

(continued)

*Table 7: Continued*

| Sample: | C38 ($n=4$) | | | C34 ($n=6$) | | | C37 ($n=4$) | | |
|---|---|---|---|---|---|---|---|---|---|
| | Average | 2σ | 2σ mean | Average | 2σ | 2σ mean | Average | 2σ | 2σ mean |
| $Fe^{3+}$ | 0·5067 | 0·0953 | 0·0550 | 0·4086 | 0·1914 | 0·0856 | 0·2941 | 0·0948 | 0·0547 |
| $Fe^{2+}$ | 0·1840 | 0·0742 | 0·0428 | 0·2765 | 0·1371 | 0·0613 | 0·2685 | 0·2396 | 0·1383 |
| Mn | 0·0099 | 0·0052 | 0·0030 | 0·0085 | 0·0065 | 0·0029 | 0·0091 | 0·0045 | 0·0026 |
| Ni | 0·0082 | 0·0095 | 0·0055 | 0·0030 | 0·0053 | 0·0024 | 0·0051 | 0·0034 | 0·0020 |
| Mg | 3·8690 | 0·3334 | 0·1925 | 3·7246 | 0·2641 | 0·1181 | 4·0292 | 0·6743 | 0·3893 |
| Ca | 1·9031 | 0·0348 | 0·0201 | 1·8745 | 0·0918 | 0·0410 | 1·9083 | 0·0678 | 0·0391 |
| Na | 0·3639 | 0·0949 | 0·0548 | 0·3359 | 0·2715 | 0·1214 | 0·2036 | 0·2284 | 0·1319 |
| K | 0·0047 | 0·0048 | 0·0028 | 0·0072 | 0·0112 | 0·0050 | 0·0015 | 0·0052 | 0·0030 |
| H | 2·0 | | | 2 | | | 2 | | |
| Mg-no.($Fe_{tot}$) | 0·848 | 0·040 | 0·023 | 0·844 | 0·035 | 0·016 | 0·876 | 0·061 | 0·035 |

| Sample: | C174 ($n=18$) | | | C03-17 ($n=4$) | | | C03-47 ($n=8$) | | |
|---|---|---|---|---|---|---|---|---|---|
| | Average | 2σ | 2σ mean | Average | 2σ | 2σ mean | Average | 2σ | 2σ mean |
| $SiO_2$ | 47·52 | 2·11 | 0·51 | 45·45 | 1·55 | 0·89 | 47·33 | 3·49 | 1·32 |
| $TiO_2$ | 0·84 | 0·21 | 0·05 | 0·73 | 0·20 | 0·11 | 0·59 | 0·39 | 0·15 |
| $Cr_2O_3$ | 9·57 | 1·46 | 0·35 | 0·54 | 0·16 | 0·09 | 0·75 | 0·33 | 0·13 |
| $Al_2O_3$ | 1·29 | 0·25 | 0·06 | 11·29 | 1·28 | 0·74 | 9·85 | 2·85 | 1·08 |
| $Fe_2O_3$ | 3·43 | 2·31 | 0·56 | 5·52 | 1·04 | 0·60 | 5·01 | 2·40 | 0·91 |
| FeO | 0·73 | 2·04 | 0·50 | 1·81 | 0·89 | 0·51 | 1·32 | 1·44 | 0·54 |
| MnO | 0·05 | 0·04 | 0·01 | 0·08 | 0·03 | 0·02 | 0·09 | 0·05 | 0·02 |
| NiO | 0·05 | 0·08 | 0·02 | 0·02 | 0·04 | 0·02 | 0·03 | 0·02 | 0·01 |
| MgO | 19·49 | 1·46 | 0·35 | 17·30 | 0·71 | 0·41 | 18·26 | 1·13 | 0·43 |
| CaO | 12·80 | 0·25 | 0·06 | 12·82 | 0·21 | 0·12 | 12·89 | 0·40 | 0·15 |
| $Na_2O$ | 1·68 | 0·34 | 0·08 | 1·57 | 0·14 | 0·08 | 1·37 | 0·63 | 0·24 |
| $K_2O$ | 0·37 | 0·30 | 0·07 | 0·03 | 0·02 | 0·01 | 0·01 | 0·02 | 0·01 |
| $H_2O$ | 2·14 | 0·04 | 0·01 | 2·11 | 0·01 | 0·01 | 2·13 | 0·02 | 0·01 |
| Total | 99·96 | | | 99·27 | | | 99·62 | | |
| Si | 6·6591 | 0·2607 | 0·0632 | 6·4732 | 0·1886 | 0·1089 | 6·6750 | 0·4440 | 0·1678 |
| Ti | 0·0887 | 0·0231 | 0·0056 | 0·0777 | 0·0217 | 0·0125 | 0·0622 | 0·0413 | 0·0156 |
| Cr | 0·1428 | 0·0279 | 0·0068 | 0·0608 | 0·0179 | 0·0103 | 0·0835 | 0·0374 | 0·0141 |
| Al | 1·5805 | 0·2548 | 0·0618 | 1·8956 | 0·2248 | 0·1298 | 1·6389 | 0·4834 | 0·1827 |
| $Fe^{3+}$ | 0·3612 | 0·2412 | 0·0585 | 0·5913 | 0·1095 | 0·0632 | 0·5323 | 0·2566 | 0·0970 |
| $Fe^{2+}$ | 0·0860 | 0·2429 | 0·0589 | 0·2159 | 0·1072 | 0·0619 | 0·1556 | 0·1687 | 0·0638 |
| Mn | 0·0064 | 0·0048 | 0·0012 | 0·0099 | 0·0040 | 0·0023 | 0·0107 | 0·0056 | 0·0021 |
| Ni | 0·0054 | 0·0085 | 0·0021 | 0·0027 | 0·0043 | 0·0025 | 0·0029 | 0·0024 | 0·0009 |
| Mg | 4·0698 | 0·2404 | 0·0583 | 3·6729 | 0·1291 | 0·0745 | 3·8389 | 0·2121 | 0·0802 |
| Ca | 1·9213 | 0·0437 | 0·0106 | 1·9558 | 0·0438 | 0·0253 | 1·9472 | 0·0518 | 0·0196 |
| Na | 0·4562 | 0·0928 | 0·0225 | 0·4335 | 0·0385 | 0·0222 | 0·3742 | 0·1746 | 0·0660 |
| K | 0·0669 | 0·0541 | 0·0131 | 0·0053 | 0·0042 | 0·0024 | 0·0025 | 0·0033 | 0·0013 |
| H | 2 | | | 2 | | | 2 | | |
| Mg-no.($Fe_{tot}$) | 0·901 | 0·019 | 0·005 | 0·820 | 0·014 | 0·008 | 0·848 | 0·028 | 0·010 |

(continued)

*Table 7: Continued*

| Sample: | C03-15 ($n=6$) | | | C194 ($n=7$) | | | C201 ($n=2$) | | |
|---|---|---|---|---|---|---|---|---|---|
| | Average | 2σ | 2σ mean | Average | 2σ | 2σ mean | Average | 2σ | 2σ mean |
| $SiO_2$ | 50·27 | 4·96 | 2·22 | 41·85 | 0·58 | 0·24 | 42·49 | 0·13 | |
| $TiO_2$ | 0·41 | 0·39 | 0·17 | 1·47 | 0·44 | 0·18 | 0·50 | 0·51 | |
| $Cr_2O_3$ | 0·46 | 0·43 | 0·19 | 15·60 | 0·69 | 0·28 | 15·30 | 0·40 | |
| $Al_2O_3$ | 6·81 | 6·08 | 2·72 | 0·43 | 0·17 | 0·07 | 0·05 | 0·04 | |
| $Fe_2O_3$ | 4·07 | 4·12 | 1·84 | 5·34 | 1·39 | 0·57 | 5·01 | 2·42 | |
| FeO | 1·15 | 2·95 | 1·32 | 4·08 | 0·97 | 0·40 | 3·18 | 1·84 | |
| MnO | 0·09 | 0·06 | 0·03 | 0·11 | 0·04 | 0·02 | 0·10 | 0·01 | |
| NiO | 0·05 | 0·03 | 0·01 | 0·02 | 0·04 | 0·02 | 0·01 | 0·01 | |
| MgO | 19·01 | 3·21 | 1·44 | 14·62 | 0·43 | 0·18 | 15·97 | 0·79 | |
| CaO | 14·94 | 9·13 | 4·09 | 11·95 | 0·27 | 0·11 | 12·94 | 0·79 | |
| $Na_2O$ | 0·60 | 0·69 | 0·31 | 2·87 | 0·21 | 0·09 | 2·57 | 0·86 | |
| $K_2O$ | 0·01 | 0·02 | 0·01 | 0·17 | 0·11 | 0·04 | 0·08 | 0·06 | |
| $H_2O$ | 2·11 | 0·18 | 0·08 | 2·10 | 0·03 | 0·01 | 2·11 | 0·04 | |
| Total | 99·97 | | | 100·62 | | | 100·28 | | |
| Si | 7·1621 | 1·1031 | 0·4933 | 5·9776 | 0·0728 | 0·0297 | 6·0541 | 0·1297 | |
| Ti | 0·0437 | 0·0409 | 0·0183 | 0·1573 | 0·0471 | 0·0192 | 0·0536 | 0·0543 | |
| Cr | 0·0518 | 0·0469 | 0·0210 | 0·0482 | 0·0189 | 0·0077 | 0·0049 | 0·0052 | |
| Al | 1·1311 | 0·9958 | 0·4453 | 2·6260 | 0·1122 | 0·0458 | 2·5695 | 0·0168 | |
| $Fe^{3+}$ | 0·4276 | 0·4313 | 0·1929 | 0·5737 | 0·1459 | 0·0596 | 0·5371 | 0·2683 | |
| $Fe^{2+}$ | 0·1437 | 0·3793 | 0·1696 | 0·4880 | 0·1208 | 0·0493 | 0·3785 | 0·2120 | |
| Mn | 0·0113 | 0·0082 | 0·0037 | 0·0135 | 0·0046 | 0·0019 | 0·0112 | 0·0013 | |
| Ni | 0·0051 | 0·0030 | 0·0013 | 0·0028 | 0·0049 | 0·0020 | 0·0006 | 0·0017 | |
| Mg | 4·0235 | 0·4244 | 0·1898 | 3·1129 | 0·0600 | 0·0245 | 3·3908 | 0·1063 | |
| Ca | 2·3050 | 1·7040 | 0·7621 | 1·8282 | 0·0395 | 0·0161 | 1·9753 | 0·0832 | |
| Na | 0·1621 | 0·1893 | 0·0847 | 0·7949 | 0·0564 | 0·0230 | 0·7081 | 0·2217 | |
| K | 0·0026 | 0·0043 | 0·0019 | 0·0309 | 0·0191 | 0·0078 | 0·0147 | 0·0083 | |
| H | 2 | | | 2 | | | 2 | | |
| Mg-no.($Fe_{tot}$) | 0·875 | 0·034 | 0·015 | 0·746 | 0·013 | 0·005 | 0·787 | 0·016 | |

| Sample: | C35 ($n=4$) | | | C203 ($n=3$) | | | C218 ($n=4$) | | |
|---|---|---|---|---|---|---|---|---|---|
| | Average | 2σ | 2σ mean | Average | 2σ | 2σ mean | Average | 2σ | 2σ mean |
| $SiO_2$ | 46·05 | 9·20 | 5·31 | 42·49 | 0·38 | 0·27 | 44·70 | 1·28 | 0·64 |
| $TiO_2$ | 1·80 | 5·30 | 3·06 | 0·78 | 0·53 | 0·38 | 0·79 | 0·12 | 0·06 |
| $Cr_2O_3$ | 3·01 | 11·08 | 6·40 | 14·48 | 1·00 | 0·71 | 13·06 | 1·51 | 0·76 |
| $Al_2O_3$ | 8·07 | 12·26 | 7·08 | 0·14 | 0·28 | 0·20 | 0·41 | 0·05 | 0·03 |
| $Fe_2O_3$ | 3·32 | 5·29 | 3·06 | 6·56 | 0·75 | 0·53 | 5·13 | 0·86 | 0·43 |
| FeO | 4·47 | 7·04 | 4·06 | 2·22 | 0·89 | 0·63 | 2·20 | 0·57 | 0·28 |
| MnO | 0·09 | 0·03 | 0·02 | 0·08 | 0·02 | 0·01 | 0·10 | 0·02 | 0·01 |
| NiO | 0·04 | 0·07 | 0·04 | 0·06 | 0·05 | 0·04 | 0·03 | 0·06 | 0·03 |
| MgO | 16·29 | 6·44 | 3·72 | 16·10 | 0·16 | 0·12 | 16·95 | 0·75 | 0·37 |
| CaO | 12·12 | 3·38 | 1·95 | 12·35 | 0·25 | 0·18 | 12·84 | 0·25 | 0·12 |

(continued)

*Table 7: Continued*

| Sample: | C35 ($n=4$) | | | C203 ($n=3$) | | | C218 ($n=4$) | | |
|---|---|---|---|---|---|---|---|---|---|
| | Average | 2σ | 2σ mean | Average | 2σ | 2σ mean | Average | 2σ | 2σ mean |
| $Na_2O$ | 1·76 | 1·50 | 0·86 | 2·68 | 0·54 | 0·38 | 2·03 | 0·41 | 0·21 |
| $K_2O$ | 0·47 | 1·76 | 1·01 | 0·25 | 0·64 | 0·45 | 0·04 | 0·02 | 0·01 |
| $H_2O$ | 2·10 | 0·08 | 0·05 | 2·10 | 0·01 | 0·01 | 2·12 | 0·01 | 0·01 |
| Total | 99·59 | | | 100·30 | | | 100·40 | | |
| Si | 6·5747 | 1·1459 | 0·6616 | 6·0589 | 0·0435 | 0·0308 | 6·3104 | 0·1878 | 0·0939 |
| Ti | 0·1969 | 0·5870 | 0·3389 | 0·0841 | 0·0563 | 0·0398 | 0·2413 | 0·7075 | 0·3538 |
| Cr | 0·0327 | 0·0465 | 0·0269 | 0·0162 | 0·0316 | 0·0223 | 0·0462 | 0·0059 | 0·0030 |
| Al | 1·8230 | 1·2049 | 0·6957 | 2·4334 | 0·1621 | 0·1146 | 2·1730 | 0·2475 | 0·1237 |
| $Fe^{3+}$ | 0·3561 | 0·5608 | 0·3238 | 0·7034 | 0·0815 | 0·0576 | 0·5447 | 0·0878 | 0·0439 |
| $Fe^{2+}$ | 0·5394 | 0·8720 | 0·5035 | 0·2653 | 0·1054 | 0·0745 | 0·2594 | 0·0663 | 0·0332 |
| Mn | 0·0114 | 0·0047 | 0·0027 | 0·0097 | 0·0029 | 0·0021 | 0·0120 | 0·0018 | 0·0009 |
| Ni | 0·0040 | 0·0079 | 0·0046 | 0·0069 | 0·0063 | 0·0044 | 0·0032 | 0·0064 | 0·0032 |
| Mg | 3·4618 | 1·2756 | 0·7365 | 3·4221 | 0·0602 | 0·0425 | 3·5672 | 0·1629 | 0·0814 |
| Ca | 1·8533 | 0·4647 | 0·2683 | 1·8875 | 0·0521 | 0·0369 | 1·9418 | 0·0405 | 0·0202 |
| Na | 0·4906 | 0·4324 | 0·2497 | 0·7400 | 0·1466 | 0·1036 | 0·5576 | 0·1119 | 0·0560 |
| K | 0·0877 | 0·3295 | 0·1902 | 0·0460 | 0·1166 | 0·0825 | 0·0063 | 0·0045 | 0·0023 |
| H | 2 | | | 2 | | | 2 | | |
| Mg-no.($Fe_{tot}$) | 0·790 | 0·205 | 0·119 | 0·779 | 0·006 | 0·004 | 0·816 | 0·026 | 0·013 |

| Sample: | C50.4 ($n=4$) | | | C50.10 ($n=3$) | | | C50.8 ($n=3$) | | |
|---|---|---|---|---|---|---|---|---|---|
| | Average | 2σ | 2σ mean | Average | 2σ | 2σ mean | Average | 2σ | 2σ mean |
| $SiO_2$ | 44·93 | 0·82 | 0·47 | 47·47 | 2·00 | 1·42 | 45·90 | 6·22 | 4·40 |
| $TiO_2$ | 1·55 | 0·30 | 0·17 | 1·16 | 0·53 | 0·37 | 1·55 | 0·86 | 0·61 |
| $Cr_2O_3$ | 10·98 | 0·44 | 0·25 | 10·05 | 0·89 | 0·63 | 10·30 | 4·03 | 2·85 |
| $Al_2O_3$ | 0·49 | 0·56 | 0·32 | 0·32 | 0·11 | 0·07 | 0·28 | 0·18 | 0·13 |
| $Fe_2O_3$ | 5·38 | 1·80 | 1·04 | 6·22 | 5·80 | 4·10 | 2·92 | 2·26 | 1·60 |
| FeO | 4·08 | 2·04 | 1·18 | 3·14 | 5·59 | 3·95 | 5·62 | 0·66 | 0·47 |
| MnO | 0·10 | 0·04 | 0·02 | 0·08 | 0·06 | 0·04 | 0·13 | 0·01 | 0·01 |
| NiO | 0·03 | 0·07 | 0·04 | 0·07 | 0·04 | 0·03 | 0·03 | 0·07 | 0·05 |
| MgO | 15·61 | 0·80 | 0·46 | 16·41 | 1·36 | 0·96 | 15·65 | 1·95 | 1·38 |
| CaO | 11·98 | 0·19 | 0·11 | 11·78 | 1·82 | 1·28 | 12·07 | 0·51 | 0·36 |
| $Na_2O$ | 1·70 | 0·21 | 0·12 | 1·32 | 0·08 | 0·06 | 1·51 | 0·72 | 0·51 |
| $K_2O$ | 0·26 | 0·11 | 0·06 | 0·30 | 0·49 | 0·35 | 0·50 | 0·31 | 0·22 |
| $H_2O$ | 2·08 | 0·04 | 0·02 | 2·13 | 0·03 | 0·02 | 2·07 | 0·06 | 0·04 |
| Total | 99·16 | | | 100·46 | | | 98·50 | | |
| Si | 6·4712 | 0·0427 | 0·0247 | 6·6828 | 0·2350 | 0·1662 | 6·6450 | 0·7163 | 0·5065 |
| Ti | 0·1678 | 0·0290 | 0·0167 | 0·1226 | 0·0543 | 0·0384 | 0·1686 | 0·0993 | 0·0702 |
| Cr | 0·0554 | 0·0637 | 0·0368 | 0·0353 | 0·0115 | 0·0081 | 0·0319 | 0·0218 | 0·0154 |
| Al | 1·8646 | 0·0601 | 0·0347 | 1·6681 | 0·1691 | 0·1196 | 1·7602 | 0·7365 | 0·5208 |
| $Fe^{3+}$ | 0·5829 | 0·1854 | 0·1071 | 0·6599 | 0·6173 | 0·4365 | 0·3188 | 0·2557 | 0·1808 |
| $Fe^{2+}$ | 0·4920 | 0·2507 | 0·1448 | 0·3696 | 0·6595 | 0·4664 | 0·6798 | 0·0626 | 0·0443 |
| Mn | 0·0120 | 0·0043 | 0·0025 | 0·0101 | 0·0064 | 0·0046 | 0·0156 | 0·0025 | 0·0018 |

(continued)

*Table 7: Continued*

| Sample: | C50.4 ($n=4$) | | | C50.10 ($n=3$) | | | C50.8 ($n=3$) | | |
|---|---|---|---|---|---|---|---|---|---|
| | Average | 2σ | 2σ mean | Average | 2σ | 2σ mean | Average | 2σ | 2σ mean |
| Ni | 0·0033 | 0·0083 | 0·0048 | 0·0078 | 0·0044 | 0·0031 | 0·0027 | 0·0076 | 0·0054 |
| Mg | 3·3511 | 0·1383 | 0·0799 | 3·4439 | 0·2508 | 0·1774 | 3·3775 | 0·3289 | 0·2326 |
| Ca | 1·8489 | 0·0641 | 0·0370 | 1·7776 | 0·2721 | 0·1924 | 1·8732 | 0·0273 | 0·0193 |
| Na | 0·4737 | 0·0639 | 0·0369 | 0·3615 | 0·0262 | 0·0185 | 0·4232 | 0·2164 | 0·1530 |
| K | 0·0479 | 0·0182 | 0·0105 | 0·0529 | 0·0875 | 0·0619 | 0·0926 | 0·0587 | 0·0415 |
| H | 2 | | | 2 | | | 2 | | |
| Mg-no.($Fe_{tot}$) | 0·757 | 0·020 | 0·012 | 0·770 | 0·037 | 0·026 | 0·050 | 0·019 | 0·783 |

| Sample: | C50.9 ($n=8$) | | | C48 ($n=8$) | | | C7 ($n=4$) | | |
|---|---|---|---|---|---|---|---|---|---|
| | Average | 2σ | 2σ mean | Average | 2σ | 2σ mean | Average | 2σ | 2σ mean |
| $SiO_2$ | 45·93 | 1·12 | 0·42 | 47·76 | 3·19 | 1·21 | 46·50 | 1·58 | 0·91 |
| $TiO_2$ | 1·50 | 0·27 | 0·10 | 1·37 | 0·66 | 0·25 | 0·82 | 0·17 | 0·10 |
| $Cr_2O_3$ | 9·86 | 1·32 | 0·50 | 8·57 | 2·13 | 0·80 | 12·44 | 0·79 | 0·46 |
| $Al_2O_3$ | 0·34 | 0·10 | 0·04 | 0·40 | 0·40 | 0·15 | 0·14 | 0·12 | 0·07 |
| $Fe_2O_3$ | 4·13 | 1·55 | 0·59 | 3·95 | 1·39 | 0·53 | 9·91 | 0·86 | 0·50 |
| FeO | 4·66 | 1·74 | 0·66 | 6·67 | 1·36 | 0·51 | 0·05 | 0·21 | 0·12 |
| MnO | 0·10 | 0·05 | 0·02 | 0·10 | 0·04 | 0·01 | 0·11 | 0·07 | 0·04 |
| NiO | 0·07 | 0·08 | 0·03 | 0·07 | 0·04 | 0·02 | 0·15 | 0·06 | 0·04 |
| MgO | 16·15 | 0·97 | 0·37 | 15·08 | 1·73 | 0·65 | 16·77 | 0·16 | 0·09 |
| CaO | 12·34 | 0·32 | 0·12 | 11·77 | 0·56 | 0·21 | 12·14 | 0·49 | 0·28 |
| $Na_2O$ | 1·37 | 0·25 | 0·09 | 1·05 | 0·38 | 0·14 | 1·21 | 0·09 | 0·05 |
| $K_2O$ | 0·39 | 0·14 | 0·05 | 0·62 | 0·25 | 0·10 | 0·11 | 0·02 | 0·01 |
| $H_2O$ | 2·08 | 0·02 | 0·01 | 2·08 | 0·05 | 0·02 | 0·01 | 0·02 | 0·01 |
| Total | 98·90 | | | 99·49 | | | 100·36 | | |
| Si | 6·6227 | 0·1444 | 0·0546 | 6·8701 | 0·3474 | 0·1313 | 6·3907 | 0·1365 | 0·0788 |
| Ti | 0·1625 | 0·0291 | 0·0110 | 0·1481 | 0·0736 | 0·0278 | 0·0846 | 0·0174 | 0·0101 |
| Cr | 0·0391 | 0·0111 | 0·0042 | 0·0458 | 0·0454 | 0·0172 | 0·0148 | 0·0133 | 0·0077 |
| Al | 1·6750 | 0·2145 | 0·0811 | 1·4543 | 0·3791 | 0·1433 | 2·0155 | 0·1167 | 0·0674 |
| $Fe^{3+}$ | 0·4484 | 0·1716 | 0·0649 | 0·4272 | 0·1488 | 0·0562 | 1·0253 | 0·1018 | 0·0588 |
| $Fe^{2+}$ | 0·5613 | 0·2062 | 0·0779 | 0·8029 | 0·1741 | 0·0658 | 0·0061 | 0·0242 | 0·0140 |
| Mn | 0·0114 | 0·0060 | 0·0023 | 0·0119 | 0·0052 | 0·0020 | 0·0126 | 0·0068 | 0·0039 |
| Ni | 0·0085 | 0·0089 | 0·0034 | 0·0077 | 0·0048 | 0·0018 | 0·0164 | 0·0072 | 0·0041 |
| Mg | 3·4710 | 0·2333 | 0·0882 | 3·2320 | 0·3219 | 0·1217 | 3·4342 | 0·0624 | 0·0361 |
| Ca | 1·9071 | 0·0610 | 0·0230 | 1·8141 | 0·0779 | 0·0295 | 1·7872 | 0·0624 | 0·0360 |
| Na | 0·3817 | 0·0672 | 0·0254 | 0·2944 | 0·1102 | 0·0416 | 0·3213 | 0·0287 | 0·0166 |
| K | 0·0712 | 0·0248 | 0·0094 | 0·1135 | 0·0479 | 0·0181 | 0·0193 | 0·0036 | 0·0021 |
| H | 2 | | | 2 | | | 2 | | |
| Mg-no.($Fe_{tot}$) | 0·772 | 0·051 | 0·036 | 0·775 | 0·029 | 0·011 | 0·769 | 0·011 | 0·007 |

(continued)

*Table 7: Continued*

| Sample: | C41 ($n=26$) | | | C172 ($n=5$) | | | C43 ($n=5$) | | |
|---|---|---|---|---|---|---|---|---|---|
| | Average | 2σ | 2σ mean | Average | 2σ | 2σ mean | Average | 2σ | 2σ mean |
| $SiO_2$ | 45·99 | 1·97 | 0·39 | 43·34 | 3·77 | 1·88 | 46·54 | 1·23 | 0·71 |
| $TiO_2$ | 1·08 | 0·35 | 0·07 | 1·02 | 0·25 | 0·12 | 0·73 | 0·11 | 0·06 |
| $Cr_2O_3$ | 10·44 | 2·02 | 0·40 | 14·40 | 3·70 | 1·85 | 11·39 | 0·97 | 0·56 |
| $Al_2O_3$ | 0·42 | 0·23 | 0·05 | 0·01 | 0·01 | 0·01 | 0·84 | 0·10 | 0·06 |
| $Fe_2O_3$ | 5·04 | 2·37 | 0·46 | 7·94 | 1·67 | 0·83 | 5·70 | 1·10 | 0·63 |
| FeO | 5·71 | 2·76 | 0·54 | 6·71 | 1·44 | 0·72 | 1·19 | 0·89 | 0·51 |
| MnO | 0·14 | 0·04 | 0·01 | 0·27 | 0·04 | 0·02 | 0·09 | 0·06 | 0·04 |
| NiO | 0·03 | 0·06 | 0·01 | 0·03 | 0·07 | 0·03 | 0·04 | 0·05 | 0·03 |
| MgO | 15·18 | 1·56 | 0·31 | 12·09 | 2·53 | 1·27 | 17·84 | 0·50 | 0·29 |
| CaO | 12·32 | 0·34 | 0·07 | 11·40 | 0·39 | 0·20 | 12·90 | 0·18 | 0·10 |
| $Na_2O$ | 1·38 | 0·31 | 0·06 | 2·00 | 0·43 | 0·21 | 1·60 | 0·22 | 0·13 |
| $K_2O$ | 0·42 | 0·11 | 0·02 | 0·34 | 0·03 | 0·02 | 0·03 | 0·01 | 0·01 |
| $H_2O$ | 2·09 | 0·05 | 0·01 | 2·08 | 0·03 | 0·01 | 2·15 | 0·02 | 0·01 |
| Total | 100·25 | | | 101·60 | | | 101·04 | | |
| Si | 6·5863 | 0·1937 | 0·0380 | 6·1963 | 0·4581 | 0·2291 | 6·4946 | 0·1386 | 0·0800 |
| Ti | 0·1164 | 0·0392 | 0·0077 | 0·1092 | 0·0257 | 0·0128 | 0·0767 | 0·0121 | 0·0070 |
| Cr | 0·0479 | 0·0262 | 0·0051 | 0·0006 | 0·0015 | 0·0008 | 0·0926 | 0·0113 | 0·0066 |
| Al | 1·7625 | 0·3461 | 0·0679 | 2·4275 | 0·6594 | 0·3297 | 1·8733 | 0·1680 | 0·0970 |
| $Fe^{3+}$ | 0·5424 | 0·2450 | 0·0480 | 0·8547 | 0·1898 | 0·0949 | 0·5982 | 0·1131 | 0·0653 |
| $Fe^{2+}$ | 0·6854 | 0·3412 | 0·0669 | 0·8021 | 0·1840 | 0·0920 | 0·1389 | 0·1039 | 0·0600 |
| Mn | 0·0167 | 0·0041 | 0·0008 | 0·0320 | 0·0042 | 0·0021 | 0·0109 | 0·0076 | 0·0044 |
| Ni | 0·0037 | 0·0065 | 0·0013 | 0·0030 | 0·0074 | 0·0037 | 0·0046 | 0·0053 | 0·0031 |
| Mg | 3·2388 | 0·2703 | 0·0530 | 2·5747 | 0·5080 | 0·2540 | 3·7103 | 0·0803 | 0·0464 |
| Ca | 1·8905 | 0·0680 | 0·0133 | 1·7458 | 0·0737 | 0·0369 | 1·9280 | 0·0329 | 0·0190 |
| Na | 0·3844 | 0·0887 | 0·0174 | 0·5534 | 0·1209 | 0·0605 | 0·4319 | 0·0618 | 0·0357 |
| K | 0·0765 | 0·0221 | 0·0043 | 0·0613 | 0·0055 | 0·0028 | 0·0055 | 0·0027 | 0·0016 |
| H | 2 | | | 2 | | | 2 | | |
| Mg-no.($Fe_{tot}$) | 0·725 | 0·038 | 0·007 | 0·608 | 0·098 | 0·049 | 0·834 | 0·009 | 0·005 |

(continued)

Mineral trace element compositions from three gabbronorites were determined: an olivine-bearing gabbronorite (C66) from the contact with ultramafic rocks; sample (C48) taken from about 1 m, and (C7) from approximately a few tens of meters from the contact, respectively. The REE concentrations of the olivine-bearing gabbronorites are low, and the LREE are depleted with respect to the MREE and HREE ($Ce_N/Gd_N$ ~0·3–0·55 and $Ce_N/Yb_N$ ~0·4–0·6); with $Gd_N/Yb_N$ ~1·2–1·47. Clinopyroxene grains with low REE concentration show a significant positive Eu anomaly. Clinopyroxene from homogeneous gabbronorite has high REE concentrations with depleted LREE with respect to the MREE ($Ce_N/Gd_N$ ~0·3–0·4). The MREE are only slightly enriched relative to the HREE ($Gd_N/Yb_N$ ~1·2).

## Orthopyroxene

Orthopyroxenes are bronzite in composition with Mg-number ranging from 0·84 to 0·72 in ultramafic rocks and from 0·76 to 0·56 in gabbronorite. The relationship between $Al_2O_3$ and Mg-number varies sympathetically with that observed for the clinopyroxene (Fig. 15), in accordance with previous measurements from deep-seated intrusions (e.g DeBari & Coleman, 1989). The $K_d$ Fe/Mg of orthopyroxene–olivine pairs is systematically lower than the $K_d$ Fe/Mg of clinopyroxene–olivine. The difference increases with increasing Fe content. It is therefore mainly due to the Mg-rich composition of clinopyroxene.

In high-temperature peridotites, a linear array is defined with a slope close to unity when the Fe/Mg ratios of olivine and orthopyroxene are plotted

*Table 7: Continued*

| Sample: | C04-9 ($n=5$) | | |
|---|---|---|---|
| | Average | 2σ | 2σ mean |
| $SiO_2$ | 44·93 | 1·53 | 0·76 |
| $TiO_2$ | 1·08 | 0·19 | 0·10 |
| $Cr_2O_3$ | 0·73 | 0·12 | 0·06 |
| $Al_2O_3$ | 12·57 | 1·22 | 0·61 |
| $Fe_2O_3$ | 2·65 | 0·74 | 0·37 |
| FeO | 5·13 | 0·59 | 0·29 |
| MnO | 0·07 | 0·04 | 0·02 |
| NiO | 0·00 | 0·00 | 0·00 |
| MgO | 15·77 | 0·81 | 0·41 |
| CaO | 12·79 | 0·33 | 0·17 |
| $Na_2O$ | 1·88 | 0·25 | 0·12 |
| $K_2O$ | 0·04 | 0·02 | 0·01 |
| $H_2O$ | 2·10 | 0·02 | 0·01 |
| Total | 99·74 | | |
| Si | 6·4198 | 0·1656 | 0·0828 |
| Ti | 0·1164 | 0·0218 | 0·0109 |
| Cr | 0·0824 | 0·0142 | 0·0071 |
| Al | 2·1170 | 0·2205 | 0·1103 |
| $Fe^{3+}$ | 0·2851 | 0·0806 | 0·0403 |
| $Fe^{2+}$ | 0·6125 | 0·0708 | 0·0354 |
| Mn | 0·0089 | 0·0043 | 0·0022 |
| Ni | 0·0000 | 0·0000 | 0·0000 |
| Mg | 3·3580 | 0·1471 | 0·0736 |
| Ca | 1·9583 | 0·0375 | 0·0188 |
| Na | 0·5197 | 0·0718 | 0·0359 |
| K | 0·0069 | 0·0037 | 0·0018 |
| H | 2 | | |
| Mg-no.($Fe_{tot}$) | 0·789 | 0·019 | 0·010 |

*Table 8: Trace element concentrations (ppm) in amphibole from the Chilas Complex*

| Sample: | C03-45 | | | C03-44 | | |
|---|---|---|---|---|---|---|
| *n*: | 6 | | | 5 | | |
| | Average | 2σ | 2σ mean | Average | 2σ | 2σ mean |
| Li | 2·84 | 3·11 | 1·17 | 0·430 | 0·303 | 0·175 |
| Sc | 165 | 136 | 51 | 179 | 15 | 7 |
| V | 283 | 248 | 94 | 463 | 60 | 30 |
| Cr | 5418 | 4892 | 1849 | 5635 | 645 | 323 |
| Co | 43·5 | 27·9 | 10·5 | 45·3 | 5·2 | 3 |
| Ni | 287 | 177 | 67 | 286 | 60 | 30 |
| Cu | 0·128 | 0·104 | 0·039 | 0·075 | 0·051 | 0·051 |
| Zn | | | | 0·0000 | 0·000 | 0·000 |
| Ga | 6·01 | 4·96 | 1·87 | 10·45 | 2·05 | 1·02 |
| Rb | 0·207 | 0·208 | 0·079 | 0·5620 | 0·766 | 0·383 |
| Sr | 67·8 | 66·8 | 25·2 | 99·3 | 22·1 | 11·0 |
| Y | 13·6 | 12·3 | 4·6 | 19·0 | 1·4 | 0·7 |
| Zr | 8·5 | 8·08 | 3·05 | 12·0 | 1·1 | 0·6 |
| Nb | 0·074 | 0·076 | 0·029 | 0·167 | 0·200 | 0·100 |
| Cs | | | | 0·016 | 0·019 | 0·010 |
| Ba | 3·36 | 4·14 | 1·56 | 3·82 | 1·88 | 1·08 |
| La | 0·605 | 0·479 | 0·181 | 0·853 | 0·145 | 0·072 |
| Ce | 2·38 | 1·91 | 0·72 | 3·54 | 0·59 | 0·29 |
| Pr | 0·509 | 0·422 | 0·160 | 0·705 | 0·082 | 0·041 |
| Nd | 3·43 | 2·85 | 1·08 | 4·92 | 0·61 | 0·30 |
| Sm | 1·51 | 1·29 | 0·49 | 2·11 | 0·37 | 0·19 |
| Eu | 0·646 | 0·519 | 0·196 | 0·947 | 0·279 | 0·139 |
| Gd | 2·07 | 1·79 | 0·68 | 2·77 | 0·40 | 0·20 |
| Tb | 0·374 | 0·339 | 0·128 | 0·547 | 0·078 | 0·039 |
| Dy | 2·62 | 2·33 | 0·88 | 3·61 | 0·54 | 0·27 |
| Ho | 0·570 | 0·514 | 0·194 | 0·746 | 0·069 | 0·035 |
| Er | 1·49 | 1·30 | 0·49 | 1·95 | 0·35 | 0·18 |
| Tm | 0·222 | 0·209 | 0·079 | 0·261 | 0·054 | 0·027 |
| Yb | 1·42 | 1·26 | 0·47 | 1·88 | 0·18 | 0·09 |
| Lu | 0·220 | 0·200 | 0·075 | 0·272 | 0·045 | 0·023 |
| Hf | 0·420 | 0·414 | 0·156 | 0·610 | 0·100 | 0·050 |
| Ta | 0·007 | 0·006 | 0·002 | 0·013 | 0·012 | 0·009 |
| Pb | 0·246 | 0·265 | 0·100 | 0·222 | 0·069 | 0·034 |
| Th | 0·017 | 0·021 | 0·008 | 0·013 | 0·005 | 0·004 |
| U | 0·020 | 0·027 | 0·010 | | | |

The concentration of trace element for which no value is shown is below detection limit.

against those of the associated clinopyroxene (Fig. 16; Obata, 1980).

The trace element patterns of orthopyroxene (Fig. 17) are characterized by LREE depletion and positive anomalies of U, Th and Pb. Orthopyroxene from the olivine-bearing gabbronorites displays a slight negative anomaly of Zr and Hf and unusually low HREE. In contrast, orthopyroxene from the gabbronorites displays a positive Zr and Hf anomaly. Orthopyroxenes within ultramafic rocks are thus not in equilibrium with clinopyroxene; this may indicate growth of orthopyroxene at the expense of olivine.

## Spinel

Spinel compositions in the Chilas Complex have been discussed in detail by Jan *et al.* (1992). Spinels in ultramafic rocks are mainly Cr-spinel, hercynite and Cr-bearing magnetite whereas in the gabbronorite sequence they are ulvöspinel and magnetite, often associated with ilmenite. Spinel compositions plot along a solvus between Al and Fe (Fig. 18; the entire dataset of spinel is presented in the

*Table 9: Major element concentrations (wt %) in plagioclase from the Chilas Complex*

| Sample: | C194 ($n=11$) | | | C218 ($n=9$) | | | C201 ($n=8$) | | |
|---|---|---|---|---|---|---|---|---|---|
| | Average | 2σ | 2σ mean | Average | 2σ | 2σ mean | Average | 2σ | 2σ mean |
| $SiO_2$ | 45·44 | 0·51 | 0·15 | 43·71 | 0·70 | 0·25 | 44·52 | 1·27 | 0·48 |
| $TiO_2$ | 0·01 | 0·02 | 0·01 | 0·01 | 0·03 | 0·01 | 0·01 | 0·03 | 0·01 |
| $Al_2O_3$ | 35·47 | 0·91 | 0·27 | 36·56 | 0·80 | 0·28 | 34·70 | 1·14 | 0·43 |
| $Cr_2O_3$ | 0·01 | 0·03 | 0·01 | 0·01 | 0·02 | 0·01 | 0·00 | 0·01 | 0·00 |
| $Fe_2O_3$ | 0·13 | 0·09 | 0·03 | 0·13 | 0·10 | 0·03 | 0·20 | 0·13 | 0·05 |
| FeO | 0·00 | 0·00 | 0·00 | 0·00 | 0·00 | 0·00 | 0·00 | 0·00 | 0·00 |
| MnO | 0·01 | 0·03 | 0·01 | 0·01 | 0·03 | 0·01 | 0·02 | 0·04 | 0·02 |
| NiO | 0·02 | 0·04 | 0·01 | 0·01 | 0·04 | 0·01 | 0·02 | 0·05 | 0·02 |
| MgO | 0·01 | 0·02 | 0·00 | 0·01 | 0·02 | 0·01 | 0·15 | 0·50 | 0·19 |
| CaO | 18·64 | 0·40 | 0·12 | 19·96 | 0·58 | 0·21 | 19·42 | 0·59 | 0·22 |
| $Na_2O$ | 1·25 | 0·25 | 0·08 | 0·38 | 0·33 | 0·12 | 0·92 | 0·64 | 0·24 |
| $K_2O$ | 0·02 | 0·03 | 0·01 | 0·01 | 0·01 | 0·01 | 0·02 | 0·02 | 0·01 |
| Total | 100·99 | | | 100·79 | | | 99·98 | | |
| Si | 2·0691 | 0·0271 | 0·0082 | 2·0039 | 0·0331 | 0·0117 | 2·0525 | 0·0268 | 0·0101 |
| Ti | 0·0003 | 0·0008 | 0·0002 | 0·0003 | 0·0009 | 0·0003 | 0·0003 | 0·0011 | 0·0004 |
| Al | 1·9036 | 0·0356 | 0·0107 | 1·9754 | 0·0395 | 0·0140 | 1·8856 | 0·0320 | 0·0121 |
| Cr | 0·0003 | 0·0010 | 0·0003 | 0·0002 | 0·0009 | 0·0003 | 0·0001 | 0·0004 | 0·0002 |
| $Fe^{3+}$ | 0·0044 | 0·0031 | 0·0009 | 0·0044 | 0·0035 | 0·0013 | 0·0070 | 0·0044 | 0·0017 |
| $Fe^{2+}$ | 0·0000 | 0·0000 | 0·0000 | 0·0000 | 0·0000 | 0·0000 | 0·0000 | 0·0000 | 0·0000 |
| Mn | 0·0004 | 0·0012 | 0·0004 | 0·0004 | 0·0010 | 0·0004 | 0·0009 | 0·0016 | 0·0006 |
| Ni | 0·0005 | 0·0016 | 0·0005 | 0·0005 | 0·0013 | 0·0005 | 0·0008 | 0·0019 | 0·0007 |
| Mg | 0·0004 | 0·0010 | 0·0003 | 0·0005 | 0·0016 | 0·0006 | 0·0103 | 0·0348 | 0·0132 |
| Ca | 0·9095 | 0·0174 | 0·0053 | 0·9804 | 0·0259 | 0·0092 | 0·9593 | 0·0362 | 0·0137 |
| Na | 0·1101 | 0·0225 | 0·0068 | 0·0336 | 0·0292 | 0·0103 | 0·0821 | 0·0562 | 0·0213 |
| K | 0·0014 | 0·0018 | 0·0005 | 0·0004 | 0·0008 | 0·0003 | 0·0010 | 0·0009 | 0·0003 |
| An | 0·891 | 0·021 | 0·006 | 0·967 | 0·029 | 0·010 | 0·921 | 0·052 | 0·020 |
| Ab | 0·108 | 0·021 | 0·006 | 0·033 | 0·029 | 0·010 | 0·078 | 0·052 | 0·020 |
| Or | 0·001 | 0·002 | 0·001 | 0·000 | 0·001 | 0·000 | 0·001 | 0·001 | 0·000 |

| Sample: | C50.4 ($n=2$) | | | C50.10 ($n=33$) | | | C50.8 ($n=2$) | | |
|---|---|---|---|---|---|---|---|---|---|
| | Average | 2σ | 2σ mean | Average | 2σ | 2σ mean | Average | 2σ | 2σ mean |
| $SiO_2$ | 44·95 | 0·83 | | 46·27 | 1·89 | 0·33 | 46·43 | 0·59 | |
| $TiO_2$ | 0·01 | 0·03 | | 0·01 | 0·02 | 0·00 | 0·03 | 0·06 | |
| $Al_2O_3$ | 33·80 | 0·76 | | 34·47 | 0·97 | 0·17 | 32·87 | 0·78 | |
| $Cr_2O_3$ | 0·03 | 0·07 | | 0·01 | 0·02 | 0·00 | 0·00 | 0·00 | |
| $Fe_2O_3$ | 0·20 | 0·06 | | 0·18 | 0·23 | 0·04 | 0·17 | 0·08 | |
| FeO | 0·00 | 0·00 | | 0·00 | 0·05 | 0·01 | 0·00 | 0·00 | |
| MnO | 0·00 | 0·00 | | 0·01 | 0·02 | 0·00 | 0·02 | 0·04 | |
| NiO | 0·00 | 0·00 | | 0·01 | 0·04 | 0·01 | 0·02 | 0·01 | |
| MgO | 0·01 | 0·01 | | 0·08 | 0·45 | 0·08 | 0·02 | 0·06 | |
| CaO | 18·17 | 0·71 | | 17·84 | 1·08 | 0·19 | 17·14 | 0·83 | |
| $Na_2O$ | 1·29 | 0·06 | | 1·48 | 0·61 | 0·11 | 1·89 | 0·47 | |

(continued)

*Table 9: Continued*

| Sample: | C50.4 ($n=2$) | | | C50.10 ($n=33$) | | | C50.8 ($n=2$) | | |
|---|---|---|---|---|---|---|---|---|---|
| | Average | 2σ | 2σ mean | Average | 2σ | 2σ mean | Average | 2σ | 2σ mean |
| $K_2O$ | 0·03 | 0·00 | | 0·03 | 0·02 | 0·00 | 0·03 | 0·00 | |
| Total | 98·48 | | | 100·39 | | | 98·59 | | |
| Si | 2·1006 | 0·0201 | | 2·1183 | 0·0636 | 0·0112 | 2·1612 | 0·0355 | |
| Ti | 0·0004 | 0·0011 | | 0·0003 | 0·0005 | 0·0001 | 0·0010 | 0·0021 | |
| Al | 1·8617 | 0·0591 | | 1·8600 | 0·0599 | 0·0106 | 1·8030 | 0·0363 | |
| Cr | 0·0010 | 0·0027 | | 0·0003 | 0·0008 | 0·0001 | 0·0000 | 0·0000 | |
| $Fe^{3+}$ | 0·0072 | 0·0018 | | 0·0063 | 0·0081 | 0·0014 | 0·0059 | 0·0031 | |
| $Fe^{2+}$ | 0·0000 | 0·0000 | | 0·0002 | 0·0018 | 0·0003 | 0·0000 | 0·0000 | |
| Mn | 0·0001 | 0·0000 | | 0·0003 | 0·0008 | 0·0001 | 0·0005 | 0·0014 | |
| Ni | 0·0000 | 0·0000 | | 0·0004 | 0·0016 | 0·0003 | 0·0004 | 0·0006 | |
| Mg | 0·0005 | 0·0013 | | 0·0058 | 0·0311 | 0·0055 | 0·0014 | 0·0040 | |
| Ca | 0·9098 | 0·0276 | | 0·8752 | 0·0586 | 0·0104 | 0·8546 | 0·0387 | |
| Na | 0·1173 | 0·0041 | | 0·1311 | 0·0529 | 0·0094 | 0·1703 | 0·0420 | |
| K | 0·0017 | 0·0006 | | 0·0015 | 0·0014 | 0·0002 | 0·0020 | 0·0001 | |
| An | 0·884 | 0·001 | | 0·868 | 0·053 | 0·009 | 0·832 | 0·040 | |
| Ab | 0·114 | 0·000 | | 0·130 | 0·052 | 0·009 | 0·166 | 0·040 | |
| Or | 0·002 | 0·000 | | 0·001 | 0·001 | 0·000 | 0·002 | 0·000 | |

| Sample: | C50.9 ($n=10$) | | | C50.6 ($n=4$) | | | C66 ($n=7$) | | |
|---|---|---|---|---|---|---|---|---|---|
| | Average | 2σ | 2σ mean | Average | 2σ | 2σ mean | Average | 2σ | 2σ mean |
| $SiO_2$ | 46·08 | 0·45 | 0·30 | 46·01 | 1·91 | 1·10 | 44·56 | 2·44 | 1·00 |
| $TiO_2$ | 0·01 | 0·01 | 0·01 | 0·01 | 0·03 | 0·02 | 0·01 | 0·02 | 0·01 |
| $Al_2O_3$ | 33·27 | 0·31 | 0·21 | 34·00 | 0·62 | 0·36 | 34·15 | 1·62 | 0·66 |
| $Cr_2O_3$ | 0·00 | 0·01 | 0·00 | 0·01 | 0·05 | 0·03 | 0·00 | 0·02 | 0·01 |
| $Fe_2O_3$ | 0·13 | 0·05 | 0·04 | 0·16 | 0·16 | 0·09 | 0·06 | 0·09 | 0·04 |
| FeO | 0·01 | 0·04 | 0·03 | 0·00 | 0·00 | 0·00 | 0·02 | 0·08 | 0·03 |
| MnO | 0·00 | 0·00 | 0·00 | 0·01 | 0·02 | 0·01 | 0·00 | 0·01 | 0·00 |
| NiO | 0·01 | 0·02 | 0·01 | 0·00 | 0·01 | 0·01 | 0·02 | 0·03 | 0·01 |
| MgO | 0·00 | 0·00 | 0·00 | 0·00 | 0·01 | 0·01 | 0·00 | 0·00 | 0·00 |
| CaO | 17·62 | 0·29 | 0·19 | 17·60 | 0·64 | 0·37 | 18·56 | 0·58 | 0·24 |
| $Na_2O$ | 1·65 | 0·16 | 0·10 | 1·74 | 0·40 | 0·23 | 1·16 | 0·34 | 0·14 |
| $K_2O$ | 0·03 | 0·01 | 0·00 | 0·03 | 0·01 | 0·01 | 0·01 | 0·02 | 0·01 |
| Total | 98·81 | | | 99·58 | | | 98·55 | | |
| Si | 2·1427 | 0·0180 | 0·0120 | 2·1200 | 0·0630 | 0·0364 | 2·0815 | 0·0998 | 0·0407 |
| Ti | 0·0003 | 0·0004 | 0·0003 | 0·0003 | 0·0010 | 0·0006 | 0·0002 | 0·0004 | 0·0002 |
| Al | 1·8231 | 0·0152 | 0·0102 | 1·8467 | 0·0522 | 0·0301 | 1·8800 | 0·0995 | 0·0406 |
| Cr | 0·0002 | 0·0003 | 0·0002 | 0·0004 | 0·0015 | 0·0009 | 0·0002 | 0·0007 | 0·0003 |
| $Fe^{3+}$ | 0·0044 | 0·0018 | 0·0012 | 0·0057 | 0·0055 | 0·0032 | 0·0022 | 0·0030 | 0·0012 |
| $Fe^{2+}$ | 0·0005 | 0·0014 | 0·0009 | 0·0000 | 0·0000 | 0·0000 | 0·0006 | 0·0034 | 0·0014 |
| Mn | 0·0001 | 0·0002 | 0·0002 | 0·0004 | 0·0008 | 0·0005 | 0·0001 | 0·0002 | 0·0001 |
| Ni | 0·0004 | 0·0005 | 0·0004 | 0·0001 | 0·0005 | 0·0003 | 0·0007 | 0·0012 | 0·0005 |
| Mg | 0·0003 | 0·0003 | 0·0002 | 0·0002 | 0·0007 | 0·0004 | 0·0000 | 0·0001 | 0·0000 |

(continued)

*Table 9: Continued*

| Sample: | C50.9 ($n=10$) | | | C50.6 ($n=4$) | | | C66 ($n=7$) | | |
|---|---|---|---|---|---|---|---|---|---|
| | Average | 2σ | 2σ mean | Average | 2σ | 2σ mean | Average | 2σ | 2σ mean |
| Ca | 0·8780 | 0·0151 | 0·0101 | 0·8691 | 0·0385 | 0·0222 | 0·9289 | 0·0325 | 0·0133 |
| Na | 0·1487 | 0·0141 | 0·0094 | 0·1553 | 0·0347 | 0·0200 | 0·1051 | 0·0300 | 0·0122 |
| K | 0·0014 | 0·0004 | 0·0002 | 0·0016 | 0·0009 | 0·0005 | 0·0005 | 0·0009 | 0·0004 |
| An | 0·854 | 0·013 | 0·009 | 0·847 | 0·035 | 0·020 | 0·898 | 0·028 | 0·012 |
| Ab | 0·145 | 0·013 | 0·009 | 0·151 | 0·034 | 0·020 | 0·102 | 0·029 | 0·012 |
| Or | 0·001 | 0·000 | 0·000 | 0·002 | 0·001 | 0·001 | 0·000 | 0·001 | 0·000 |

| Sample: | C48 | | | C48II ($n=22$) | | | C41 ($n=20$) | | |
|---|---|---|---|---|---|---|---|---|---|
| | Average | 2σ | 2σ mean | Average | 2σ | 2σ mean | Average | 2σ | 2σ mean |
| $SiO_2$ | 49·03 | 1·08 | 0·36 | 53·61 | 0·83 | 0·18 | 45·83 | 0·55 | 0·24 |
| $TiO_2$ | 0·01 | 0·02 | 0·01 | 0·01 | 0·02 | 0·00 | 0·01 | 0·01 | 0·00 |
| $Al_2O_3$ | 33·23 | 1·00 | 0·33 | 29·30 | 1·05 | 0·22 | 34·15 | 0·46 | 0·20 |
| $Cr_2O_3$ | 0·01 | 0·02 | 0·01 | 0·01 | 0·03 | 0·01 | 0·01 | 0·01 | 0·01 |
| $Fe_2O_3$ | 0·24 | 0·21 | 0·07 | 0·16 | 0·11 | 0·02 | 0·11 | 0·06 | 0·03 |
| FeO | 0·00 | 0·00 | 0·00 | 0·01 | 0·07 | 0·02 | 0·00 | 0·02 | 0·01 |
| MnO | 0·01 | 0·02 | 0·01 | 0·01 | 0·02 | 0·00 | 0·01 | 0·01 | 0·01 |
| NiO | 0·01 | 0·02 | 0·01 | 0·01 | 0·03 | 0·01 | 0·02 | 0·02 | 0·01 |
| MgO | 0·02 | 0·11 | 0·04 | 0·02 | 0·03 | 0·01 | 0·01 | 0·01 | 0·01 |
| CaO | 15·51 | 0·90 | 0·30 | 11·84 | 0·60 | 0·13 | 18·31 | 0·37 | 0·17 |
| $Na_2O$ | 2·83 | 0·44 | 0·15 | 4·84 | 0·35 | 0·07 | 1·50 | 0·20 | 0·09 |
| $K_2O$ | 0·04 | 0·05 | 0·02 | 0·24 | 0·05 | 0·01 | 0·03 | 0·02 | 0·01 |
| Total | 100·95 | | | 100·03 | | | 99·97 | | |
| Si | 2·2168 | 0·0460 | 0·0153 | 2·4221 | 0·0345 | 0·0073 | 2·1067 | 0·0231 | 0·0103 |
| Ti | 0·0003 | 0·0006 | 0·0002 | 0·0002 | 0·0006 | 0·0001 | 0·0002 | 0·0003 | 0·0001 |
| Al | 1·7704 | 0·0419 | 0·0140 | 1·5598 | 0·0397 | 0·0085 | 1·8505 | 0·0220 | 0·0098 |
| Cr | 0·0003 | 0·0007 | 0·0002 | 0·0003 | 0·0009 | 0·0002 | 0·0003 | 0·0004 | 0·0002 |
| $Fe^{3+}$ | 0·0083 | 0·0074 | 0·0025 | 0·0053 | 0·0036 | 0·0008 | 0·0038 | 0·0020 | 0·0009 |
| $Fe^{2+}$ | 0·0000 | 0·0000 | 0·0000 | 0·0003 | 0·0027 | 0·0006 | 0·0001 | 0·0009 | 0·0004 |
| Mn | 0·0003 | 0·0008 | 0·0003 | 0·0003 | 0·0006 | 0·0001 | 0·0004 | 0·0005 | 0·0002 |
| Ni | 0·0003 | 0·0008 | 0·0003 | 0·0004 | 0·0011 | 0·0002 | 0·0006 | 0·0008 | 0·0004 |
| Mg | 0·0015 | 0·0072 | 0·0024 | 0·0011 | 0·0016 | 0·0004 | 0·0005 | 0·0008 | 0·0004 |
| Ca | 0·7512 | 0·0444 | 0·0148 | 0·5729 | 0·0282 | 0·0060 | 0·9019 | 0·0196 | 0·0088 |
| Na | 0·2484 | 0·0373 | 0·0124 | 0·4235 | 0·0301 | 0·0064 | 0·1335 | 0·0172 | 0·0077 |
| K | 0·0023 | 0·0029 | 0·0010 | 0·0138 | 0·0031 | 0·0007 | 0·0015 | 0·0012 | 0·0005 |
| An | 0·750 | 0·039 | 0·013 | 0·567 | 0·029 | 0·006 | 0·870 | 0·017 | 0·008 |
| Ab | 0·248 | 0·038 | 0·013 | 0·419 | 0·028 | 0·006 | 0·129 | 0·017 | 0·007 |
| Or | 0·002 | 0·003 | 0·001 | 0·014 | 0·003 | 0·001 | 0·001 | 0·001 | 0·000 |

(continued)

electronic supplement). Spinel from dunite (with high Mg-number in olivine) is partly shifted towards the Cr apex, approaching the trend defined by Cr-spinel from the Jijal Complex (Jan & Windley, 1990). Spinels from the high Mg-number dunitic samples display an Mg-number enrichment trend with constant Cr-number. A similar trend at higher Cr-number values has been reported for spinels from the Jijal Complex

*Table 9: Continued*

| Sample: | C7 ($n=19$) | | | C129 ($n=18$) | | | C138 ($n=19$) | | |
|---|---|---|---|---|---|---|---|---|---|
| | Average | 2σ | 2σ mean | Average | 2σ | 2σ mean | Average | 2σ | 2σ mean |
| $SiO_2$ | 53·64 | 0·37 | 0·17 | 55·38 | 3·55 | 0·86 | 54·88 | 3·04 | 0·72 |
| $TiO_2$ | 0·01 | 0·02 | 0·01 | 0·01 | 0·02 | 0·01 | 0·02 | 0·04 | 0·01 |
| $Al_2O_3$ | 29·35 | 0·82 | 0·38 | 28·11 | 2·57 | 0·62 | 27·87 | 2·43 | 0·57 |
| $Cr_2O_3$ | 0·00 | 0·01 | 0·01 | 0·01 | 0·02 | 0·01 | 0·01 | 0·03 | 0·01 |
| $Fe_2O_3$ | 0·13 | 0·06 | 0·03 | 0·12 | 0·09 | 0·02 | 0·16 | 0·19 | 0·04 |
| FeO | 0·00 | 0·01 | 0·01 | | 0·00 | | | 0·00 | |
| MnO | 0·01 | 0·02 | 0·01 | 0·01 | 0·02 | 0·00 | 0·01 | 0·02 | 0·00 |
| NiO | 0·01 | 0·05 | 0·02 | | | | | 0·00 | |
| MgO | 0·02 | 0·03 | 0·01 | 0·01 | 0·01 | 0·00 | 0·01 | 0·02 | 0·01 |
| CaO | 11·82 | 0·29 | 0·13 | 10·36 | 2·83 | 0·69 | 10·75 | 2·23 | 0·53 |
| $Na_2O$ | 4·90 | 0·24 | 0·11 | 4·87 | 1·41 | 0·34 | 4·80 | 1·10 | 0·26 |
| $K_2O$ | 0·24 | 0·05 | 0·02 | 0·34 | 0·16 | 0·04 | 0·40 | 0·17 | 0·04 |
| Total | 100·14 | 1·11 | 0·51 | 99·21 | | | 98·88 | | |
| Si | 2·4193 | 0·0221 | 0·0102 | 2·5076 | 0·1463 | 0·0355 | 2·4987 | 0·1295 | 0·0305 |
| Ti | 0·0005 | 0·0007 | 0·0003 | 0·0003 | 0·0007 | 0·0002 | 0·0006 | 0·0015 | 0·0003 |
| Al | 1·5599 | 0·0294 | 0·0135 | 1·5004 | 0·1447 | 0·0351 | 1·4960 | 0·1335 | 0·0315 |
| Cr | 0·0002 | 0·0005 | 0·0002 | 0·0003 | 0·0008 | 0·0002 | 0·0003 | 0·0011 | 0·0003 |
| $Fe^{3+}$ | 0·0044 | 0·0023 | 0·0010 | 0·0042 | 0·0031 | 0·0007 | 0·0056 | 0·0064 | 0·0015 |
| $Fe^{2+}$ | 0·0001 | 0·0005 | 0·0002 | | | | | 0·0000 | |
| Mn | 0·0004 | 0·0010 | 0·0004 | 0·0003 | 0·0008 | 0·0002 | 0·0003 | 0·0008 | 0·0002 |
| Ni | 0·0005 | 0·0016 | 0·0007 | | | | | 0·0000 | |
| Mg | 0·0013 | 0·0020 | 0·0009 | 0·0004 | 0·0008 | 0·0002 | 0·0004 | 0·0015 | 0·0003 |
| Ca | 0·5712 | 0·0133 | 0·0061 | 0·5028 | 0·1407 | 0·0341 | 0·5247 | 0·1099 | 0·0259 |
| Na | 0·4283 | 0·0192 | 0·0088 | 0·4274 | 0·1223 | 0·0297 | 0·4234 | 0·0964 | 0·0227 |
| K | 0·0140 | 0·0029 | 0·0013 | 0·0194 | 0·0093 | 0·0022 | 0·0230 | 0·0101 | 0·0024 |
| An | 0·564 | 0·015 | 0·007 | 0·529 | 0·139 | 0·034 | 0·540 | 0·110 | 0·026 |
| Ab | 0·423 | 0·015 | 0·007 | 0·450 | 0·131 | 0·032 | 0·436 | 0·101 | 0·024 |
| Or | 0·014 | 0·003 | 0·001 | 0·020 | 0·010 | 0·002 | 0·024 | 0·010 | 0·002 |

| Sample: | C134 ($n=14$) | | | C135 ($n=9$) | | | C46 ($n=9$) | | |
|---|---|---|---|---|---|---|---|---|---|
| | Average | 2σ | 2σ mean | Average | 2σ | 2σ mean | Average | 2σ | 2σ mean |
| $SiO_2$ | 55·99 | 1·37 | 0·38 | 54·48 | 0·71 | 0·25 | 56·28 | 3·74 | 1·32 |
| $TiO_2$ | 0·02 | 0·03 | 0·01 | | | | 0·01 | 0·03 | 0·01 |
| $Al_2O_3$ | 27·65 | 0·79 | 0·22 | 28·83 | 0·39 | 0·14 | 28·95 | 2·61 | 0·92 |
| $Cr_2O_3$ | 0·01 | 0·03 | 0·01 | | | | 0·01 | 0·02 | 0·01 |
| $Fe_2O_3$ | 0·13 | 0·11 | 0·03 | 0·00 | 0·00 | 0·00 | 0·04 | 0·16 | 0·06 |
| FeO | | | | 0·14 | 0·07 | 0·03 | 0·04 | 0·07 | 0·03 |
| MnO | 0·01 | 0·01 | 0·00 | | | | 0·01 | 0·03 | 0·01 |
| NiO | | | | | | | 0·02 | 0·05 | 0·02 |
| MgO | 0·00 | 0·01 | 0·00 | 0·00 | 0·01 | 0·00 | 0·01 | 0·02 | 0·01 |
| CaO | 9·73 | 0·56 | 0·16 | 10·48 | 0·31 | 0·11 | 10·33 | 2·92 | 1·03 |
| $Na_2O$ | 5·06 | 0·41 | 0·11 | 5·12 | 0·17 | 0·06 | 5·76 | 1·77 | 0·62 |

(continued)

*Table 9: Continued*

| Sample: | C134 ($n=14$) | | | C135 ($n=9$) | | | C46 ($n=9$) | | |
|---|---|---|---|---|---|---|---|---|---|
| | Average | 2σ | 2σ mean | Average | 2σ | 2σ mean | Average | 2σ | 2σ mean |
| $K_2O$ | 0·43 | 0·10 | 0·03 | 0·34 | 0·03 | 0·01 | 0·03 | 0·02 | 0·01 |
| Total | 99·03 | 0·94 | 0·26 | 99·40 | 0·38 | 0·13 | 101·46 | 1·86 | 0·66 |
| Si | 2·5353 | 0·0416 | 0·0115 | 2·4724 | 0·0261 | 0·0092 | 2·4953 | 0·1365 | 0·0483 |
| Ti | 0·0006 | 0·0011 | 0·0003 | | | | 0·0004 | 0·0009 | 0·0003 |
| Al | 1·4760 | 0·0489 | 0·0136 | 1·5420 | 0·0242 | 0·0086 | 1·5133 | 0·1434 | 0·0507 |
| Cr | 0·0003 | 0·0010 | 0·0003 | 0·0000 | 0·0000 | 0·0000 | 0·0004 | 0·0008 | 0·0003 |
| $Fe^{3+}$ | 0·0046 | 0·0036 | 0·0010 | | | | 0·0012 | 0·0053 | 0·0019 |
| $Fe^{2+}$ | | | | 0·0054 | 0·0028 | 0·0010 | 0·0013 | 0·0028 | 0·0010 |
| Mn | 0·0002 | 0·0005 | 0·0001 | | | | 0·0003 | 0·0010 | 0·0004 |
| Ni | | | | | | | 0·0008 | 0·0017 | 0·0006 |
| Mg | 0·0002 | 0·0006 | 0·0002 | 0·0002 | 0·0007 | 0·0002 | 0·0003 | 0·0012 | 0·0004 |
| Ca | 0·4720 | 0·0304 | 0·0084 | 0·5095 | 0·0152 | 0·0054 | 0·4912 | 0·1419 | 0·0502 |
| Na | 0·4443 | 0·0335 | 0·0093 | 0·4505 | 0·0140 | 0·0050 | 0·4945 | 0·1456 | 0·0515 |
| K | 0·0250 | 0·0059 | 0·0016 | 0·0199 | 0·0015 | 0·0005 | 0·0015 | 0·0011 | 0·0004 |
| An | 0·501 | 0·032 | 0·009 | 0·520 | 0·015 | 0·005 | 0·498 | 0·145 | 0·051 |
| Ab | 0·472 | 0·032 | 0·009 | 0·460 | 0·015 | 0·005 | 0·501 | 0·145 | 0·051 |
| Or | 0·027 | 0·006 | 0·002 | 0·020 | 0·002 | 0·001 | 0·001 | 0·001 | 0·000 |

(continued)

(Fig. 19, Jan & Windley, 1990). Spinel constitutes <3 vol. % of the gabbronorite. An apparent continuous solid-solution between ilmenite and ulvöspinel, and between ulvöspinel and magnetite, is developed.

## Amphibole

It is generally difficult to differentiate between magmatic and metamorphic amphibole in deep-seated plutons. Amphibole rimming pyroxene within the gabbronorites is interpreted as a late magmatic phase or an early metamorphic overgrowth. In more evolved units amphibole forming euhedral centimeter-sized grains with quartz intergrowths is considered magmatic. The amphibole interpreted as magmatic is essentially a pargasitic, tschermakitic to magnesio-hornblende (Fig. 20). In secondary peridotites interstitial magnesio-hornblende between olivine grains is replaced by metamorphic tremolitic amphibole. Trace elements measured on magnesium-hornblende in the ol-websterites (Fig. 21) define a pattern very similar to that of clinopyroxene with a $K_d^{REE}$ of 3–5, higher than the usually observed $K_d^{REE}$ of 1–2 (Chazot *et al.*, 1996; Hermann *et al.*, 2001). Accordingly, a metamorphic re-equilibration or origin for the magnesio-hornblende is likely. The trace element pattern is characterized by LREE depletion and a negative Hf and Zr anomaly. The lack of negative Eu and Sr anomalies indicates that amphibole did not equilibrate with plagioclase.

## Plagioclase

The anorthite (An) content of plagioclase in the mafic rocks varies continuously from $An_{91}$ to $An_{48}$ between samples (Fig. 22); large variations in An content (e.g. from $An_{88}$ to $An_{73}$) can be found within single mafic samples as a result of normal core–rim zoning. Plagioclase-bearing ultramafic rocks have slightly more homogeneous plagioclase (varying from $An_{98}$ to $An_{80}$). Grain zonation is generally reverse, which has been attributed to diffusion exchange of Na between plagioclase and amphibole (Khan *et al.*, 1989). Whereas plagioclases from primitive pyroxene-bearing pegmatites plot on the high-An side of the trend, plagioclases from evolved hornblende-bearing pegmatites are distinctively lower in $K_2O$ at a given An content than in the mafic sequence (Fig. 22).

Trace element concentrations have been determined on 6–9 mineral grains separated from four samples: two gabbronorites (C7 and C48), one olivine-bearing gabbronorite (C66) and one plagioclase-bearing lherzolite (C218). The averaged, primitive mantle normalized (Sun & McDonough, 1989), trace element patterns of all analyses are similar (Fig. 23). The trace element concentrations increase with decreasing An content from plagioclase-bearing lherzolite ($An_{96}$) to

*Table 9: Continued*

| Sample: | C219 ($n=7$) | | | C172 ($n=9$) | | |
|---|---|---|---|---|---|---|
| | Average | 2σ | 2σ mean | Average | 2σ | 2σ mean |
| $SiO_2$ | 45·29 | 1·46 | 0·60 | 55·10 | 2·11 | 0·75 |
| $TiO_2$ | 0·00 | 0·01 | 0·00 | 0·01 | 0·03 | 0·01 |
| $Al_2O_3$ | 36·73 | 0·97 | 0·40 | 29·00 | 1·30 | 0·46 |
| $Cr_2O_3$ | 0·02 | 0·03 | 0·01 | 0·00 | 0·01 | 0·00 |
| $Fe_2O_3$ | 0·01 | 0·07 | 0·03 | 0·04 | 0·06 | 0·02 |
| FeO | 0·09 | 0·11 | 0·04 | 0·01 | 0·05 | 0·02 |
| MnO | 0·01 | 0·02 | 0·01 | 0·00 | 0·01 | 0·00 |
| NiO | 0·02 | 0·05 | 0·02 | 0·01 | 0·04 | 0·02 |
| MgO | 0·00 | 0·01 | 0·00 | 0·00 | 0·02 | 0·01 |
| CaO | 19·08 | 1·15 | 0·47 | 10·78 | 1·56 | 0·55 |
| $Na_2O$ | 0·65 | 0·65 | 0·27 | 5·53 | 1·01 | 0·36 |
| $K_2O$ | 0·00 | 0·01 | 0·00 | 0·02 | 0·03 | 0·01 |
| Total | 101·91 | 0·34 | 0·14 | 100·53 | 0·54 | 0·19 |
| Si | 2·0509 | 0·0605 | 0·0247 | 2·4674 | 0·0744 | 0·0263 |
| Ti | 0·0002 | 0·0003 | 0·0001 | 0·0004 | 0·0007 | 0·0003 |
| Al | 1·9608 | 0·0568 | 0·0232 | 1·5308 | 0·0800 | 0·0283 |
| Cr | 0·0006 | 0·0009 | 0·0004 | 0·0002 | 0·0004 | 0·0001 |
| $Fe^{3+}$ | 0·0005 | 0·0024 | 0·0010 | 0·0013 | 0·0019 | 0·0007 |
| $Fe^{2+}$ | 0·0033 | 0·0041 | 0·0017 | 0·0005 | 0·0019 | 0·0007 |
| Mn | 0·0003 | 0·0007 | 0·0003 | 0·0002 | 0·0004 | 0·0001 |
| Ni | 0·0007 | 0·0018 | 0·0007 | 0·0004 | 0·0015 | 0·0005 |
| Mg | 0·0002 | 0·0004 | 0·0002 | 0·0002 | 0·0008 | 0·0003 |
| Ca | 0·9255 | 0·0585 | 0·0239 | 0·5176 | 0·0790 | 0·0279 |
| Na | 0·0567 | 0·0571 | 0·0233 | 0·4799 | 0·0844 | 0·0298 |
| K | 0·0003 | 0·0004 | 0·0002 | 0·0012 | 0·0017 | 0·0006 |
| An | 0·942 | 0·058 | 0·024 | 0·518 | 0·082 | 0·029 |
| Ab | 0·058 | 0·058 | 0·024 | 0·480 | 0·081 | 0·029 |
| Or | 0·000 | 0·000 | 0·000 | 0·001 | 0·002 | 0·001 |

gabbronorite ($An_{56}$). The incompatible elements are variably enriched (1–30 times primitive mantle) and HREE are strongly depleted (0·01–0·1 times primitive mantle). Ba, Pb, Sr, Eu display positive anomalies with respect to LREE.

## DISCUSSION

### *P–T* conditions during intrusion

The granoblastic texture and the partly exsolved pyroxenes indicate slow cooling of the gabbronorite. Two-pyroxene thermometry (Wood & Banno, 1973; Wells, 1977) yields a temperature range of 840–950°C, regardless of the lithology (see Table 11), in accordance with previously published estimates (Jan & Howie, 1981). These temperatures are probably re-equilibration temperatures that prevailed during granulite-facies conditions. The Ca-in-opx thermometer (Brey & Köhler, 1990) applied to the ultramafic rocks yields a significantly higher temperature of 1040–1160°C (Table 11). Significantly higher liquidus temperatures of 1214–1265°C (Table 11) are obtained for the most primitive dunite samples using the low-*P* relationship between olivine Mg-number and basaltic liquidus temperature (Niu *et al.*, 2002). Using the relationship of Herzberg & O'Hara (2002) to correct for the inferred higher intrusion pressure of the Chilas Complex (see below) yields higher temperatures of 1250–1302°C. The presence of magmatic amphibole indicates a hydrous parental magma and constrains the upper limit of the crystallization temperature at the onset of amphibole fractionation to less than 1100°C (Allen *et al.*, 1975). There is a significant variability in the predicted effect of $H_2O$ on liquidus olivine temperatures (Falloon & Danyushevsky, 2000; Sugawara, 2000). Especially at low water contents (<1·5 wt%) the effect is probably non-linear (Medard & Grove, 2007; Almeev *et al.*, 2007). However, the addition of 1–2 wt% of $H_2O$ lowers the liquidus temperature by some 40–60°C (Almeev *et al.*, 2007). Accordingly we estimate magmatic temperatures to have been in the range of 1190–1220°C.

Pressure estimates within gabbronoritic mineral-assemblages are not straightforward. The clinopyroxene barometer (Nimis & Ulmer, 1998) yields pressures between 0·6 and 1·3 GPa depending on the assumed crystallization temperature. Pressure estimates for the intrusion above 0·8 GPa are possibly too high, as magmatic garnet should form at such a high pressure (e.g. Müntener *et al.*, 2000). There is no garnet in the Chilas Complex. The plag–grt–bio–qz barometer (Hoisch, 1990) and Fe–Mg grt–bio exchange thermometer, applied to a metapelite sampled within the Khiner Valley, less than 1 km to the north of the boundary with the Chilas gabbronorite, yield peak metamorphic conditions of ~0·7 GPa and ~700°C (Jagoutz, unpublished data). An intrusion pressure >0·6 GPa is consistent with the two-pyroxene–spinel symplectites between olivine and plagioclase in ultramafic rocks; these indicate pressure of ~0·6–0·7 GPa (Kushiro & Yoder, 1966). Accordingly, the pressure during intrusion of the Chilas Complex can be constrained around 0·6–0·7 GPa. These pressures are lower than those for the garnet granulites of the Jijal Complex (Ringuette *et al.*, 1999). This difference is consistent with the interpretation that the Chilas Complex intruded during rifting and associated decompression (Khan *et al.*, 1989; Burg *et al.*, 2006).

### Attainment of phase equilibrium and preservation of original magmatic chemistry

The *P–T* conditions calculated for the Chilas Complex indicate granulite-facies conditions, which is a consequence

*Table 10: Trace element concentrations (ppm) in plagioclase from the Chilas Complex*

| Sample: | C218 | | | C66 | | | C48 | | | C7 | | |
|---|---|---|---|---|---|---|---|---|---|---|---|---|
| *n*: | 6 | | | 7 | | | 7 | | | 9 | | |
| | Average | 2σ | 2σ mean | Average | 2σ | 2σ mean | Average | 2σ | 2σ mean | Average | 2σ | 2σ mean |
| Li | 1·81 | 2·25 | 1·01 | 0·139 | 0·053 | 0·022 | 9·01 | 1·39 | 0·57 | 4·30 | 2·34 | 0·83 |
| Sc | 0·245 | 0·043 | 0·019 | 0·286 | 0·055 | 0·021 | 0·264 | 0·047 | 0·019 | 0·217 | 0·055 | 0·019 |
| V | | | | | | | 0·254 | 0·211 | 0·086 | 0·222 | 0·083 | 0·029 |
| Cr | 2·91 | 1·13 | 0·51 | 2·72 | 2·05 | 0·77 | 1·86 | 0·67 | 0·27 | 1·27 | 0·31 | 0·11 |
| Co | 0·043 | 0·034 | 0·015 | 0·329 | 1·556 | 0·588 | 0·125 | 0·104 | 0·043 | 0·124 | 0·173 | 0·061 |
| Ni | 1·75 | 1·03 | 0·46 | 1·78 | 4·15 | 1·86 | 0·799 | 0·495 | 0·202 | 1·12 | 0·89 | 0·31 |
| Cu | | | | | | | 0·351 | 0·688 | 0·281 | 0·145 | 0·130 | 0·046 |
| Zn | | | | | | | 15·55 | 65·44 | 26·72 | 4·22 | 7·07 | 2·50 |
| Ga | 18·4 | 7·3 | 3·3 | 17·0 | 1·6 | 0·6 | 22·6 | 2·0 | 0·8 | 21·7 | 1·9 | 0·7 |
| Rb | | | | | | | 0·585 | 0·227 | 0·093 | 0·503 | 0·081 | 0·029 |
| Sr | 1062 | 768 | 344 | 602 | 67 | 25 | 566 | 21 | 9 | 547 | 34 | 12 |
| Y | | | | 0·010 | 0·008 | 0·004 | 0·111 | 0·050 | 0·021 | 0·245 | 0·044 | 0·015 |
| Zr | | | | | | | | | | | | |
| Nb | | | | | | | | | | 0·009 | 0·012 | 0·004 |
| Cs | | | | | | | | | | 0·007 | 0·007 | 0·002 |
| Ba | 4·11 | 3·0 | 1·33 | 7·93 | 0·99 | 0·37 | 68·0 | 6·7 | 2·7 | 71·9 | 4·9 | 1·7 |
| La | 0·152 | 0·066 | 0·029 | 0·258 | 0·035 | 0·013 | 1·44 | 0·16 | 0·07 | 2·12 | 0·12 | 0·04 |
| Ce | 0·122 | 0·067 | 0·030 | 0·404 | 0·083 | 0·031 | 2·27 | 0·35 | 0·14 | 3·47 | 0·23 | 0·08 |
| Pr | 0·011 | 0·006 | 0·003 | 0·037 | 0·019 | 0·007 | 0·213 | 0·048 | 0·020 | 0·364 | 0·044 | 0·016 |
| Nd | 0·029 | 0·024 | 0·011 | 0·109 | 0·068 | 0·026 | 0·738 | 0·224 | 0·091 | 1·31 | 0·12 | 0·04 |
| Sm | | | | 0·062* | | | 0·101 | 0·031 | 0·013 | 0·187 | 0·036 | 0·013 |
| Eu | 0·057 | 0·017 | 0·008 | 0·105 | 0·022 | 0·008 | 0·420 | 0·088 | 0·036 | 0·540 | 0·110 | 0·039 |
| Gd | | | | | | | 0·078 | 0·025 | 0·010 | 0·118 | 0·032 | 0·011 |
| Tb | | | | | | | 0·006 | 0·004 | 0·002 | 0·015 | 0·004 | 0·001 |
| Dy | | | | | | | 0·026 | 0·018 | 0·007 | 0·062 | 0·028 | 0·010 |
| Ho | | | | | | | 0·005 | 0·003 | 0·001 | 0·010 | 0·003 | 0·001 |
| Er | | | | | | | 0·011 | 0·007 | 0·004 | 0·021 | 0·010 | 0·003 |
| Tm | | | | | | | 0·002 | 0·001 | 0·001 | 0·005 | 0·003 | 0·001 |
| Yb | | | | | | | | | | | | |
| Lu | | | | | | | | | | | | |
| Hf | | | | | | | | | | 0·011 | 0·001 | 0·001 |
| Ta | | | | | | | | | | 0·005 | 0·003 | 0·001 |
| Pb | 0·820 | 0·230 | 0·103 | 0·378 | 0·057 | 0·022 | 1·81 | 0·324 | 0·132 | 1·96 | 0·13 | 0·05 |
| Th | | | | | | | | | | 0·003 | 0·001 | 0·000 |
| U | 0·015 | 0·009 | 0·004 | 0·004 | 0·002 | 0·001 | | | | 0·005 | 0·006 | 0·002 |

The concentration of trace element for which no value is shown is below detection limit.
*Concentration determined using isotopic dilution method and TIMS (unpublished data).

of deep-seated intrusions re-equilibrating during cooling into the granulite-facies field. At such elevated temperatures diffusive, sub-solidus, re-equilibration potentially obliterates the original magmatic mineral chemistry. Analysed samples are extremely fresh and no alteration products associated with infiltration of water are observed in thin section. Therefore re-equilibration in the studied samples should have occurred dominantly by solid-state diffusion or recrystallization. The lower temperature for the opx–cpx exchange thermometer (Wood & Banno, 1973; Wells, 1977) compared with the Ca-in-opx thermometer (Brey & Köhler, 1990), the granoblastic texture,

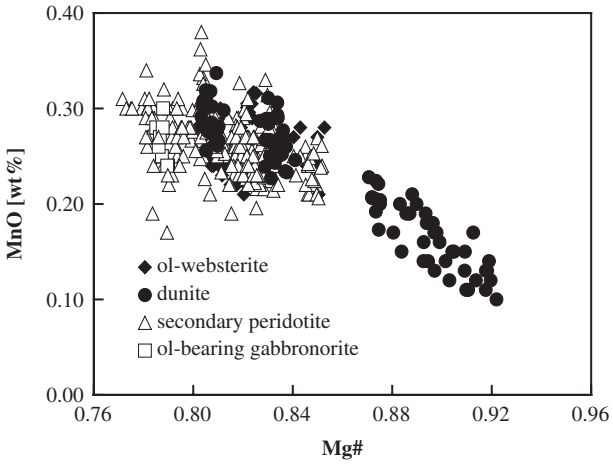


**Fig. 12.** Olivine composition in dunite, lherzolite, pyroxenite and olivine-bearing gabbronorite. (Note compositional gap between Mg-number 0·87 and 0·85.)

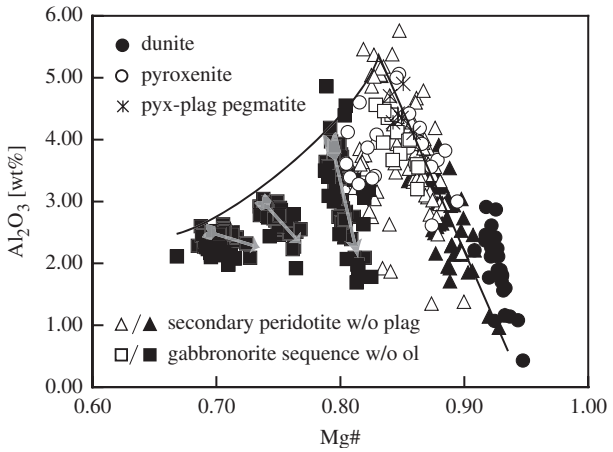


**Fig. 13.** $Al_2O_3$ vs Mg-number for clinopyroxene. The continuous line represents an igneous trend determined from core compositions. Grey arrows represent metamorphic cooling deduced from zoned clinopyroxene. The igneous trend is characterized by an increasing $Al_2O_3$ content with decreasing Mg-number until plagioclase is present in the rocks. The metamorphic trend represents a Tschermak $(Fe,Mg)SiAl_{-2}$ exchange during cooling. (See text for discussion.) Symbols as indicated or as in Fig. 12.

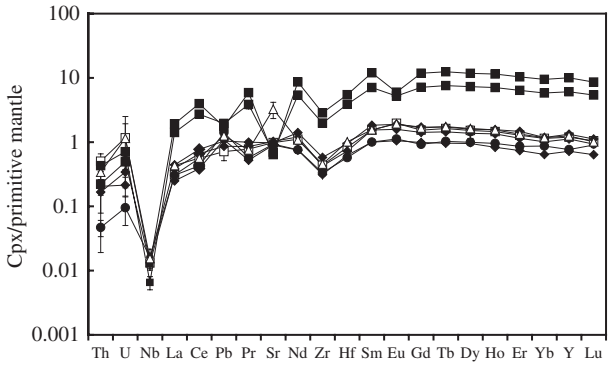


**Fig. 14.** Abundance of trace elements in clinopyroxene normalized to primitive mantle (Sun & McDonough, 1989). The average value of 6–11 mineral grains per sample is plotted, with error bars indicating the 2σ mean inter-mineral variance of single samples. Symbols as in Fig. 13.

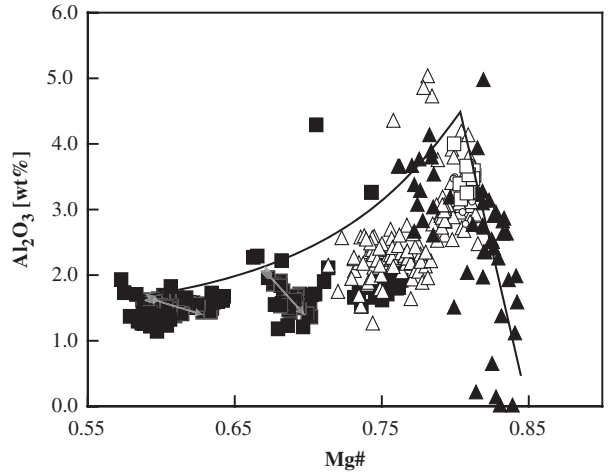


**Fig. 15.** $Al_2O_3$ vs Mg-number for orthopyroxene from the Chilas Complex. Symbols as in Fig. 13.

exsolution trails in pyroxene and the Tschermak exchange observed in clinopyroxene confirm that metamorphic re-equilibration did occur. However, there are several lines of evidence that metamorphic re-equilibration affected, but did not obliterate the original magmatic phase equilibrium. First, the presence of sharply defined centimeter-scale layering and the preservation of millimeter-scale veinlets in thin section (Burg *et al.*, 2006) preclude re-equilibration beyond the grain scale. Additionally, the presence of exsolved pyroxene indicates that diffusion rates were too low compared with cooling rates. This observation is consistent with the temperatures calculated with the Ca-in-opx thermometer ($1105 \pm 33$°C) being higher than temperatures from the cpx–opx thermometer (850–920°C). Reverse and normal zoning in plagioclase (see below) and the absence of a significant Eu anomaly in clinopyroxene in plagioclase-bearing rocks (see below and Fig. 24) indicate that the preserved mineral chemistry for elements with low diffusion coefficients reflects or closely approaches that of the original igneous protolith. Similarly, using the empirical relationship between temperature and equilibrium distribution of trace elements (Witt-Eickschen & O'Neill, 2005) in a four-phase ol-websterite (C03-44) for a range of trace elements generally yields similar temperatures to the Ca-in-opx thermometer (Table 11).

## A composite Chilas Complex

Based on the different mineral chemistry of plagioclase in the UMA sequence ($An_{98-83}$) and in the main

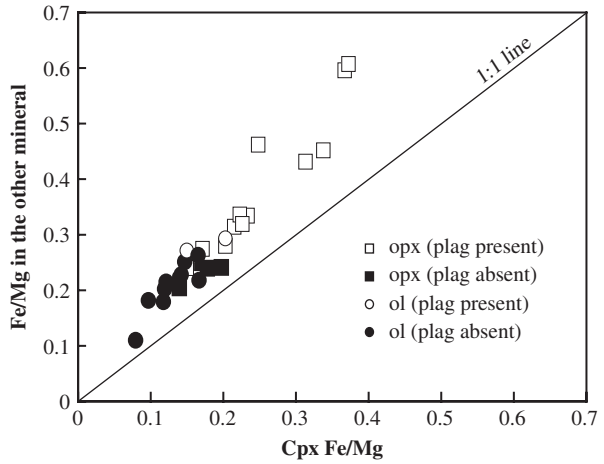


**Fig. 16.** Plot of Fe/Mg in clinopyroxene vs Fe/Mg in olivine and orthopyroxene. The 1:1 line is shown for comparison.

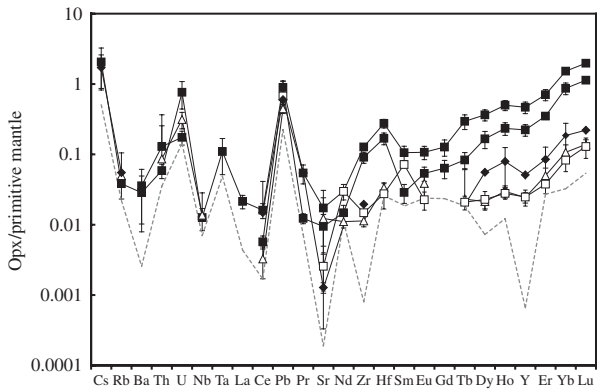


**Fig. 17.** Abundance of trace elements in orthopyroxene normalized to primitive mantle (Sun & McDonough, 1989). The average value of 5–10 mineral grains per sample is plotted. Errors bars indicate the $2\sigma$ mean inter-mineral variance of single samples. Grey dotted line illustrates the detection limit. Symbols as in Fig. 13.

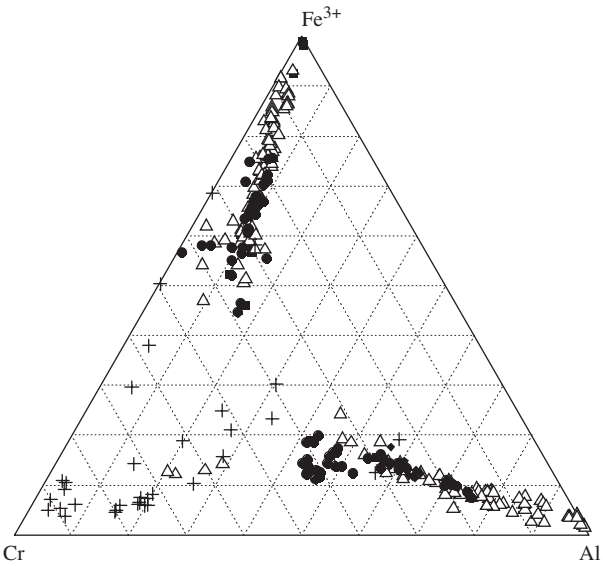


**Fig. 18.** Ternary plot ($Fe^{3+}$–Cr–Al) illustrating spinel compositions from the Chilas Complex compared with those from the Jijal Complex (Jan & Windley, 1990). Symbols as in Fig. 13, except that for presentation reasons secondary peridotites are shown as open triangles regardless of the presence or absence of plagioclase. +, Data from the Jijal Complex.

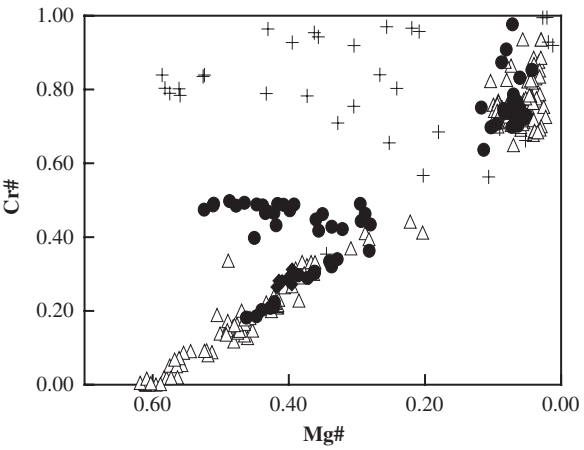


**Fig. 19.** Cr-number [Cr-number = Cr/(Al + Cr)] vs Mg-number for spinel in ultramafic rocks compared with spinel compositions in the ultramafic Jijal Complex (Jan & Windley, 1990). Symbols as in Fig. 17.

gabbronorite ($An_{64–40}$) (Fig. 22), the UMA associations were inferred to have crystallized from a more mafic magma than the gabbronorites (Jan *et al.*, 1984; Khan *et al.*, 1989). Our results show that there is no real difference despite a conspicuous paucity of compositions between $An_{80}$ and $An_{65}$. However, traverses across plagioclase grains within individual gabbronorite samples show large variations spanning the composition range of the inferred gap. We also note that the data of Khan (1988) plot within the supposed compositional gap. The normalized trace element patterns of plagioclase from plagioclase-bearing lherzolite, olivine-bearing gabbronorite and gabbronorite are consistent with differentiation (Fig. 23 and, for example, increasing Ba/Sr with decreasing anorthite content; Blundy & Wood, 1991). Our plagioclase data do not support the formation of the ultramafic and gabbronorite sequences from compositionally different magma batches. Continuous differentiation trends are also observed in the major element chemistry of olivine (Fig. 12), clinopyroxene (Fig. 13) and orthopyroxene (Fig. 15). In addition, the Nd isotopic composition indicates equilibrium between the gabbronorite sequence and the ultramafic bodies at the time of emplacement (Jagoutz *et al.*, 2006). Therefore, our analyses suggest that both the ultramafic and gabbronorite sequences were derived from a common differentiating magma, albeit structural observations imply different intrusive batches (Burg *et al.*, 2006). We propose that the term UMA should be abandoned, and a distinction

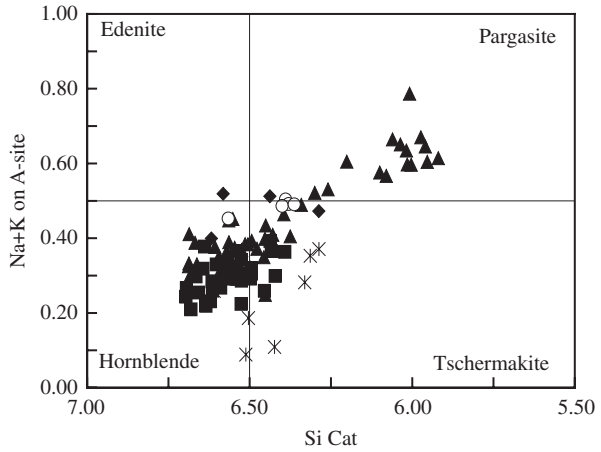


**Fig. 20.** Magmatic amphibole compositions from various lithologies of the Chilas Complex. Nomenclature after Leake (1978). Symbols as in Fig. 13.

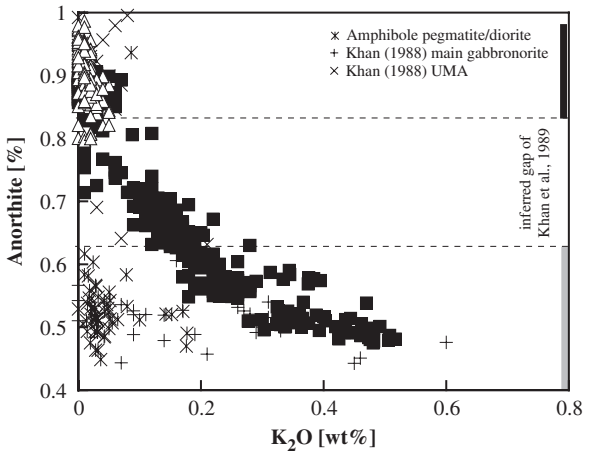


**Fig. 22.** Compositional variation of plagioclase. The compositional gap between $An_{83}$ and $An_{64}$ invoked by Khan *et al.* (1989) in plagioclase composition between UMA associations and gabbronorite (bars on the left side) is not verified. Symbols for data from this study as in Fig. 13; literature data are from Khan (1988).

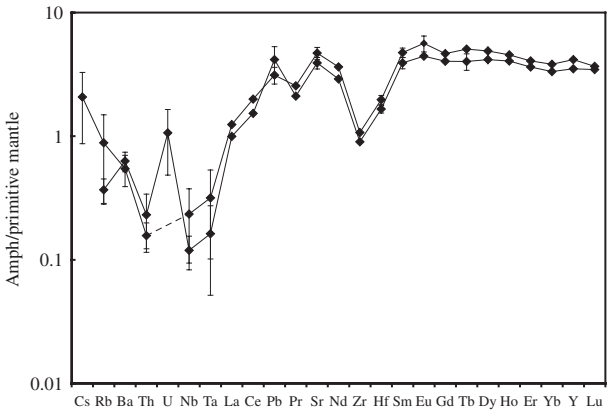


**Fig. 21.** Averaged primitive mantle (Sun & McDonough, 1989) normalized trace element patterns of amphibole from the ol-websterite. Error bars indicate the 2σ mean inter-mineral variance. Symbols as in Fig. 13.

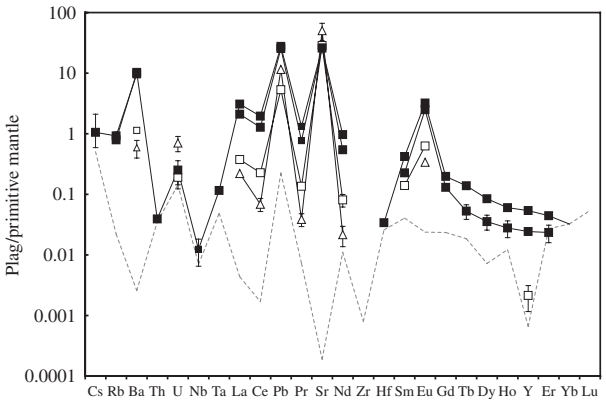


**Fig. 23.** Primitive mantle (Sun & McDonough, 1989) normalized average trace element composition of plagioclase from gabbronorite (C7 and C48), olivine-bearing gabbronorite (C66) and a plagioclase-bearing secondary peridotite (C218). The dashed line indicates the detection limit of LA-ICP-MS. Inter-mineral variations within single samples are given as $2\sigma_{mean}$ error bars. Symbols as in Fig. 13.

should be made between olivine-dominated ultramafic and plagioclase-dominated gabbronorite sequences.

It is worth noting that the transition from high to lower An content across the supposed compositional gap (Khan *et al.*, 1989) occurs over less than a few meters outcrop. Transitional samples could easily be overlooked by statistical sampling throughout the Chilas Complex. Field evidence supports the thinning and smearing out of meter-scale layered sequences towards the contact with the ultramafite [Fig. 7 and Jagoutz *et al.* (2006, Fig. 3a)]. We propose that an initially much wider transition zone was disrupted during diapiric emplacement of the ultramafic rocks, thereby juxtaposing primitive, high-An rocks next to evolved, low-An rocks and obliterating an originally continuous, 'stratigraphic' An trend.

The lower $K_2O$ concentration at a given An content of plagioclase from evolved amphibole-bearing pegmatites or diorites compared with the gabbronorite sequence (Fig. 22) could be interpreted to imply a different source for the earlier units. However, as field observations indicate a comagmatic relationship between the gabbronorite sequence and the pegmatites (Fig. 6e) we consider this interpretation unlikely. Similarly, as the $K_2O$ depletion is also found in samples devoid of biotite, biotite crystallization cannot be solely responsible for the relative depletion in $K_2O$. We currently favour the interpretation that the low $K_2O$ content of plagioclase is due to the escape of a very late stage, small-degree, $K_2O$-rich liquid from the system.

*Table 11: Comparism of temperature estimates using different thermometers applied to various samples from the Chilas Complex*

| Sample | Ca-in-opx thermometer, Brey & Köhler (1990)* | cpx–opx thermometer, Wood & Banno (1973) | Ol-liquidus temp., Niu *et al.* (2002) | Trace element partitioning thermometer, Witt-Eickschen & O'Neil (2005)† |
|---|---|---|---|---|
| C66 | – | 950 ± 52 | 1159 ± 6 | – |
| C48 | – | 876 ± 49 | – | – |
| C218 | 1100 ± 64 | 859 ± 48 | 1159 ± 2 | – |
| C201 | 1097 ± 82 | 842 ± 63 | 1161 ± 10 | – |
| C35 | 1084 ± 22 | 881 ± 8 | 1174 ± 6 | – |
| C04-09 | 1040 ± 38 | 818 ± 65 | – | – |
| C174 | – | – | 1242 ± 25 | – |
| C123 | – | – | 1216 ± 3 | – |
| C03-44 | 1109 ± 60 | 840 ± 76 | 1173 ± 3 | 1099 ± 111 |
| T6 | 1108 ± 57 | 890 ± 62 | 1175 ± 10 | – |

Errors are given as 2σ variation. (For details of the samples see Table 1.)
*Samples with italic numbers are plag-lherzolite samples and are therefore not fully applicable to the four-phase lherzolite thermometer.
†We used the empirical relationship of Witt-Eickschen & O'Neil (2005) between cpx/opx $K_d$ and temperature, to calculate a temperature from measured cpx/opx trace element partitioning.

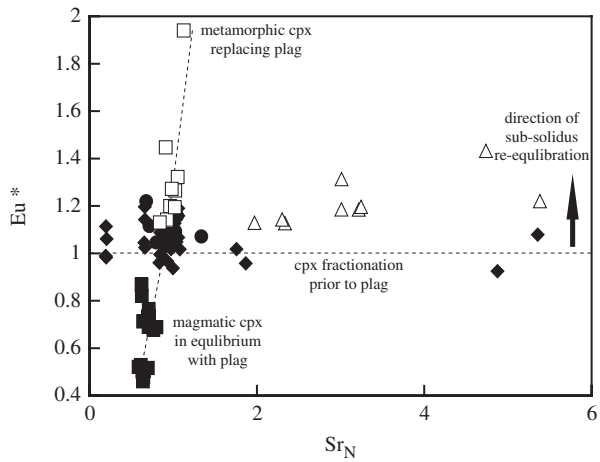


**Fig. 24.** Primitive mantle normalized (Sun & McDonough, 1989) Sr vs Eu* [$Eu^* = Eu/\sqrt{(Sm \times Gd)}$]. Clinopyroxenes fractionated before plagioclase have no significant Eu anomaly ($Eu^* \sim 1$) and variable Sr concentrations; subsequent sub-solidus re-equilibration produces a positive Eu* anomaly. Within clinopyroxene in equilibrium with plagioclase Eu* is positively correlated with the Sr content: magmatic clinopyroxenes have a negative Eu anomaly (i.e. $Eu^* < 1$) and metamorphic pyroxenes growing at the expense of plagioclase inherit a positive Eu anomaly ($Eu^* > 1$). Symbols as in Fig. 13.

## Changing crystallization sequence

Petrographic evidence indicates that the crystallization sequence is different for the ultramafic and the mafic sequences of the Chilas Complex. In ultramafic rocks the crystallization sequence is ol (+ sp) → ol + cpx (+ sp) → ol–cpx–opx (+ sp) → ol–cpx–opx–plag (+ sp + amph). Accordingly, clinopyroxene fractionated before plagioclase, which explains the positive Sr and Pb anomalies and the lack of a significant Eu anomaly in primitive clinopyroxenes (Fig. 24). The granoblastic texture of the gabbronorites has obliterated much of the igneous crystallization sequence. However, frequent inclusions of plagioclase within clinopyroxene imply crystallization of plagioclase prior to clinopyroxene. This observation matches the mineral trace element data. In clinopyroxene from gabbronorite samples C48 and C7, the increase in incompatible element concentrations is associated with continuously more pronounced negative Eu, Sr and Pb anomalies and decreasing Mg-number (Fig. 24). Only clinopyroxenes from the most primitive ol-gabbronorite (C66) do not show a negative Eu anomaly. These display a positive Eu anomaly ($Eu^* \sim 1{\cdot}1$–$1{\cdot}9$), which is positively correlated with the Sr content (Fig. 24). Primitive clinopyroxene with a positive Eu anomaly is produced by subsolidus metamorphic reaction (Seifert & Chadima, 1989). The original magmatic assemblage within the primitive gabbronorite was dominated by olivine and plagioclase with only minor amounts of magmatic clinopyroxene. This change in crystallization sequence from ol–cpx–plag to ol–plag–cpx can be explained by compositional ($H_2O$ and/or Na content) and pressure effects (Elthon & Scarfe, 1984; Gust & Perfit, 1987; Bartels *et al.*, 1991). Experimental petrology studies indicate that the crystallization sequence, especially of plagioclase and clinopyroxene, depends on the ambient pressure and the water content of the

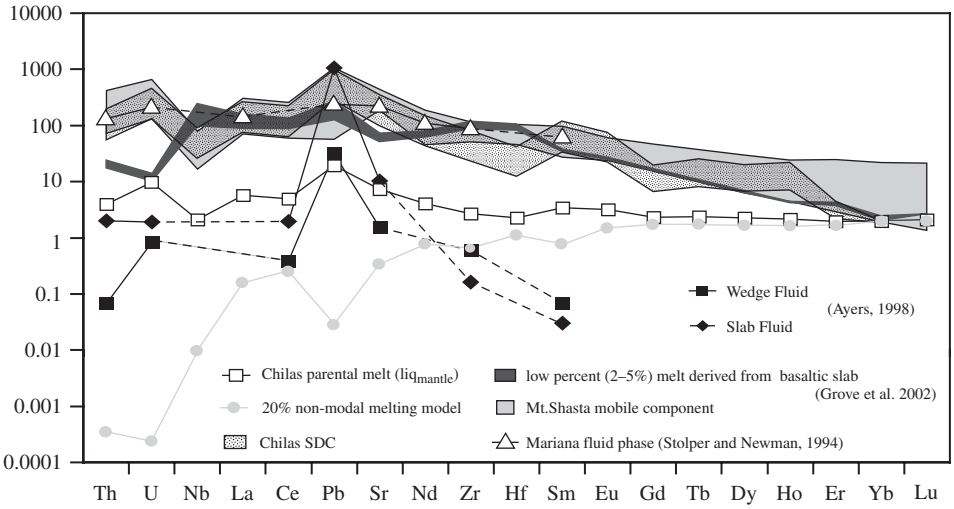


**Fig. 25.** Primitive mantle normalized trace element diagram comparing the Chilas parental melt composition (liq$_{mantle}$), the result of 20% non-modal batch melting (ol 80%, opx 20) of a depleted source (Grove *et al.*, 2002) and the trace element characteristics of a slab-derived component. The slab-derived component (dotted field) is compared with a fluid component inferred for Mt. Shasta (grey field) (Grove *et al.*, 2002), a fluid in equilibrium with the mantle wedge, eclogitized slab (Ayers, 1998) and with a fluid involved in the Marianas primitive magma formation (Stolper & Newman, 1994). The Chilas slab-derived component is most similar to a low percentage melt or supercritical liquid derived from the basaltic part of a subducted slab. (See text for more details.)

system (e.g. Gaetani *et al.*, 1993; Sisson & Grove, 1993; Panjasawatwong *et al.*, 1995; Villiger *et al.*, 2007). At 1·2 GPa, in the presence of $H_2O$, clinopyroxene fractionates prior to plagioclase, the crystallization of which is suppressed (Müntener *et al.*, 2001). At lower pressure (0·2 GPa), even in the presence of water, plagioclase crystallizes prior to clinopyroxene (Sisson & Grove, 1993). We propose that the gabbronorite sequence crystallized close to conditions corresponding to the clinopyroxene–plagioclase crossover, which occurs around 0·5–0·7 GPa. In the light of our new results, we suggest that the ol–cpx–plag crystallization sequence in the ultramafic rocks changed to ol–plag–cpx in the gabbronorite sequence. This difference is explained by different crystallization depths and/or water contents. As the transitional sample C66 is from the reactional contact and sample C48 a few meters from the contact with the ultramafic rocks, different crystallization pressures are now recorded at the same exposure level. This feature is consistent with the syn-magmatic emplacement model of Jagoutz *et al.* (2006).

## Parental liquid composition

### *Composition of the mantle-derived melt*

The high Mg-number of olivine in dunite [C174 Mg-number(average) = 0·90] indicates that olivine equilibrated with a liquid that had a high average Mg-number(melt) = 0·73 [assuming $K\mathrm{d}_{ol}$(Fe–Mg) = 0·3; Roeder & Emslie, 1970] and was, therefore, originally in equilibrium with mantle olivine. The REE and selected trace element concentrations of that parental magma can be calculated by assuming that it was in equilibrium with the most primitive clinopyroxene of dunite C174, using the $K_d$ values of Hart & Dunn (1993) with an interpolated value for Eu (Ionov *et al.*, 2002). The calculated liquid (hereafter termed liq$_{mantle}$) is extremely primitive and slightly LREE enriched (Fig. 25). The flat MREE to HREE and the high Mg-number(melt) are similar to those of basalts from the Izu–Bonin arc described by Arculus *et al.* (1992).

Trace element modeling of non-modal batch melting (Shaw, 1970) is used to constrain the degree of partial melting of the mantle source to explain the observed composition. As the Nd isotopic composition indicates a depleted mantle source (Jagoutz *et al.*, 2006) we used the depleted mantle composition of Grove *et al.* (2002) as a starting source for the trace element modeling. The result indicates that the HREE element characteristics of the liq$_{mantle}$ is best reproduced by ~20% of partial melting in the spinel field. Pearce & Peate (1995) estimated that flux melting as a result of volatile addition from the subducted slab accounts for ~10 ± 5% melting. Following this line of argument we ascribe a significant part of the degree of melting to decompression associated with arc extension (Burg *et al.*, 2006). The more incompatible trace elements, however, are progressively less well reproduced through this model. Even though it is often assumed that incompatible elements in island-arc magmas are derived from the subducted slab (e.g. McCulloch & Gamble, 1991) there is evidence that, even in primitive arc lavas, intra-crustal assimilation processes are, at least in part, responsible for enrichment in incompatible elements (Dungan & Davidson, 2004; Leeman *et al.*, 2005). Hence, it is difficult to differentiate between 'intra-crustal' and 'source-derived'

trace element signatures in subduction zone lavas. As the clinopyroxenes used in this study to calculate the $liq_{mantle}$ are from a mantle-derived melt channel at the base of the arc (Jagoutz *et al.*, 2006), they provide an unrivalled opportunity to study the trace element budget of a supra-subduction zone magma at the mantle–crust transition. In the following discussion, we estimate the trace element budget of an external component, which we consider to be derived from the slab, to balance the observed mismatch.

### *Modeled composition of the subduction-derived component*

A main factor needed to quantify the trace element characteristics of the slab-derived component is the assumption concerning the percentage of this material added to the mantle source region, and this is poorly constrained. However, as the original water content of the upper mantle is believed to be low (Hirth & Kohlstedt, 1996; Asimow & Langmuir, 2003), the bulk water content of subduction zone magmas is attributed to dewatering of the subducted slab (e.g. Grove *et al.*, 2002). Following this line of thought we make a simplified assumption that the amount of $H_2O$ within the Chilas Complex magma should be correlated with the amount of slab-derived components added at source. Magmatic amphibole fixes a lower limit of at least 4 wt% $H_2O$ (Cawthorn & OHara, 1976). However, the initial water content must have been lower (~2–3 wt%) because amphibole crystallized the earliest after fractionation of olivine and clinopyroxene, which in the Aleutians accounts for 15–30% of the mass crystallized (Conrad & Kay, 1984). Similar, in anhydrous system at 0·7 GPa ~25% ultramafic cumulates are formed before plagioclase saturation (Villiger *et al.*, 2007). We assume that a minimum of ~30% of mass crystallized before amphibole saturation. An upper limit of 7–8 wt% $H_2O$ is given by the plagioclase–melt hygrometer of Housh & Luhr (1991) using the high-An plagioclase composition of the primitive ol-gabbronorite C66 and the inferred gabbronorite parental composition ($liq_{gnr}$; see below). The hygrometer calculation probably overestimates the original water content. We have assumed that the water content of the $liq_{mantle}$ could have been between 2 and 7 wt%. The primary value is likely to have been towards the lower end of this range.

To infer the trace element characteristics of the slab-derived component, we followed the procedure of Grove *et al.* (2002). We calculated the trace element concentration of the liquid:

$$C(\mathrm{liq}_{\mathrm{mantle}}) = C_{\mathrm{non-modal\,mantle}}(1 - X_{\mathrm{sl}}/\mathrm{a}) + (X_{\mathrm{sl}}/\alpha)C_{\mathrm{sl}} \quad (3)$$

where $C(\mathrm{liq}_{\mathrm{mantle}})$, $C_{\mathrm{non\text{-}modal\ mantle}}$ and $C_{\mathrm{sl}}$ is the concentration of the element of interest in the $liq_{mantle}$, in the modeled mantle-derived melt and in the slab-derived component, respectively. $X_{\mathrm{sl}}$ is the weight fraction of water in the $liq_{mantle}$, and $\alpha$ is a correction factor to account for the fact that the slab-derived component has additional major elements besides $H_2O$. The results of Grove *et al.* (2002) indicate a rather constant correction factor of ~0·6, which was adopted for the calculation here.

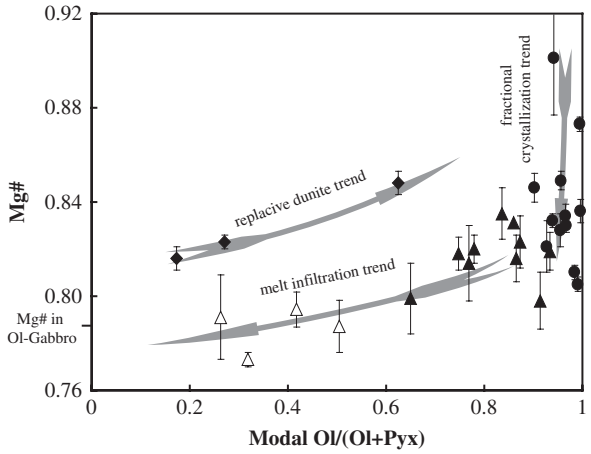


**Fig. 26.** Relationship between modal abundance of olivine and pyroxene vs the Mg-number in olivine in dunite (●), secondary peridotite (▲) and plagioclase-bearing secondary peridotite (△). The Mg-number of olivine in gabbronorite is indicated on the *y*-axis. (See text for discussion.)

### *Results*

The trace element composition of the slab-derived component is strongly enriched in LREE and incompatible elements and depleted in HREE (Fig. 27). It accounts for 90–99% of the highly incompatible elements (Th, U, Nb, La, Ce, Pb, Sr), 40–80% of the less incompatible elements (Nd, Zr, Hf, Sm, Eu) and less than ~20% of the HREE elements. The trace element concentration is comparable with the composition of slab-derived components for the Mt. Shasta (Grove *et al.*, 2002) and the Mariana Trough magmas (Stolper & Newman, 1994) (Fig. 26). The absolute trace element concentrations are similar to those of a low-degree melt (2–5%) or supercritical liquid (Kessel *et al.*, 2005) derived from the eclogitized basaltic part of the subducted slab (Grove *et al.*, 2002). The elevated Pb/Ce ratio requires an additional component, which could be a fluid with high Pb/Ce ratios in equilibrium with an eclogitic slab or mantle wedge (Ayers, 1998). It is important to emphasize that our model documents that between 40 and 99% of the radiogenic isotopic tracers and high field strength elements (Th, Pb, Sr, Nd, Hf and Nb) is contributed by the slab-derived component. This result influences models using apparent conservative elements to infer mantle signatures.

## Fractionation mechanism

### *Ultramafic sequence*

Apart from the secondary peridotites and the older ol-websterites, the ultramafic bodies are dominated by

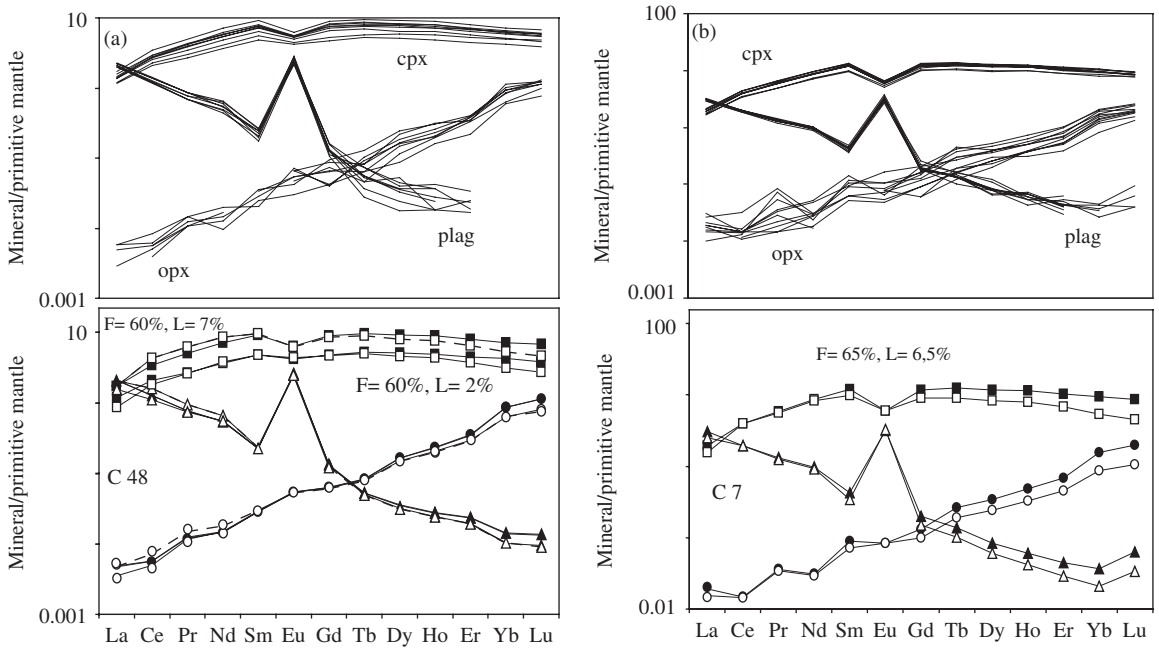


**Fig. 27.** Primitive mantle normalized (Sun & McDonough, 1989) results from the trace element modeling following the approach of Hermann *et al.* (2001). The mean modal composition of the gabbronorite has been approximated as plag 60%, opx 30% and cpx 10%, based on an average value of grid counting and modal calculation based on whole-rock analyses. Squares, clinopyroxene; triangles, plag; circles, opx. The composition of plag and opx has been averaged and assumed to be constant, whereas the spread in cpx can be explained by equilibration with different amounts of interstitial liquid. The upper diagram displays the measured values. In the lower diagram the open symbols are model results;solid symbols are measured values of the sample. (a) Sample C48 can be reproduced by 60% differentiation. The spread in cpx composition indicates equilibration with different amounts of interstitial liquid: solid line, 2% of interstitial liquid; dashed line, 7% of interstitial liquid. (b) Sample C7 modeled with 65% differentiation and an average of 6·5% of interstitial liquid. The spread in cpx compositions is modeled with an amount of interstitial liquid between 5 and 8% (not shown).

homogeneous dunite. None of the dominantly monomineralic ultramafic rock compositions are close to any original liquid composition.

A good correlation is observed between the olivine Mg-number and the modal amount of pyroxene (Fig. 26). The transition from ol-websterite to dunite is related to a decrease in pyroxene content and a slight increase in Mg-number from 0·81 to ~0·85, implying that during dissolution of pyroxene the Mg-number was buffered by the rock assemblage and a high Mg-number melt. We speculate that the initial modal composition of the protolith of the ol-websterite was pyroxene-dominated, similar to the pyroxenite now exposed in the Jijal section. Within dunite samples the Mg-number decreases from 0·90 to ~0·80–0·82 with only a minor change of the olivine/pyroxene ratio, indicating that fractionation of olivine exerts an important control on the Mg-number. Based on these observations we infer that the dunitic bodies are formed by percolative fractional crystallization combining melt–rock reactions and fractional crystallization (Harte *et al.*, 1993). The gradual dunite–lherzolite–pyroxenite transition is associated with a decrease in modal content of olivine, associated with a decrease in olivine Mg-number from ~0·82 to 0·77. The Mg-number asymptotically approaches the olivine Mg-number value measured in olivine-bearing gabbronorite at the contact between ultramafite and gabbronorite (Fig. 26). We interpret the concentric zoning as an result of a melt–rock reaction between melt present within a unconsolidated gabbronoritic crystal mush and the more rigid dunite during emplacement of the ultramafite bodies.

### *Gabbronorite sequence*

Whole-rock trace element data show that the gabbronorite sequence evolved through *in situ* crystallization (Jagoutz *et al.* 2006). Trace element modeling suggests that the mafic rocks correspond either to 'solid compositions' or to 'liquid compositions'. The 'solid compositions' are cumulate-dominated rocks with various amounts of interstitial liquid, whereas 'liquid compositions' are approaching crystallized liquid compositions. To estimate the degree of fractionation of cumulative gabbronorite the mineral trace element data have been modeled following the method of Hermann *et al.* (2001), based on the model of Langmuir (1989). The rationale behind this approach is that zoning of the minerals has been obliterated during slow cooling under granulite-facies conditions. If interstitial liquid was present, it equilibrated with the cumulus assemblage. The basis of the model is to simulate REE patterns of mineral phases fractionated

from a primitive liquid. The unknown is the amount of interstitial liquid (L) and the degree of fractionation ($F$) of a particular sample. These two parameters are modeled to reproduce the measured REE patterns of the mineral phases.

Because of the 'evolved' nature of the mafic gabbronorite sequence and the inferred switch in crystallization sequence it is inappropriate to use $liq_{mantle}$ as a starting composition for this model. Therefore we constrain a liquid composition at the onset of plagioclase crystallization (hereafter called $liq_{gnr}$). $Liq_{gnr}$ corresponds to $liq_{mantle}$ after the latter had produced the ultramafic sequence. The REE composition of $liq_{gnr}$ has been calculated in equilibrium with the mean composition of the magmatic clinopyroxene in the primitive olivine-bearing gabbronorite (C66); that is, clinopyroxene grains with no significant europium anomaly. The trace element composition of $liq_{gnr}$ has the same characteristics as the average bulk composition of the gabbronorite sequence (Jagoutz *et al.*, 2006). The trace element concentration of $liq_{gnr}$ is about 30–50% higher than for $liq_{mantle}$. However, the trace element characteristics of both liquids are similar but $liq_{mantle}$ is slightly more enriched in LREE compared with MREE and HREE [$liq_{gnr}$ $(Ce/Sm)_N$ ~1·10, $(Ce/Yb)_N$ ~2·28; $liq_{mantle}$ $(Ce/Sm)_N$ ~1·45, $(Ce/Yb)_N$ ~2·46]. Simple Rayleigh fractionation modeling (Shaw, 1970) indicates that the change in concentration is due to ~30–50% mass fractionation dominated by olivine (~70%) and accompanied by smaller amounts of clinopyroxene (~30%) and spinel.

Starting from $liq_{gnr}$, the REE patterns of clinopyroxene, plagioclase and orthopyroxene in the gabbronorite samples have been modeled. As the model used can only be applied to relatively primitive samples devoid of the significant amounts of apatite and Ti-pargasite found in more evolved rocks, which influence the REE budget (Hermann *et al.*, 2001), two homogeneous primitive gabbronorite samples (C48 and C7) have been chosen to evaluate the degree of fractionation and to approximate the amount of trapped liquid equilibrated with the cumulus mineral assemblage.

### *Results of mineral trace element modeling*

The *in situ* crystallization model reproduces the mineral trace element patterns of the gabbronorite samples (Fig. 27). The mineral REE patterns of sample C48 are consistent with 60% differentiation. The variation of trace element concentration in clinopyroxene is reproduced by varying the amount of interstitial liquid between 2 and 7 vol. %. Mineral trace element patterns of sample C7 were reproduced with 65% differentiation and 5–8% of interstitial liquid. In accordance with the whole-rock model (Jagoutz *et al.*, 2006), we conclude that both samples C48 and C7 represent cumulate-dominated rocks equilibrated with small amounts of interstitial liquid.

## CONCLUSIONS

The ultramafic rocks and the gabbronorite sequence of the Chilas Complex crystallized from a common, hydrous and mantle-derived magma. Phase petrology indicates that the ultramafic rocks crystallized at higher pressure than the gabbronorite sequence. Mineral data further indicate a difference in crystallization mechanism. The ultramafic rocks were dominantly formed by fractional crystallization and melt–rock reaction at ~0·7 GPa, whereas the gabbronorite sequence was dominantly formed by *in situ* crystallization at 0·6–0·7 GPa. Exposure of the two rock units at the same structural level, without tectonic discontinuity, supports diapirism of the ultrabasic rocks into the unconsolidated gabbronorite (Jagoutz *et al.*, 2006). According to this model of emplacement, the ultramafic bodies represent kilometer-scale upper mantle melt conduits. The new data presented here imply that percolative fractional crystallization and magmatic differentiation were the dominant fractionation mechanisms in the upper mantle that sourced the Chilas magma. Within the lower crust, however, the already fractionated liquid evolved at lower pressure through *in situ* crystallization.

## ACKNOWLEDGEMENTS

H. Williams is thanked for help and support during a long field season in Pakistan. The owners of the Chilas Inn Hotel are thanked for their hospitality during field work. This paper benefited from discussion with M. Schmidt, S. Villiger and J.-L. Bodinier. Reviews by Yaoling Niu and Richard Price are highly appreciated and greatly improved the paper. Marjorie Wilson is thanked for careful and professional editorial handling. The Swiss National Science Foundation supported O.J.'s and J.P.B.'s work (grants NF 20-49372.96 and NF 20-61465.00). Final preparation of the manuscript was supported by an SNF grant to O.M. (PP002-102809).

## SUPPLEMENTARY DATA

Supplementary data for this paper are available at *Journal of Petrology* online.

## REFERENCES

Allen, J. C., Boettcher, A. L. & Marland, G. (1975). Amphiboles in andesite and basalt; I, Stability as a function of $P$–$T$–$f\,O_2$. *American Mineralogist* **60**(11–12), 1069–1085.

Almeev, R. A., Holtz, F., Koepke, J., Parat, F. & Botcharnikov, R. (2007). The effect of $H_2O$ on olivine crystallization in MORB: Experimental calibration at 200 MPa. *American Mineralogist* **92**, 670–674.

Annen, C., Blundy, J. D. & Sparks, R. S. J. (2006). The genesis of intermediate and silicic magmas in deep crustal hot zones. *Journal of Petrology* **47**(3), 505–539.

Arculus, R. J., Pearce, J. A., Murton, B. J. & van der Laan, S. R. (1992). Igneous stratigraphy and major-element geochemistry of Holes 786A

and 786B. In: Fryer, P., Pearce, J. A. & Stokking, LL. B., *et al.* (eds) *Proceedings of the Ocean Drilling Program, Scientific Results*. College Station, TX: Ocean Drilling Program **125**, pp. 143–169.

Asimow, D. & Langmuir, C. H. (2003). The importance of water to oceanic mantle melting regimes. *Nature* **421**(6925), 815–820.

Asrarullah, A. Z. & Abbas, G. (1979). Ophiolites in Pakistan; an introduction. In: Abul, F. & DeJong, K. A. (eds) *Geodynamics of Pakistan*. Quetta: Geological Survey of Pakistan, pp. 181–192.

Ayers, J. (1998). Trace element modeling of aqueous fluid–peridotite interaction in the mantle wedge of subduction zones. *Contributions to Mineralogy and Petrology* **132**(4), 390–404.

Bard, J. (1983). Metamorphism of an obducted island arc; example of the Kohistan Sequence (Pakistan) in the Himalayan collided range. *Earth and Planetary Science Letters* **65**(1), 133–144.

Bartels, K. S., Kinzler, R. J. & Grove, T. L. (1991). High pressure phase relations of primitive high-alumina basalts from Medicine Lake Volcano, Northern California. *Contributions to Mineralogy and Petrology* **108**(3), 253–270.

Barth, M., McDonough, W. & Rudnick, R. L. (2000). Tracking the budget of Nb and Ta in the continental crust. *Chemical Geology* **165**(3–4), 197–213.

Blundy, J. D. & Wood, B. J. (1991). Crystal-chemical controls on the partitioning of Sr and Ba between plagioclase feldspar, silicate melts, and hydrothermal solutions. *Geochimica et Cosmochimica Acta* **55**(1), 193–209.

Boudier, F. & Nicolas, A. (1972). Fusion partielle gabbroique dans la lherzolite de Lanzo (Alpes piemontaises). *Schweizerische Mineralogische und Petrographische Mitteilungen* **52**(1), 39–56.

Brey, G. P. & Köhler, T. (1990). Geothermobarometry in four-phase lherzolites; II, New thermobarometers, and practical assessment of existing thermobarometers. *Journal of Petrology* **31**(6), 1353–1378.

Burg, J. P., Bodinier, J. L., Chaudhry, S., Hussain, S. & Dawood, H. (1998). Infra-arc mantle–crust transition and intra-arc mantle diapirs in the Kohistan Complex (Pakistani Himalaya); petro-structural evidence. *Terra Nova* **10**(2), 74–80.

Burg, J. P., Jagoutz, O., Hamid, D. & Hussain, S. (2006). Pre-collision tilt of crustal blocks in rifted island arcs: structural evidence from the Kohistan Arc. *Tectonics* **25**(5), doi:10.1029/2005TC001835.

Butt, K. A., Chaudhry, M. N. & Ashraf, M. (1980). An interpretation of petrotectonic assemblage west of western Himalayan syntaxis in Dir District and adjoining areas in northern Pakistan. In: Tahirkheli, R. A. K., Jan, M. Q. & Majid, M. (eds) *Proceedings of the Internatioanl Committee on Geodynamics, Group 6 Meeting. Geological Bulletin, University of Peshawar* **13**, 79–86.

Cawthorn, R. G. (1996). Models for incompatible trace-element abundances in cumulus minerals and their application to plagioclase and pyroxenes in the Bushveld Complex. *Contributions to Mineralogy and Petrology* **123**(1), 109–115.

Cawthorn, R. G. & O'Hara, M. J. (1976). Amphibole fractionation in calc-alkaline magma genesis. *American Journal of Science* **276**(3), 309–329.

Chaudhry, M. N., Ghazantar, M. & Ashraf, M. (1983). A plate tectonic model for northwest Himalayas. *Kashmir Journal of Geology* **1**, 109–112.

Chazot, G., Menzies, M. A. & Harte, B. (1996). Determination of partition coefficients between apatite, clinopyroxene, amphibole, and melt in natural spinel lherzolites from Yemen: implications for wet melting of the lithospheric mantle. *Geochimica et Cosmochimica Acta* **60**(3), 423–437.

Conrad, W. K. & Kay, R. W. (1984). Ultramafic and mafic inclusions from Adak Island; crystallization history, and implications for the nature of primary magmas and crustal evolution in the Aleutian Arc. *Journal of Petrology* **25**(1), 88–125.

Coward, M. P., Jan, M. Q., Rex, D., Tarney, J., Thirlwall, M. F. & Windley, B. F. (1982). Structural evolution of a crustal section in the western Himalaya. *Nature* **295**(5844), 22–24.

Coward, M. P., Windley, B. F., Broughton, R. D., Luff, I. W., Petterson, M. G., Pudsey, C. J., Rex, D. C. & Asif, K. M. (1986). Collision tectonics in the NW Himalayas. In: Coward, M. P. & Ries, A. C. (eds) . *Collision Tectonics. Geological Society, London, Special Publications* **19**, 203–219.

DeBari, S., Kay, S. M. & Kay, R. W. (1987). Ultramafic xenoliths from Adagdak Volcano, Adak, Aleutian Islands, Alaska; deformed igneous cumulates from the Moho of an island arc. *Journal of Geology* **95**(3), 329–341.

DeBari, S. M. (1994). Petrogenesis of the Fiambala gabbroic intrusion, northwestern Argentina, a deep crustal syntectonic pluton in a continental magmatic arc. *Journal of Petrology* **35**(3), 679–713.

DeBari, S. M. & Coleman, R. G. (1989). Examination of the deep levels of an island arc; evidence from the Tonsina ultramafic–mafic assemblage, Tonsina, Alaska. In: Page, R. A. (ed.) *Special Section on Northern Chugach Mountains–Southern Copper River Basin Segment of the Alaskan Transect; Part 1. Journal of Geophysical Research, B, Solid Earth and Planets* **94**, 4373–4391.

Dungan, M. A. & Davidson, J. (2004). Partial assimilative recycling of the mafic plutonic roots of arc volcanoes: An example from the Chilean Andes. *Geology* **32**(9), 773–776.

Elthon, D. & Scarfe, C. M. (1984). High-pressure phase equilibria of a high-magnesia basalt and the genesis of primary oceanic basalts. *American Mineralogist* **69**(1–2), 1–15.

Falloon, T. J. & Danyushevsky, L. (2000). Melting of refractory mantle at 1·5, 2 and 2·5 GPa under anhydrous and $H_2O$-undersaturated conditions: implications for the petrogenesis of high-Ca boninites and the influence of subduction components on mantle melting. *Journal of Petrology* **41**(2), 257–283.

Gaetani, G. A., Grove, T. L. & Bryan, W. B. (1993). The influence of water on the petrogenesis of subduction-related igneous rocks. *Nature* **365**, 332–334.

Gasparik, T. (1984). Two-pyroxene thermobarometry with new experimental data in the system CaO–MgO–$Al_2O_3$–$SiO_2$. *Contributions to Mineralogy and Petrology* **87**(1), 87–97.

Grove, T. L., Parman, S. W., Bowring, S. A., Price, R. C. & Baker, M. B. (2002). The role of an $H_2O$-rich fluid component in the generation of primitive basaltic andesites and andesites from the Mt. Shasta region, N California. *Contributions to Mineralogy and Petrology* **142**(4), 375–396.

Gust, D. A. & Perfit, M. R. (1987). Phase relations of a high-Mg basalt from the Aleutian Island Arc: implications for primary island arc basalts and high-Al basalts. *Contributions to Mineralogy and Petrology* **97**, 7–18.

Hart, S. R. & Dunn, T. (1993). Experimental cpx/melt partitioning of 24 trace elements. *Contributions to Mineralogy and Petrology* **113**(1), 1–8.

Harte, B., Hunter, R. H. & Kinny, D. (1993). Melt geometry, movement and crystallization, in relation to mantle dikes, veins and metasomatism. *Philosophical Transactions of the Royal Society of London, Series A* **342**(1663), 1–21.

Heinrich, C. A., Pettke, T., Halter, W. E., Aigner-Torres, M., Audetat, A., Gunther, D., Hattendorf, B., Bleiner, D., Guillong, M. & Horn, I. (2003). Quantitative multi-element analysis of minerals, fluid and melt inclusions by laser-ablation inductively-coupled-plasma mass-spectrometry. *Geochimica et Cosmochimica Acta* **67**(18), 3473–3497.

Hermann, J., Müntener, O. & Günther, D. (2001). Differentiation of mafic magma in a continental crust-to-mantle transition zone. *Journal of Petrology* **42**(1), 189–206.

Herzberg, C. & O'Hara, M. J. (2002). Plume-associated ultramafic magmas of Phanerozoic age. *Journal of Petrology* **43**(10), 1857–1883.

Hirth, G. & Kohlstedt, D. L. (1996). Water in the oceanic upper mantle; implications for rheology, melt extraction and the evolution of the lithosphere. *Earth and Planetary Science Letters* **144**(1–2), 93–108.

Hoisch, T. D. (1990). Empirical calibration of six geobarometers for the mineral assemblage quartz + muscovite + biotite + plagioclase + garnet. *Contributions to Mineralogy and Petrology* **104**(2), 225–234.

Housh, T. B. & Luhr, J. F. (1991). Plagioclase–melt equilibria in hydrous systems. *American Mineralogist* **76**(3–4), 477–492.

Howells, S. & O'Hara, M. J. (1978). Low solubility of alumina in enstatite and uncertainties in estimated geotherms. *Philosophical Transactions of the Royal Society of London, Series A* **288**, 471–486.

Ionov, D. A., Bodinier, J.-L., Mukasa, S. B. & Zanetti, A. (2002). Mechanisms and sources of mantle metasomatism: major and trace element compositions of peridotite xenoliths from Spitsbergen in the context of numerical modelling. *Journal of Petrology* **43**(12), 2219–2259.

Jagoutz, O., Müntener, O., Burg, J.-P., Ulmer, P. & Jagoutz, E. (2006). Lower continental crust formation through focused flow in km-scale melt conduits: The zoned ultramafic bodies of the Chilas Complex in the Kohistan Island arc (NW Pakistan). *Earth and Planetary Science Letters* **242**(3–4), 320–342.

Jan, M. Q. & Howie, R. A. (1980). Ortho- and clinopyroxenes from the pyroxene granulites of Swat Kohistan, northern Pakistan. *Mineralogical Magazine* **43**(330), 715–726.

Jan, M. Q. & Howie, R. A. (1981). The mineralogy and geochemistry of the metamorphosed basic and ultrabasic rocks of the Jijal Complex, Kohistan, NW Pakistan. *Journal of Petrology* **22**(1), 85–126.

Jan, M. Q., Khattak, M. U. K., Parvez, M. K. & Windley, B. F. (1984). The Chilas stratiform complex; Field and mineralogical aspects. *Geological Bulletin, University of Peshawar* **17**, 163–169.

Jan, M. Q., Khan, M. A. & Windley, B. F. (1992). Exsolution in Al–Cr–$Fe^{3+}$-rich spinels from the Chilas mafic–ultramafic complex, Pakistan. *American Mineralogist* **77**(9–10), 1074–1079.

Jan, M. Q. & Windley, B. F. (1990). Chromian spinel–silicate chemistry in ultramafic rocks of the Jijal Complex Northwest Pakistan. *Journal of Petrology* **31**(3), 667–715.

Kay, S. M. & Kay, R. W. (1985). Aleutian tholeiitic and calc-alkaline magma series; I, The mafic phenocrysts. *Contributions to Mineralogy and Petrology* **90**(2–3), 276–290.

Kelemen, B. (1990). Reaction between ultramafic rock and fractionating basaltic magma; I, Phase relations, the origin of calc-alkaline magma series, and the formation of discordant dunite. *Journal of Petrology* **31**(1), 51–98.

Kessel, R., Schmidt, M. W., Ulmer, P. & Pettke, T. (2005). Trace element signature of subduction-zone fluids, melts and supercritical liquids at 120–180 km depth. *Nature* **437**(7059), 724–727.

Khan, M. A. (1988). Petrology and structure of the Chilas ultramafic–mafic complex, Kohistan Arc, NW Himalayas. PhD thesis, University of London..

Khan, N. A. & Khan, T. (1998). Geology of the Chilas Quadrangle (43-I/3) Diamir District, Northern Areas, Pakistan. Quetta: Geological Survey of Pakistan.

Khan, M. A., Habib, M. & Jan, M. Q. (1985). Ultramafic and mafic rocks of the Thurley Gah and their relationship to the Chilas complex. *Geological Bulletin, University of Peshawar* **18**, 83–102.

Khan, M. A., Jan, M. Q., Windley, B. F., Tarney, J. & Thirlwall, M. F. (1989). The Chilas mafic–ultramafic igneous complex; the root of the Kohistan island arc in the Himalaya of northern Pakistan. In: Malinconico, L. L., Jr & Lillie, R. J. (eds) *Tectonics of the Western Himalayas. Geological Society of America, Special Papers* **232**, 75–94.

Khan, M.A., Jan, M.Q., and Weaver, B.L., (1993). Evolution of the lower arc crust in Kohistan, N. Pakistan; temporal arc magmatism through early, mature and intra-arc rift stages. In Treloar, P.J., and Searle, M.P., (eds) *Himalayan Tectonics*. Geological Society, London, Special Publications **74**, 123–138.

Khan, N. A., Khan, T., Mujtaba, G., Hussain, H. & Khan, R. (1999a). Geology of the Kiner Gah Quadrangle (43-I/2) Diamir District, Northern Areas, Pakistan. Quetta: Geological Survey of Pakistan.

Khan, N. A., Latif, M., Bakht, M. S. & Fayaz, A. (1999b). Geology of the Gunar Quardangle (43-I/7), Diamir District, Northern Areas, Pakistan. Quetta: Geological Survey of Pakistan.

Kretz, R. (1983). Symbols for rock-forming minerals. *American Mineralogist* **68**(1–2), 277–279.

Kubo, K., Swada, Y., Takahashi, Y., Kausar, A. B., Seki, Y., Khan, I. H., Khan, T., Khan, N. A. & Takahashi, Y. (1996). The Chilas Igneous Complex in the Western Himalayas of Northern Pakistan. *Proceedings of Geoscience Colloquium, Geoscience Laboratory, Geological Survey, Islamabad* **15**, 63–68.

Kushiro, I. & Yoder, H. S., Jr (1966). Anorthite–forsterite and anorthite–enstatite reactions and their bearing on the basalt–eclogite transformation. *Journal of Petrology* **7**(3), 337–362.

Langmuir, C. H. (1989). Geochemical consequences of *in situ* crystallization. *Nature* **340**(6230), 199–205.

Leake, B. E. (1978). Nomenclature of amphiboles. *American Mineralogist* **63**(11–12), 1023–1052.

Leeman, W., Streck, M., Chesley, J. & Tonarini, S. (2005). Evidence for magma-mixing and disequilibrium in 'primitive' basaltic andesites from Mount Shasta, Northern California. *EOS Transactions, American Geophysical Union* **86**(52), Fall Meeting Supplement, Abstract V11A-06.

Longerich, H. P., Jackson, S. E. & Gunther, D. (1996). Laser ablation inductively coupled plasma mass spectrometric transient signal data acquisition and analyte concentration calculation. *Journal of Analytical Atomic Spectrometry* **11**(9), 899–904.

McBirney, A. R. & Noyes, R. M. (1979). Crystallization and layering of the Skaergaard Intrusion. *Journal of Petrology* **20**(3), 487–554.

McCulloch, M. T. & Gamble, J. A. (1991). Geochemical and geodynamical constraints on subduction zone magmatism. *Earth and Planetary Science Letters* **102**(3–4), 358–374.

Médard, E. & Grove, T. L. (2007). Liquidus temperatures in the basalt-$H_2O$ system: Influence of $H_2O$ on the olivine-melt equilibrium. *Contributions to Mineralogy and Petrology* (submitted).

Müntener, O., Hermann, J. & Trommsdorff, V. (2000). Cooling history and exhumation of lower-crustal granulite and upper mantle (Malenco, eastern Central Alps). *Journal of Petrology* **41**(2), 175–200.

Müntener, O., Kelemen, B. & Grove, T. L. (2001). The role of $H_2O$ during crystallization of primitive arc magmas under uppermost mantle conditions and genesis of igneous pyroxenites; an experimental study. *Contributions to Mineralogy and Petrology* **141**(6), 643–658.

Niida, K., Kausar, A. B. & Khan, S. R. (1996). Ultramafic crystal mush intrusion into the crystallizing magma chamber: field evidence from the Chilas complex, northern Pakistan. *Proceedings of Geoscience Colloquium, Geoscience Laboratory, Geological Survey, Islamabad* **15**, 157–172.

Nimis, P. & Ulmer, P. (1998). Clinopyroxene geobarometry of magmatic rocks; Part I, An expanded structural geobarometer for anhydrous and hydrous, basic and ultrabasic systems. *Contributions to Mineralogy and Petrology* **133**(1–2), 122–135.

Niu, Y., Gilmore, T., Mackie, S., Greig, A. & Bach, W. (2002). Mineral chemistry, whole-rock compositions, and petrogenesis of leg 176 gabbros: data and discussion. In: Natland, J. H., Dick, H. J. B., Miller, D. J. & Von Herzen, R. P. (eds) *Proceedings of the Ocean Drilling Program, Scientific Results*. College Station, TX: Ocean Drilling Program **176**, 1–60.

Obata, M. (1980). The Ronda peridotite; garnet-, spinel-, and plagioclase-lherzolite facies and the *P–T* trajectories of a high-temperature mantle intrusion. *Journal of Petrology* **21**(3), 533–572.

Panjasawatwong, Y., Danyushevsky, L. V., Crawford, A. J. & Harris, K. L. (1995). An experimental study of the effects of melt composition on plagioclase; melt equilibria at 5 and 10 kbar; implications for the origin of magmatic high-An plagioclase. *Contributions to Mineralogy and Petrology* **118**(4), 420–432.

Pearce, J. A. & Peate, D. W. (1995). Tectonic implications of the composition of volcanic arc magmas. *Annual Review Earth and Planetary Sciences* **23**, 251–285.

Petterson, M. G. & Windley, B. F. (1985). Rb–Sr dating of the Kohistan arc-batholith in the Trans-Himalaya of North Pakistan, and tectonic implications. *Earth and Planetary Science Letters* **74**(1), 45–57.

Pettke, T., Halter, W. E., Webster, J. D., Aigner-Torres, M. & Heinrich, C. A. (2004). Accurate quantification of melt inclusion chemistry by LA-ICPMS: a comparison with EMP and SIMS and advantages and possible limitations of these methods. *Lithos* **78**(4), 333–361.

Pudsey, C. J., Coward, M. P., Luff, I. W., Shackleton, R. M., Windley, B. F. & Jan, M. Q. (1985). Collision zone between the Kohistan Arc and the Asian Plate in NW Pakistan. *Transactions of the Royal Society of Edinburgh: Earth Sciences* **76**(4), 463–479.

Ringuette, L., Martignole, J. & Windley, B. F. (1999). Magmatic crystallization, isobaric cooling, and decompression of the garnet-bearing assemblages of the Jijal Sequence (Kohistan Terrane, western Himalayas). *Geology* **27**(2), 139–142.

Roeder, L. & Emslie, R. F. (1970). Olivine–liquid equilibrium. *Contributions to Mineralogy and Petrology* **29**(4), 275–289.

Rudnick, R. L. (1995). Making continental crust. *Nature* **378**, 571–578.

Santos, J. F., Schaerer, U., Gil, I. J. I. & Girardeau, J. (2002). Genesis of pyroxenite-rich peridotite at Cabo Ortegal (NW Spain); geochemical and Pb–Sr–Nd isotope data. *Journal of Petrology* **43**(1), 17–43.

Schaltegger, U., Zeilinger, G., Frank, M. & Burg, J. (2002). Multiple mantle sources during island arc magmatism; U–Pb and Hf isotopic evidence from the Kohistan arc complex, Pakistan. *Terra Nova* **14**(6), 461–468.

Searle, M. P., Khan, M. A., Fraser, J. E., Gough, S. J. & Qasim, J. M. (1999). The tectonic evolution of the Kohistan–Karakoram collision belt along the Karakoram Highway transect, North Pakistan. *Tectonics* **18**(6), 929–949.

Seifert, K. E. & Chadima, S. A. (1989). Depletion of heavy rare-earth elements in metamorphic minerals from Adirondack anorthosites. *Geology* **17**, 1004–1006.

Shaw, D. M. (1970). Trace element fractionation during anatexis. *Geochimica et Cosmochimica Acta* **34**(2), 237–243.

Sisson, T. W. & Grove, T. L. (1993). Experimental investigations of the role of $H_2O$ in calc-alkaline differentiation and subduction zone magmatism. *Contributions to Mineralogy and Petrology* **113**(2), 143–166.

Stolper, E. & Newman, S. (1994). The role of water in the petrogenesis of Mariana Trough magmas. *Earth and Planetary Science Letters* **121**(3–4), 293–325.

Sugawara, T. (2000). Empirical relationships between temperature, pressure, and MgO content in olivine and pyroxene saturated liquid. *Journal of Geophysical Research, B, Solid Earth and Planets* **105**(4), 8457–8472.

Sun, S. S. & McDonough, W. F. (1989). Chemical and isotopic systematics of oceanic basalts; implications for mantle composition and processes. In: Saunders, A. D. & Norry, M. J. (eds) *Magmatism in the Ocean Basins. Geological Society, London, Special Publications* **42**, 313–345.

Tahirkheli, R. A. K., Mattauer, M., Proust, F. & Tapponnier, P. (1979). The India–Eurasia suture zone in northern Pakistan; synthesis and interpretation of recent data at plate scale. In: Abul, F. & DeJong, K. A. (eds) *Geodynamics of Pakistan*. Quetta: Geological Survey of Pakistan, pp. 125–130.

Takahashi, E., Uto, K. & Schilling, J. G. (1987). Primary magma compositions and Mg/Fe ratios of their mantle residues along Mid Atlantic Ridge 29°N to 73°N. *Technical Report of Institute for Study of the Earth's Interior, Okayama University, Series A*, 14 pp.

Takahashi, Y., Mikoshiba, M. U., Takahashi, Y., Kausar, A. B., Khan, T. & Kubo, K. (2007). Geochemical modelling of the Chilas Complex in the Kohistan Terrane, northern Pakistan. *Journal of Asian Earth Sciences* **29**(2–3), 336–349.

Treloar, J., Petterson, M. G., Jan, M. Q. & Sullivan, M. A. (1996). A re-evaluation of the stratigraphy and evolution of the Kohistan Arc sequence, Pakistan Himalaya; implications for magmatic and tectonic arc-building processes. *Journal of the Geological Society, London* **153**(5), 681–693.

Villiger, S., Ulmer, P. & Müntener, O. (2007). Equilibrium and fractional crystallization experiments at 0·7 GPa—the effect of pressure on phase relations, liquid compositions and mineral–liquid exchange reactions of tholeiitic magmas. *Journal of Petrology* **48**, 159–184.

Voshage, H., Hofmann, A. W., Mazzucchelli, M., Rivalenti, G., Sinigoi, S., Raczek, I. & Demarchi, G. (1990). Isotopic evidence from the Ivrea Zone for a hybrid lower crust formed by magmatic underplating. *Nature* **347**(6295), 731–736.

Wells, R. A. (1977). Pyroxene thermometry in simple and complex systems. *Contributions to Mineralogy and Petrology* **62**(2), 129–139.

Witt-Eickschen, G. & O'Neill, H. S. C. (2005). The effect of temperature on the equilibrium distribution of trace elements between clinopyroxene, orthopyroxene, olivine and spinel in upper mantle peridotite. *Chemical Geology* **221**(1–2), 65–101.

Wood, B. J. & Banno, S. (1973). Garnet–orthopyroxene and orthopyroxene–clinopyroxene relationships in simple and complex systems. *Contributions to Mineralogy and Petrology* **42**(2), 109–124.

Yoder, H. S., Jr & Tilley, C. E. (1962). Origin of basalt magmas; an experimental study of natural and synthetic rock systems. *Journal of Petrology* **3**(3), 342–529.

Zaman, H. & Torii, M. (1999). Palaeomagnetic study of Cretaceous red beds from the eastern Hindukush ranges, northern Pakistan; palaeoreconstruction of the Kohistan–Karakoram composite unit before the India–Asia collision. *Geophysical Journal International*, **136**(3), 719–738.

Zeitler, K. (1985). Cooling history of the NW Himalaya, Pakistan. *Tectonics* **4**(1), 127–151.

Zeitler, K., Sutter, J. F., Williams, I. S., Zartman, R. E. & Tahirkheli, R. A. K. (1989). Geochronology and temperature history of the Nanga Parbat–Haramosh Massif, Pakistan. In: Malinconico, L. L., Jr & Lillie, R. J. (eds) *Tectonics of the Western Himalayas. Geological Society of America, Special Papers* **232**, 1–22.

Zeitler, K., Chamberlain, C. P. & Smith, H. A. (1993). Synchronous anatexis, metamorphism, and rapid denudation at Nanga Parbat (Pakistan Himalaya). *Geology* **21**(4), 347–350.